NOAA OAR Special Report

PMEL Tsunami Forecast Series: Vol. 19

A Tsunami Forecast Model for Homer, Alaska

Utku Kânoğlu[1,2]

[1]Department of Engineering Sciences, Middle East Technical University, Ankara, Turkey

[2]NOAA/Pacific Marine Environmental Laboratory (PMEL), Seattle, WA

July 24, 2014

NOTICE from NOAA

Mention of a commercial company or product does not constitute an endorsement by NOAA/OAR. Use of information from this publication concerning proprietary products or the tests of such products for publicity or advertising purposes is not authorized. Any opinions, findings, and conclusions or recommendations expressed in this material are those of the authors and do not necessarily reflect the views of the National Oceanic and Atmospheric Administration.

Contribution No. 3353 from NOAA/Pacific Marine Environmental Laboratory
Contribution No. 1774 from Joint Institute for the Study of the Atmosphere and Ocean (JISAO)

Also available from the National Technical Information Service (NTIS)
(http://www.ntis.gov)

Contents

List of Figures

List of Tables

Foreword

Tsunamis have been recognized as a potential hazard to United States coastal communities since the mid-twentieth century, when multiple destructive tsunamis caused damage to the states of Hawaii, Alaska, California, Oregon, and Washington. In response to these events, the United States, under the auspices of the National Oceanic and Atmospheric Administration (NOAA), established the Pacific and Alaska Tsunami Warning Centers, dedicated to protecting United States interests from the threat posed by tsunamis. NOAA also created a tsunami research program at the Pacific Marine Environmental Laboratory (PMEL) to develop improved warning products.

The scale of destruction and unprecedented loss of life following the December 2004 Sumatra tsunami served as the catalyst to refocus efforts in the United States on reducing tsunami vulnerability of coastal communities, and on 20 December 2006, the United States Congress passed the "Tsunami Warning and Education Act" under which education and warning activities were thereafter specified and mandated. A "tsunami forecasting capability based on models and measurements, including tsunami inundation models and maps..." is a central component for the protection of United States coastlines from the threat posed by tsunamis. The forecasting capability for each community described in the PMEL Tsunami Forecast Series is the result of collaboration between the National Oceanic and Atmospheric Administration office of Oceanic and Atmospheric Research, National Weather Service, National Ocean Service, National Environmental Satellite, Data, and Information Service, the University of Washington's Joint Institute for the Study of the Atmosphere and Ocean, National Science Foundation, and United States Geological Survey.

NOAA Center for Tsunami Research

Abstract

A tsunami forecast model was designed for Homer, Alaska and implemented into the tsunami forecasting system known as Short-term Inundation Forecast System for Tsunamis (SIFT) developed by the National Oceanic and Atmospheric Administration Center for Tsunami Research at the Pacific Marine and Environmental Laboratory, Seattle, Washington, United States of America. This is part of a larger effort to provide tsunami forecast models for the seventy-five communities along vulnerable United States coastlines. Homer is located in the Kenai Peninsula, Alaska and has important commercial and recreational fishing harbor. A Reference Model (RM) and a Forecast Model (FM) were developed using the validated and verified tsunami numerical model of Method of Splitting Tsunami (MOST) both having three telescoping grids in increasing resolution towards Homer, Alaska. Community Modeling Interface for Tsunamis (ComMIT) software which is an interface to the MOST model is used for the development. Synthetic tsunami events originating from subduction zones around the Pacific were considered to test the stability and sensitivity of the Homer FM. It is demonstrated that the RM and FM remained stable in the case of extreme events, i.e., mega- and micro-tsunamis. In addition, FM showed good agreement with the RM in leading wave height and reasonable agreement for later waves indicating accuracy of the FM. FM is optimized to have 4 hours of wave propagation in approximately 10 minutes of CPU time. Unfortunately, there was no tide gage at Homer, Alaska to verify the modeling approach, unlike the FMs which were developed elsewhere. Tide gage in Homer, Alaska was destroyed during the 1964 tsunami and was not rebuild. Therefore, another model similar to the one developed for Homer was developed for Seldovia, Alaska where a tide gage exists. Seldovia model incorporates same outer grids as Homer but different near-shore grid. The tsunami from the 11 March 2011 Japan earthquake was recorded in Seldovia tide gage and has provided data for verification of the modeling approach used for the region. Comparison of the model results with tide gage records of the 11 March 2011 tsunami in Selvodia provided confidence for the FM developed for Homer. After the FM development, the Homer, Alaska FM was tested in SIFT. It is found that FM behaves same in the forecasting environment as in the model development.

Chapter 1

Introduction

The National Oceanic and Atmospheric Administration (NOAA) Center for Tsunami Research (NCTR) at the Pacific Marine Environmental Laboratory (PMEL), Seattle, Washington, United States of America has been developing tsunami forecasting capabilities for the coastlines of the United States and its territories. The NCTR tsunami forecasting products can be classified into two categories: operational (short-term) forecast products (Tang *et al.*, 2012; Wei *et al.*, 2008; Tang *et al.*, 2009) in support of Tsunami Warning Centers (TWCs) operated by the NOAA's National Weather Service (NWS) of the United States –Pacific Tsunami Warning Center (PTWC), Hawai'i and West Coast and Alaska Tsunami Warning Center (WC/ATWC), Alaska– (Titov, 2009; Titov *et al.*, 2005a); and long-term forecast products such as inundation maps to mitigate tsunami disasters and to plan for emergency response by member states in the National Tsunami Hazard Mitigation Program (NTHMP) (González *et al.*, 2005), tsunami hazard assessment (Uslu *et al.*, 2013, 2010a, 2010b) or probabilistic tsunami flooding maps (González *et al.*, 2009; Tsunami Pilot Study Working Group, 2006).

The NCTR has been developing the operational forecasting system known as Short-term Inundation Forecast of Tsunamis (SIFT) to attain short-term forecasting capabilities. The SIFT is designed to efficiently provide basin-wide warning of approaching tsunami, i.e., timely and accurately. The SIFT system integrates several key components: real-time deep-ocean observations of a passing tsunami from Deep-ocean Assessment and Reporting of Tsunamis (DART), also known as tsunameters (Spillane *et al.*, 2008); a basin-wide pre-computed propagation database of wave amplitudes and flow velocities based on potential tsunamigenic unit sources (Gica *et al.*, 2008); an inversion algorithm to refine the tsunami source based on deep-ocean observations using tsunamigenic unit source combination during an event (Percival *et al.*, 2009); and high-resolution models to provide accurate and timely forecast for tsunami prone coastal communities (Tang *et al.*, 2009; Tang *et al.*, 2008a). After rigorous testing at the NCTR, the current version of the SIFT system was distributed to the warning centers for operational test and evaluation (OT&E). The SIFT system was accepted for operational use at the NWS's two warning centers by executive panel on June 7, 2013 (Vasily Titov, personal communication, 8 June 2013). Nonetheless, the SIFT system is under continuous testing and development at the NCTR. The NCTR is also extending SIFT to a web base forecasting tool (tweb) (Burger *et al.*, 2013).

The bottom pressure recorder to measure long wave in deep-sea, which was the basis of what is now known as tsunameters, was developed by PMEL and presented first time during the workshop in Twin Harbors, Catalina Island, California in 1990 (Liu *et al.*, 1991). Then, with

further developments at PMEL and deployment of them in deep-sea, measurements from the network of tsunameters are now critical component of the SIFT. Tsunameters are deployed at specific locations to provide rapid measurements of a passing tsunami (Bernard *et al.*, 2006). The methodology behind the buoy site selection process is explained in Spillane *et al.* (2008). Note that until the direct measurements of tsunamis in deep-sea, the only available recordings were from tide gages, which are most often located in sheltered locations inside harbors or inlets. Tide gage measurements reliably only provide arrival time and possibly the character of the first wave but not enough to identify the initial deformation. Besides, once tsunami reaches tide gages it is too late for warning.

Both the short- and long-term forecasting methodologies of the NCTR use a pre-computed propagation database of tsunami evolution from unit earthquakes. These unit earthquakes are generated by a 100 km long 50 km wide fault planes with a slip value of 1 m, i.e., an equivalent moment magnitude, Mw 7.5. Hence, they are called unit sources. They are placed along the subduction zones of the world oceans in several rows, depending on the width of the subduction zone (Gica *et al.*, 2008). The ocean-bottom deformation is calculated with the Okada (1985) formulation for each unit earthquake. The specific characteristics –dip and rake angles, and source depth– are determined depending on the subduction zone geometry and known history of earthquakes. The nonlinear shallow-water model is used to evaluate propagation from each unit earthquake source for entire basin. The propagation results are contained in a set of ocean-specific tsunami propagation databases, i.e., the Pacific, the Atlantic and the Indian Oceans.

Databases have been created and maintained at NCTR.[1] Currently, there are 1,725 pre-computed unit source propagation model results covering the worlds oceans, forming the propagation database. It is also under continuous expansion as need arises. Similar idea is also in use at the Bureau of Meteorology, Australia[2], see Greenslade *et al.* (2007). However, Australian database uses different approach. Rather than employing unit sources, each source location has four scenarios associated with it, i.e., magnitudes of 7.5, 8, 8.4 and 9 events. Comparison of the same inundation model results with boundary conditions from the NCTR and Australian scenario databases is provided in Greenslade and Titov (2008). Also, same kind of database is in the process of development in the Mediterranean and Aegean Seas (Kânoğlu *et al.*, 2012).

The propagation database is used to obtain offshore scenario wave kinematics for the production of short- and long-term forecast products at the NCTR. The linearity of tsunami propagation in the open ocean allows scaling and/or combination of the pre-computed propagation results of unit sources from database to create scenario events. Even though the numerical model which is used for the calculation of propagation is nonlinear, in deep water, the contributions of the nonlinear terms in the wave evolution are negligible. Once in shallow water, the superposition probably is not applicable, hence a site-specific inundation model is created to study the terminal effects (Uslu, 2008). This combination becomes the boundary and/or initial conditions for near-shore models. Most importantly, the basin-wide database of pre-computed water elevations and flow velocities for unit sources covering worldwide subduction zones helps to reduce computation time substantially and expedites forecast during an event.

For real-time warning, the deep-ocean tsunami propagation for a specific event, i.e., the offshore scenario, is obtained through the scaling and/or combination of unit sources constrained with tsunameter measurement(s) through the methodology explained in Percival *et*

[1] http://sift.pmel.noaa.gov

[2] http://opendap.bom.gov.au:8080/thredds/catalogs/bmrc-atws-catalog.html

al. (2009), in real time. As the tsunami propagates across the ocean and successively reaches tsunameter observation sites, recorded sea levels are ingested into the tsunami forecast tool SIFT in near real-time and incorporated into an inversion algorithm to produce an improved estimate of the tsunami source over a magnitude estimate. A linear combination of the pre-computed unit tsunami sources from the database, combination of water elevations and flow velocities, is then performed based on this tsunami source, now reflecting the transfer of energy to the fluid body, to produce boundary and/or initial conditions of water elevation and flow velocities to initiate the near-shore forecast model computation. While methodology is explained in detail in Tang *et al.* (2009), specific examples of the real-time forecast results are summarized in Tang *et al.* (2012) and (Wei *et al.*, 2008) for the 11 March 2011 Japan and the 15 August 2007 Peru events respectively.

Tsunami numerical models are prominent in both types of tsunami forecasting products, short- and long-term tsunami forecasting. The NCTR uses the Method of Splitting Tsunamis (MOST) numerical model (Titov and González, 1997; Titov and Synolakis, 1998, 1997, 1995; Titov, 1997). The MOST model is a finite difference model based on method of characteristic which is capable of simulating tsunami evolution, i.e., transoceanic propagation and inundation over dry land. Also, MOST takes input from a propagation database and then, a series of nested grids which resolves the near-shore bathymetry and topography are used to estimate the water level and inundation at coastal site. The MOST model has gone through extensive validation and verification as outlined in Synolakis *et al.* (2008, 2007) using analytical solutions, experimental results, and field measurements and was successfully used for simulations of many historical tsunami events. Development of tsunami science is summarized in Synolakis and Kânoğlu (2009) with perspective of validation and verification. Validation and verification of tsunami numerical models is essential, especially the ones will be used in forecasting environment and design of critical structures such as nuclear power plants (González *et al.* (Science Review Working Group), 2007). Note also that numerical dispersion of MOST may appropriately mimics frequency dispersion at optimized grid resolution as shown in Burwell *et al.* (2007) and Zhou *et al.* (2012). Therefore, it is applicable dispersive propagation of tsunamis. Previous and present development of forecast models in the Pacific (Titov *et al.*, 2005; Titov, 2009; Tang *et al.*, 2008b; Wei *et al.*, 2008) have validated the accuracy and efficiency of each forecast model currently implemented in the real-time tsunami forecast system. Models are tested when the opportunity arises and are used for scientific research.

At the NCTR, specifically, two types of models are developed for the tsunami prone sites, i.e., a high-resolution reference model (RM) and forecast model (FM). Both models utilize MOST and consist of three levels of telescoping grids with increasing resolution to model the tsunami dynamics and inundation onto dry land. First, RM is developed for the site. Then RM is used as the basis for the development of a FM to be used operationally to provide an estimate of arrival time, wave height, flow velocities at prone site while a tsunami is still propagating in the open ocean. FMs are optimized for their grid resolution and run time comparing their results with high spatial and temporal resolution RM results to make sure that FMs mimic the interested quantities reasonably well. Also comparing FM results, if available for the location, with historical data is an essential way to verify FMs' accuracy. The goal of FM is to maximize the length of time that the community at-risk could react to a tsunami threat by providing accurate information as quickly as possible to emergency managers and other officials responsible for the community and infrastructure. Therefore, RM grids are optimized by coarsening the resolution and/or considering smaller spatial extend of the overall grid dimensions. While the aim

of the RM is accuracy, the FM is optimized in run-time to be used operationally considering the significant portion of the modeled tsunami, typically 4 to 10 hours of modeled tsunami time, to pass through the model domain without too much signal degradation. Tang *et al.* (2009) describe the technical aspects of FM development, stability testing and robustness. Currently, 75 FMs were constructed for populous coastal communities at risk in the Pacific, Atlantic and Caribbean for the United States and its territorial coastlines and integrated to SIFT system. Previous and present development of FM in the Pacific has shown the accuracy and efficiency of the up-to-date FMs which are implemented in SIFT for the real-time tsunami forecast (Tang *et al.*, 2012; Wei *et al.*, 2008) as well as in hind-cast studies (Wei *et al.*, 2013).

This is one of the report in the FM development series which outlines the one developed for the town of Homer, Alaska. The development and testing of the FM for the town of Homer which is located at the shore of Kachemak Bay in the Kenai Peninsula, Alaska is explained (Figures 1- 2). A population of 5,003 is reported in the 2010 census. Homer's distinct feature is the 7.2 km (4.5 mi) long gravel bar, known as the Homer Spit which extends into the bay (Figure 3). Much of the Homer coastline and spit sank after the 1964 Alaska earthquake resulting also distraction of Homer tide gage. Homer's fishing harbor is used commercially and recreationally. Homer is the southernmost town on the Alaska Highway system. It is also a stopping point for the Alaska ferry and regional air flights. The FM is incorporated into the SIFT system at the NCTR and will be incorporated into the SIFT in use at the PTWC and WC/ATWC during the version update.

Chapter 2

Model Development

Accurate forecasting of the tsunami impact on a coastal community largely relies on the usage of validated and verified tsunami numerical model as explained. In addition, accurate bathymetry and topography are crucial inputs to developing the RM and FM, especially for the inundation calculation. The high spatial and temporal grid resolution necessary for modeling accuracy poses a challenge in the run-time requirement for real-time forecasts. The FM need to utilize the most recent bathymetry and topography available to reproduce the correct wave dynamics during the inundation computation. Each RM and resulted FM consist of three telescoping grids with increasing spatial resolution and, consequently, temporal resolution for simulation of wave inundation onto dry-land. Referred to as A-, B-, and C-grids, each of which becomes successively finer in resolution as they telescope into the population and economic center of the community of interest. Offshore is covered by the largest and lowest resolution A-grid while the near-shore details are resolved within the finest scale C-grid to the point that tide gauge observations recorded during historical tsunamis, if available, and signal from incoming waves are resolved within expected accuracy limits. The procedure is to start with large spatial extent merged bathymetric topographic grids at high resolution, referred to as RM, and then these grids are optimized coarsening the grid resolution and/or reducing the modeling region –the grid size– allowing for the significant portion of the modeled tsunami waves, typically 4 to 10 hours of modeled tsunami time, to pass through the model domain without too much signal degradation. This final model is referred to as the FM. Here, development of RM and consequently FM is outlined for Homer, Alaska. In addition to the development, testing of FM using synthetic and historical events is summarized.

2.1 Forecast Area

Homer, Alaska is located at the southwestern tip of the Kenai Peninsula (Figure 1). The Kenai Peninsula extends approximately 240 km (150 miles) southwest from the Chugach Mountains located south of Anchorage. It is separated by main land by the Cook Inlet in the west and is bordered by the Gulf of Alaska and Prince William Sound to the east. Kachemak Bay is a small inlet off the Cook Inlet where Homer is located. Homer is the southernmost town on the Alaska Highway system. It is also a stopping point for the Alaska ferry and regional air flights. Local, state, and federal government offices are located in downtown Homer, at elevations well above the reach of a distant tsunamis.

Homer, population 5,003 reported at the 2010 census, is the largest of the Kachemak Bay communities. The Homer small boat harbor is home to more than 700 charter and commercial boat operations year round, growing to 1,500 in the summer months. Even though commercial fishing has been the major source of income for residents of Kachemak Bay tourism also plays a very important role in the local economy. The community of Homer and the rest of the Kachemak Bay area have been one of the earliest areas of south-central Alaska to develop a significant tourism industry. Thousands of people come to sightsee, fish, hike, and view wildlife, mostly during the summer months.

Town's most distinguishing feature is the Homer Spit, approximately 7.2 km (4.5 mi) narrow long gravel bar that extends from town into the Kachemak Bay, on which the Homer Harbor is located (Figure 3). Much of the coastline as well as the Homer Spit sank dramatically during the Good Friday Earthquake on 27 March 1964. After the earthquake, very little vegetation was able to survive on the Homer Spit. The commercial and industrial center of the community is located on the Spit. It is used for heavily for recreational activities during summer and is especially vulnerable to large sea waves. Severe storms accompanied by high water levels and waves have occasionally overtopped the roadway on the Homer Spit, causing the road to close.

Even though it is not the tsunami forecasting area, as explained before, because of existence of tide gage, FM similar to the one developed for Homer was also developed for Seldovia, Alaska. Seldovia city in Kenai Peninsula Borough, Alaska is one of five first-class and home-rule communities located within the Kenai Peninsula Borough, State of Alaska. Its population was 255 at the 2010 census. Seldovia is located along Kachemak Bay, 27 km (17 mi) southwest of Homer (Figure 2). Commercial fishing and shellfish processing are local economic activities. There are timber operations in Seldovia Bay and nearby Jakolof Bay, and tourism is increasing. There is no road system connecting the town to other communities. Seldovia is accessible by boat or plane. A state-owned 562 m (1,845 ft) long by 18 m (60 ft) wide gravel airstrip and a seaplane base are available. The city is served by several scheduled and chartered aircraft services.

2.2 Model Set-up

The basis for the FMs and RMs grids are high-resolution digital elevation model (DEM) constructed by the NOAA's National Geophysical Data Center (NGDC) and NCTR using the best and all available bathymetric, topographic, and shoreline data to reproduce the wave dynamics during the inundation computation for at-risk communities. For each community, data are compiled from a variety of sources to produce a DEM referenced to Mean High Water in the vertical and to the World Geodetic System 1984 (WGS-84) in the horizontal.[1]

The best available data for the Homer area is gathered and used to develop RM and FM. The bathymetry and topography used in the development of both models were based on a DEM provided by NGDC. This was considered to an adequate representation of the local bathymetric and topographic features that will effect tsunami propagation and inundation. Grids may be updated if newer, more accurate data are available. This model is an already improvement over the previous models since it incorporates new DEM and new set of stability and robustness tests applied to newly developed FMs.

Development of an optimized tsunami FM for Homer, Alaska began to develop RM with the

[1] http://ngdc.noaa.gov/mgg/inundation/tsunami/inundation.html

spatial extent merged bathymetric/topographic grids shown in Figure 4. The high-resolution Homer, Alaska RM consists of three nested grids. The outermost A-grid covers from approximately 4,000 m depth (maximum depth 5,547 m) at Pacific Ocean including some part of Gulf of Alaska and extends to the north including Cook Inlet and Anchorage, Alaska. This region (Figure 4) was modeled by 24 arc-second resolution which corresponds approximately 742 m grid resolution in latitude and approximately 390 m in longitude. This dataset is generated from Southern Alaska Coastal Relief Model (Lim *et al.*, 2011). 24 arc-second resolution RM A-grid is sampled to generate FM A-grid in 72 arc-second resolution, i.e., to approximately 2,226 m and 1,169 m resolution for latitude and longitude respectively. Extent of RM A-grid and FM A-grid are kept same (Figure 5). Parameters for the RM and FM A-grids are summarized in Table 1.

Both RM and FM intermediate B-grids were produced using 1/3 arc-second resolution grid which covers Kenai Peninsula (Friday *et al.*, 2010). The intermediate B-grid covers Kenai Peninsula to a depth of 175 m with 6 arc-second resolution in RM and 12 arc-second resolution in FM. These resolutions correspond approximately 186 m in latitude and 94 m in longitude for RM and 371 m in latitude and 188 m in longitude for FM. Again extent of RM (Figure 4) and FM (Figure 5) B-grids are kept same. Parameters for each B-grid are summarized in Table 1.

The innermost RM and FM C-grids were again produced using 1/3 arc-second resolution grid which covers Kenai Peninsula (Friday *et al.*, 2010). While RM C-grid employs 1/3 arc-second grid resolution FM C-grid employs 1.5 arc-second grid resolution. These grid resolutions correspond grid resolution 10 m in latitude and 5 m in longitude for RM and 47 m in latitude and 24 m in longitude for FM. C-grid extents are shown in Figures 4 and 5 for RM and FM respectively and parameters are given in Table 1. Unlike RM and FM A- and B-grid which are kept at same extent C-grids is chosen to be slightly different in extent in RM and FM to reduce the computation time. In addition, as explained, FM like C-grid is developed for Seldovia, Alaska.[2] FM C-grid resolution for Seldovia model is chosen same as Homer C-grid (Figure 6), i.e., 1.5 arc-second (Table 1). However, Seldovia FM shares the same A- and B-grids with Homer FM.

Once the RM and optimized FM grids are finalized adjustable parameters such as time steps for each grid, number of time steps, A- and B-grids near shore wet/dry boundary depth, friction coefficient, output time step are also determined and they are given in Appendix A1 and A2 for RM and FM respectively. These parameters remain fixed from run to run, under the assumption that the parameters may be location dependent (sharp bathymetric changes, high resolution needed for channels, bars etc.) but should not depend on the flow field, i.e., the particular tsunami being modeled.

During the development of RM and consequently FM for Homer, Alaska, Community Modeling Interface for Tsunamis (ComMIT) software is used substantially (Titov *et al.*, 2011). After the Indian Ocean tsunami of 2004, the Intergovernmental Coordination Group (ICG)/ the Indian Ocean Tsunami Warning and Mitigation System (IOTWS) recommended to develop a web-based community tsunami model and, in response, the NCTR was developed ComMIT, which is in essence a rich graphical interface to a precomputed tsunami scenario database and to the MOST model. ComMIT is designed in Java programming language, analogously to MOST's command-line operation, and is easy to use. Detail of modeling with ComMIT is summarized in Titov *et al.* (2011). In short, ComMIT uses initial conditions from a precomputed propagation database, has an easy graphical interface to output modeling results, and requires

[2] If a FM was to be developed for Seldovia, Alaska, probably, it could have been higher resolution and smaller in extent. Here, it is kept at same resolution as Homer grid to understand resolution effect.

minimal hardware. Both deep-ocean propagation and inundation tsunami models require information on: (1) bathymetry and coastal topography, (2) initial and boundary conditions, and (3) model run-specific information such as spatial resolution, time step, and length of model run. The aim of ComMIT is to provide an interface which allows for the selection of model input data (initial condition, bathymetry grids, etc.) as well as a platform to display model output through a graphical user interface (GUI). The interface also allows for Internet sharing of the model results, either as a Google Earth animation, or through the use of shared databases via the OPeNDAP protocol.[3] The ComMIT output comprises universally accepted and standardized NetCDF format files, providing access to the model results either via ComMIT itself, or via a number of software packages for model data presentation and analysis (e.g., Matlab, IDL, Ferret, etc.).

2.3 Model Robustness and Stability

After RM and FM models are developed as described, the numerical stability and robustness of the Homer, Alaska RM and FM are tested with a total of nineteen synthetic mega-tsunami, one medium-tsunami and three micro-tsunami synthetic scenarios listed in Table 2 (see also Figure 7) for their robustness and stability. As given in Table 2, the synthetic mega-tsunami events is composed of 20 unit sources covering area of 1000 × 100 km^2 with a slip value of 25 m. This is equivalent to an earthquake of Mw 9.3. At least one mega-tsunami scenario is tested for every subduction zone in the Pacific Basin (Gica *et al.*, 2008). The propagation database is summarized in the Appendix B for the Pacific Basin. It contains unit sources from Aleutian–Alaska–Cascadia Subduction Zone (ACSZ) (Figure B.1, Table B.1), Central and South America Subduction Zone (CSSZ) (Figure B.2, Table B.2), Eastern Philippines Subduction Zone (EPSZ) (Figure B.3, Table B.3), Kamchatka–Bering Subduction Zone (KBSZ) (Figure B.4, Table B.4), Kamchatka–Kuril–Japan–Izu–Mariana–Yap Subduction Zone (KISZ) (Figure B.5, Table B.5), Manus–Oceanic Convergent Boundary Subduction Zone (MOSZ) (Figure B.6, Table B.6), New Guinea Subduction Zone (NGSZ) (Figure B.7, Table B.7), New Zealand–Kermadec–Tonga Subduction Zone (NZSZ) (Figure B.8, Table B.8), New Britain–Solomons–Vanuatu Subduction Zone (NVSZ) (Figure B.9, Table B.9), New Zealand–Puysegur Subduction Zone (NPSZ) (Figure B.10, Table B.10), and Ryukyu–Kyushu–Nankai Subduction Zone (RNSZ) (Figure B.11, Table B.11).

Figures 8-26 show the time series of water surface elevations from all 19 synthetic mega-tsunami scenarios comparing results from RM and FM. First, both models maintains stability in all the events presented. Second, RM and FM models compare well, i.e., FM model mimics arrival time, initial wave amplitude, maximum wave amplitude. Overall, later waves also compare reasonably well. Usually, warning points for the developed FMs are chosen as tide gage locations and time series of sea surface elevations for RM and FM are compared at this point. However, non-existence of a tide gage in Homer presented challenge for developing of Homer, Alaska. The Homer tide gauge was destroyed in the 1964 Alaska event. Therefore, Homer, Alaska warning point was chosen as at ($59°36.35'N$, $151°25.08'W$) at 5.3 m water depth Mean-Sea-Level; outside of the Homer Spit the North East side of the entrance into harbor (Figure 2). The new tide gauge was established in Seldovia, across the Cook Inlet from Homer (Figure 2) on 24 May 1964 with present installation dating on 9 July 1990. National Ocean Survey (NOS) tide gage station (ID: 9455500) located in Seldovia ($59°26.40'N$, $151°43.20'W$). The

[3] http://opendap.org

mean range in Seldovia is 4.73 m and the diurnal range is 5.50 m. Mean sea level is 5.08 m. The tide gauge at Seldovia has recordings of the 2011 Japan tsunami that are used in validation of the RM and FM for Seldovia. This is the only way to have confidence for the tsunami FM developed for Homer, Alaska. Since the FM will be used mostly for tsunamis generated by medium size earthquakes, it is essential to test it with medium and micro tsunamis. The model performs well with one medium size tsunami originated from New Zealand–Kermadec–Tonga region (Table 2). Comparisons between RM and FM models are given in Figure 27. FM model was also tested with three micro-tsunami events listed in Table 2. FM behaved as expected, i.e., no instabilities (Figures 28-30).

Results of the Homer, Alaska tsunami forecast model showed that optimized model reduces the computation time of 4 hours simulation to 8.9 minutes of wall-clock time. A significant portion of the modeled tsunami waves, typically 4 to 10 hr of modeled tsunami time, pass through the model domain without appreciable signal degradation.

2.4 Model Validation with Historical Events

In addition to synthetic event tests presented in the previous section, FM requires validation against historical events if there are reliable sources of data, such as the runup, inundation, and time-series of water surface elevations recorded at tide gage stations. As explained previously, Homer tide gage was destroyed during the 1964 Alaska earthquake and was not rebuilt. However, there is tide gage station at Seldovia, Alaska across from Cook Inlet. The 11 March 2011 Japan tsunami was recorded in Seldovia tide gage. Therefore, only 11 March 2011 Japan tsunami was used and tide gage records are compared with FM and RM results (Figure 32). Comparisons of the results for Seldovia model confirms that FM modeled the event as expected. Model estimates wave height measurements at Seldovia gage for the 11 March 2011 Japan tsunami reasonably well (Figure 32). During the FM development it is necessary to validate as many historical events as possible. Usual events used in testing are listed in Table 3 and shown in Figure 31. In the other events, the signals are too weak and noisy to be applied for model validations at Seldovia.

Chapter 3

Summary and Conclusions

The FM was developed for Homer, Alaska to be incorporated into the SIFT which is designed for the support of NOAA's tsunami warning centers. First, a set of grids have been developed for the Homer, Alaska RM and, then, optimized for the FM. Homer FM is optimized such that 4 hours wave propagation is modeled in approximately 10 minutes, satisfying forecasting time requirement. The computational grids were derived from the best available bathymetric and topographic data at the time of grid construction. The stability and sensitivity of FM is investigated by simulating nineteen mega, one medium and three micro size synthetic tsunamis. The good stability of the FM is observed and this guarantees its reliability during real-time forecast. FM and RM agree with each other for initial waves for all synthetic events modeled.

Since there was no tide gauge at Homer, Alaska after the 1964 earthquake, there was not any historical tide gauge data to verify FM developed. However, additional FM like model developed for Seldovia, Alaska sharing same outer grids with Homer, i.e., the same A- and B-grids for both models. The 11 March 2011 Japan tsunami was modeled for Seldovia and results are compared with tide gauge measurement. Comparison shows reasonable agreement at Seldovia tide gauge implying the validity of the developed model for Homer, Alaska. Once all the testing is completed in the development phase FM is submitted to the SIFT developer team to be integrated into SIFT. After the integration, FM is tested in the forecasting environment. Results of SIFT testing are presented in Appendix C. The results show that the FM is stable and robust across geographically distributed mega-tsunami events in forecasting environment as in the development environment with consistent and high quality results.

Kachemak Bay where Homer and Seldovia located was given high-priority for Alaska inundation mapping project. Suleimani *et al.* (2005) consider 1964 great Alaska earthquake and a hypothetical scenario to produce inundation map for the region. Note that it is not the intention of this study to develop such a map. However, RM developed here can be definitely utilized for the development such products.

Note also that, development of this optimized tsunami FM was based on the digital elevation model (DEM) provided by the National Geophysical Data Center and the author considers it to be an adequate representation of the local bathymetry and topography. This report is already development over the previous modeling effort which was employing previous bathymetry and topography. As new DEMs become available, FM will be updated and report updates will be posted.[1]

[1] http://nctr.pmel.noaa.gov/forecast_reports/

Chapter 4

Acknowledgments

Author acknowledges the work of Dr. Arun Chawla who prepared previous FM with a limited topographic and bathymetric data, and thanks to Dr. Edison Gica providing location maps of synthetic scenarios and historical events. Author also wish to thank the NOAA Center for Tsunami Research for the support during summer visits from 2004 to 2013. The Author also appreciates group for discussions, comments, and editorial assistance. Collaborative contributions of the National Weather Service, the National Geophysical Data Center, and the National Data Buoy Center were invaluable. The National Oceanic and Atmospheric Administration provided funding for all work culminating in the development of the Homer, Alaska tsunami forecast model and report. This publication was partially funded by the Joint Institute for the Study of the Atmosphere and Ocean (JISAO) under NOAA Cooperative Agreement No. NA17RJ1232, JISAO Contribution No. XXXX. This is PMEL Contribution No. XXXX.

Chapter 5

References

Bernard, E. N., Mofjeld, H. O., Titov, V., Synolakis, C. E., and González F. I. (2006). Tsunami: scientific frontiers, mitigation, forecasting, and policy implications. *Philos. T. R. Soc. A*, 364, 1989–2007. doi: 10.1098/rsta.2006.1809

Burger, E. F., Kamb, L., and Nakamura, T. (2013) A WEB based tsunami-forecating tool: Design approach and implementation *29th Conference on Environmental Information Processing Technologies (formerly IIPS), 93rd Annual Meeting of the AMS in Austin, TX*.

Burwell, D., Tolkova, E., and Chawla, A. (2007), Diffusion and dispersion characterization of a numerical tsunami model, *Ocean Modelling, 19*, 10–30.

Friday, D. Z., Taylor, L. A., Eakins, B. W., Carignan, K. S., Caldwell, R. J., Grothe, P. R. and Lim, E. (2010) Digital Elevation Model of Kachemak Bay, Alaska: Procedures, Data Sources and Analysis. *NOAA Tech. Memo.*, The Pacific Marine Environmental Laboratory (PMEL) NOAA Center for Tsunami Research by the NOAA National Geophysical Data Center (NGDC), 24 pp.

Gica, E., Spillane, M. C., Titov, V. V., Chamberlin, C. D., and Newman, J. C. (2008). Development of the forecast propagation database for NOAA's Short-term Inundation Forecast for Tsunamis (SIFT). NOAA Tech. Memo. OAR PMEL-139, NTIS: PB2008-109391, NOAA/Pacific Marine Environmental Laboratory, Seattle, WA, 89 pp.

González, F. I., Geist, E. L., Jaffe, B., Kânoğlu, U., Mofjeld, H., Synolakis, C. E., Titov, V V., Arcas, D., Bellomo, D., Carlton, D., Horning, T., Johnson, J., Newman, J., Parsons, T., Peters, R., Peterson, C., Priest, G., Venturato, A., Weber, J., Wong, F., and Yalciner, A. (Tsunami Pilot Study Working Group) (2009) Probabilistic tsunami hazard assessment at Seaside, Oregon for near- and far-field seismic sources. *Journal of Geophysical Research-Ocean*, 114, C11023 (2009). doi: 10.1029/2008JC005132

González, F.I., E. Bernard, P. Dunbar, E. Geist, B. Jaffe, U. Kânoğlu, J. Locat, H. Mofjeld, A. Moore, C. Synolakis, V. Titov, and R. Weiss (Science Review Working Group) (2007). Scientific and technical issues in tsunami hazard assessment of nuclear power plant sites. NOAA Tech. Memo. OAR PMEL-136, Pacific Marine Environmental Laboratory, Seattle, WA, 125 pp. +appendices on CD.

González, F. I., Titov, V. V., Mofjeld, H. O., Venturato, A., Simmons, S.,Hansen, R., Combellick, R., Eisner, R., Hoirup, D., Yanagi, B., Yong, S., Darienzo, M., Priest, G., Crawford, G., and Walsh

T. (2005) Progress in NTHMP hazard assessment. *Nat. Hazards* 35, 89–110. Special Issue, US National Tsunami Hazard Mitigation Program. doi:10.1007/s11069-004-2406-0.

Greenslade, D. J. M. and Titov V. V. (2008). A comparison study of two numerical tsunami forecasting systems. *Pure Appl. Geophys.* 165(11-12), 1991?2001. doi: 10.1007/s00024-008-0413-x.

Greenslade D. J. M., Simanjuntak, M. A., Chittleborough, J., and Burbidge, D. (2007). A first-generation realtime tsunami forecasting system for the Australian region. *BMRC Research Report* No. 126, Bur. Met., Australia.

Kânoğlu, U., Hoto, O., Kalligeris, N., Flouri, E., Aydin, B., Moore, C. W., and Synolakis, C. E. (2012) Tsunami Propagation Database for the Mediterranean and Aegean Seas *AGU abstract* CONTROL ID: 1500513

Lim, E., Eakins, B.W., and Wigley, R. (2011), Coastal Relief Model of Southern Alaska: Procedures, Data Sources and Analysis, *NOAA Tech. Memo*, *NESDIS NGDC-43*, National Geophysical Data Center, Marine Geology and Geophysics Division Boulder, Colorado, USA 28 pp.

López, A. and Okal, E. A (2006) A seismological reassessment of the source of the 1946 Aleutian 'tsunami' earthquake. *Geophys. J. Int.* doi: 10.1111/j.1365-246X.2006.02899.x

Okada, Y. (1985) Surface deformation due to shear and tensile faults in a half-space, *B. Seismol. Soc. Am.*, 75, 1135–1154.

Percival, D. B., Arcas, D., Denbo, D. W., Eble, M. C., Gica, E., Mofjeld, H. O., Spillane, M. C., Tang, L., and Titov, V. V. (2009), Extracting tsunami source parameters via inversion of DART buoy data, *NOAA Tech. Memo. OAR PMEL-144*, Pacific Marine Environmental Laboratory, NOAA, Seattle, WA, 22 pp.

Spillane, M. C., Gica, E., Titov, V. V. and Mofjeld, H. O. (2008). Tsunameter network design for the U.S. DARTő arrays in the Pacific and Atlantic Oceans. *NOAA Tech. Memo.* PMEL-143, 165 pp.

Suleimani, E. N., Combellick, R. A., Marriott, D., Hansen, R. A., Venturato, A. J., and Newman, J. C. (2005). Tsunami Hazard Maps of the Homer and Seldovia Areas, Alaska. Report of Investigations 2005–2, Division of Geological & Geophysical Surveys, Department of Natural Resources, State of Alaska.

Synolakis, C. E., and Kânoğlu, U., (2009). Chapter 8 – Tsunami modelling: Development of benchmarked models. In: E. N. Bernard and A. R. Robinson (edited) *The Sea: Ideas and Observations on Progress in the Study of the Seas, Volume 15: Tsunamis*, Harvard University Press, Cambridge, MA, and London, U.K., 237–294.

Synolakis, C. E., Bernard, E., Titov, V., Kânoğlu, U., and González, F. (2008). Validation and verification of tsunami numerical models. *Pure Appl. Geophys*, 165, 2197–2228.

Synolakis, C. E., Bernard, E., Titov, V., Kânoğlu, U., and González, F. (2007): Standards, criteria, and procedures for NOAA evaluation of tsunami numerical models Tech. Memo. OAR PMEL-135, NOAA/Pacific Marine Environmental Laboratory, Seattle, WA, 55 pp.

Tang, L., Titov, V. V., Bernard, E., Wei, Y., Chamberlin, C., Newman, J. C., Mofjeld, H., Arcas, D., Eble, M., Moore, C., Uslu, B., Pells, C., Spillane, M. C., Wright, L. M., and Gica, E. (2012): Direct energy estimate of the 2011 Japan tsunami using deep-ocean pressure measurements. *J. Geophys. Res. Oceans*, 117, C08008. doi: 10.1029/2011JC007635

Tang L., Titov, V. V., and Chamberlin, C. D. (2009), Development, testing, and applications of site-specific tsunami inundation models for real-time forecasting, *J. Geophys. Res.*, C12025, doi: 10.1029/2009JC005476.

Tang, L., Chamberlin, C., and Titov, V. (2008a). Developing tsunami forecast inundation models for Hawaii: procedures and testing. Tech. Memo. OAR PMEL-141, NOAA.

Tang, L., Titov, V., Wei, Y., Mofjeld, H., Spillane, M., Arcas, D., Bernard, E., Chamberlin, C., Gica, E., and Newman, J. (2008b). Tsunami forecast analysis for the May 2006 Tonga tsunami. *J. Geophys. Res.*, 113, C12015, doi: 10.1029/2008JC004922.

Titov, V. V., Moore, C. W., Greenslade, D. J. M., Pattiaratchi, C., Badal, R., Synolakis, C. E, Kânoğlu, U. (2011) A new tool for inundation modeling: Community Modeling Interface for Tsunamis (ComMIT). *Pure Appl. Geophys.* 168, 2121s. doi: 10.1007/s00024-011-0292-4

Titov, V. V. (2009). Chapter 12 – Tsunami forecasting. In: E. N. Bernard and A. R. Robinson (edited) *The Sea: Ideas and Observations on Progress in the Study of the Seas, Volume 15: Tsunamis*, Harvard University Press, Cambridge, MA, and London, U.K., 371–400.

Titov, V. V., González, F. I., Bernard, E. N., Eble, M. C., Mofjeld, H. O., Newman, J. C., and Venturato, A. J. (2005a). Real-Time Tsunami Forecasting: Challenges and Solutions. *Natural Hazards*, 35(1):35–41 (41–58).

Titov, V. V., Rabinovich, A. B., Mofjeld, H. O., Thomson, R. E., and González, F. I. (2005b). The global reach of the 26 December 2004 Sumatra Tsunami. *Science*, 309:2045–2048.

Titov, V. V. and Synolakis, C. E. (1998). Numerical modelling of tidal wave runup. *J. Waterw. Port Coast. Ocean Eng.*, 124:157–171.

Titov, V. V. and González, F. (1997). Implementation and testing of the method of splitting tsunami (MOST) model. NOAA Tech. Memo. ERL PMEL-112 (PB98-122773), NOAA/Pacific Marine Environmental Laboratory, Seattle, WA, 11 pp. Technical Memorandum ERL PMEL 112, NOAA.

Titov, V. V. and Synolakis, C. E. (1997). Extreme inundation flows during the Hokkaido-Nansei-Oki tsunami. *Geophys. Res. Lett.*, 24(11):1315–1318.

Titov, V. V. (1997). Numerical modeling of long wave runup. *Ph.D. Thesis*, University of Southern California, Los Angeles, California, 90089-2531, 141 pp.

Titov, V. V. and Synolakis, C. E. (1995). Modeling of breaking and non-breaking long-wave evolution and runup using VTCS-2. *J. Waterw. Port C-ASCE*, 121, 308–316. doi: 10.1061/(ASCE)0733- 950X(1995)121:6(308)

Tsunami Pilot Study Working Group (2006) Seaside, Oregon Tsunami Pilot Study: Modernization of FEMA flood hazard maps NOAA/OAR Special Report, NOAA/OAR/PMEL, Seattle, Washington, 94 pp. + 7 appendices.

Uslu, B., Eble, M., Arcas, D., and Titov, V. (2013). Tsunami Hazard Assessment for the Commonwealth of the Northern Mariana Islands, *Tsunami Hazard Assessment Special Series, NOAA OAR Special Report*, V. 3, 188 pp.

Uslu, B., Eble, M., Titov, V., and Bernard, E. (2010a). Distant tsunami threats to the ports of Los Angeles and Long Beach, California, *Tsunami Hazard Assessment Special Series, NOAA OAR Special Report*, V. 2, 100 pp.

Uslu, B., Eble, M., and Chamberlin, C. (2010b). Tsunami Hazard Assessment for Guam, *Tsunami Hazard Assessment Special Series, NOAA OAR Special Report*, V. 1, 186 pp.

Uslu, B. (2008). *Deterministic and Probabilistic tsunami studies in California from near and farfield sources.* PhD thesis, University of Southern California, Los Angeles, California.

Wei, Y., Chamberlin, C., Titov, V. V. , Tang, L., Bernard, E. N. (2013) Modeling of the 2011 Japan tsunami: lessons for near-field forecast. *Pure Appl. Geophys.* doi:10.1007/s00024-012-0519-z

Wei, Y., Bernard, E. N., Tang, L., Weiss, R., Titov, V. V., Moore, C., Spillane, M., Hopkins, M., and Kânoğlu, U. (2008). Real-time experimental forecast of the Peruvian tsunami of August 2007 for U.S. coastlines. *Geophys. Res. Let.*, *35*, L04609, doi: 10.1029/2007GL032250.

Zhou, H., Wei, Y., and Titov, V. V. (2012), Dispersive modeling of the 2009 Samoa tsunami, *Geophys. Res. Lett.*, *39*(16), L16603, doi:1029/2012GL053068.

Liu, P. L.-F., Synolakis, C. E., and Yeh, H. H. (2012), Report on the International Workshop on long-wave run-up, *J. Fluid Mech.*, *229*, 675–688, doi: 10.1017/S0022112091003221.

Figures

(a)

(b)

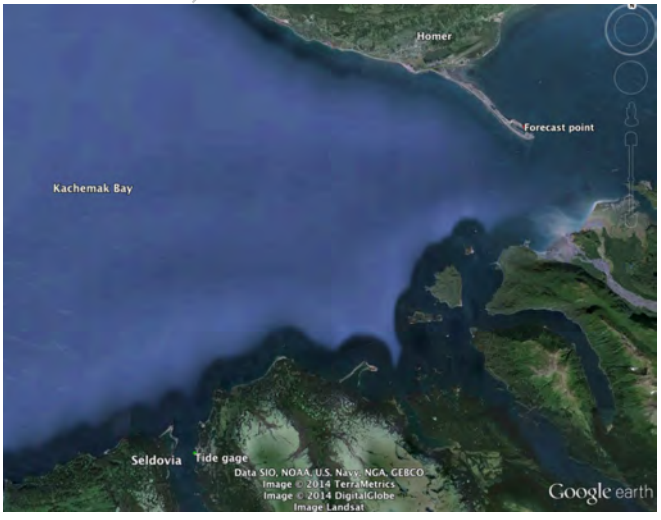

Figure 1: An aerial Google Earth image of (a) the forecasting area and (b) close up view. The red and green circles show locations of forecast point at Homer, Alaska ($59°36.35'N$, $151°25.08'W$) and tide gage location (station ID: 9455500) in Seldovia ($59°26.40'N$, $151°43.20'W$) respectively.

(a)

(b)

Figure 2: An aerial Google Earth image of (a) Homer (b) Seldovia. The red and green circles show locations of forecast point at Homer, Alaska ($59°36.35'N$, $151°25.08'W$) and tide gage location (station ID: 9455500) in Seldovia ($59°26.40'N$, $151°43.20'W$) respectively.

(a)

(b)

Figure 3: (a) Aerial photograph and (b) close up view showing the Homer Spit. (Wikipedia Commons http://en.wikipedia.org/wiki/Homer_Spit).

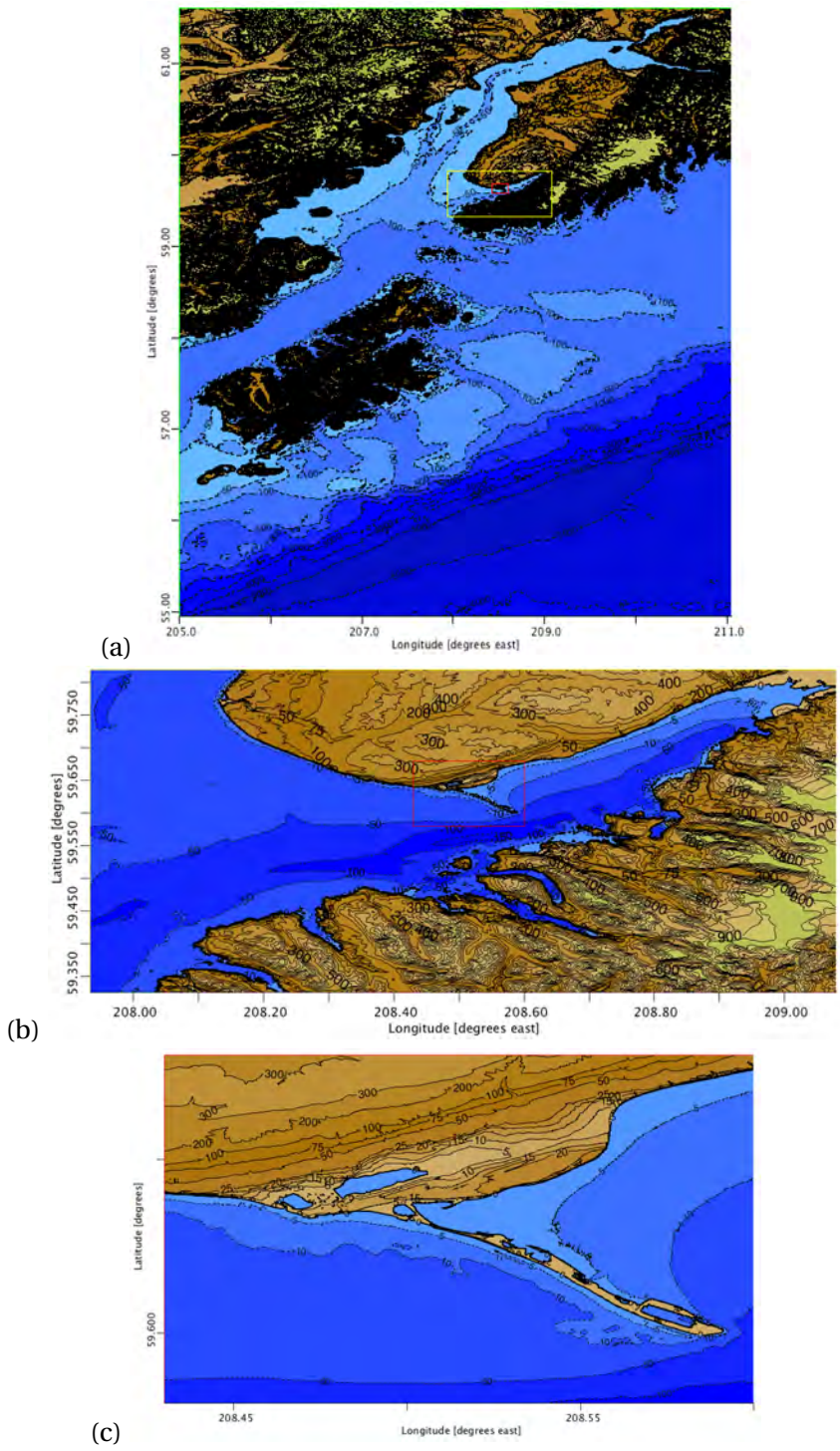

Figure 4: Extent of Homer, Alaska RM grids: (a) A-grid, (b) B-grid, (c) C-grid. Yellow and red rectangles in insets show B-grid and C-grid extensions respectively. Grid extents, resolutions and sources are summarized in Table 1.

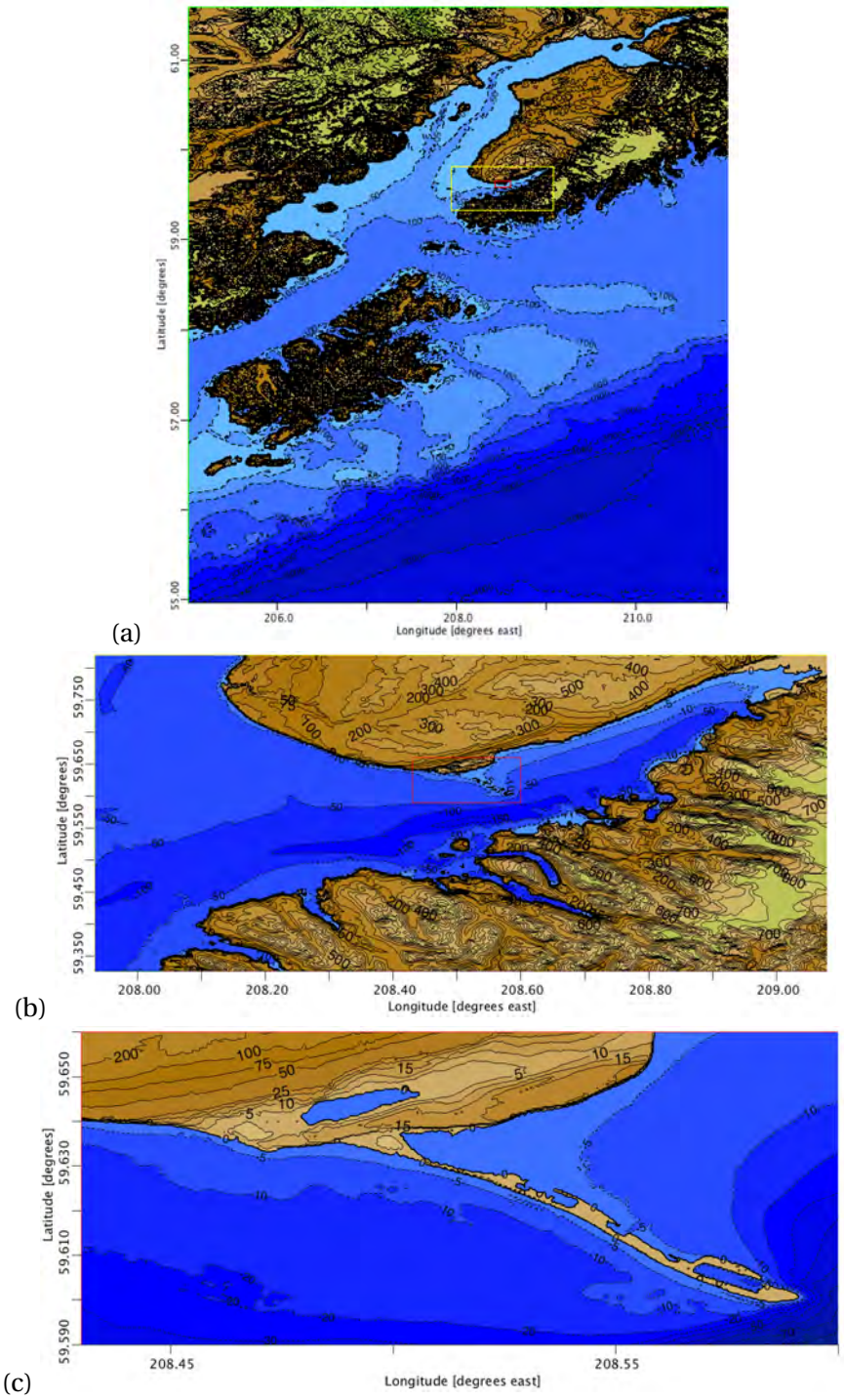

Figure 5: Extent of Homer, Alaska FM grids: (a) A-grid, (b) B-grid, and (c) C-grid. Yellow and red rectangles in insets show B-grid and C-grid extensions respectively. Grid extents, resolutions and sources are summarized in Table 1.

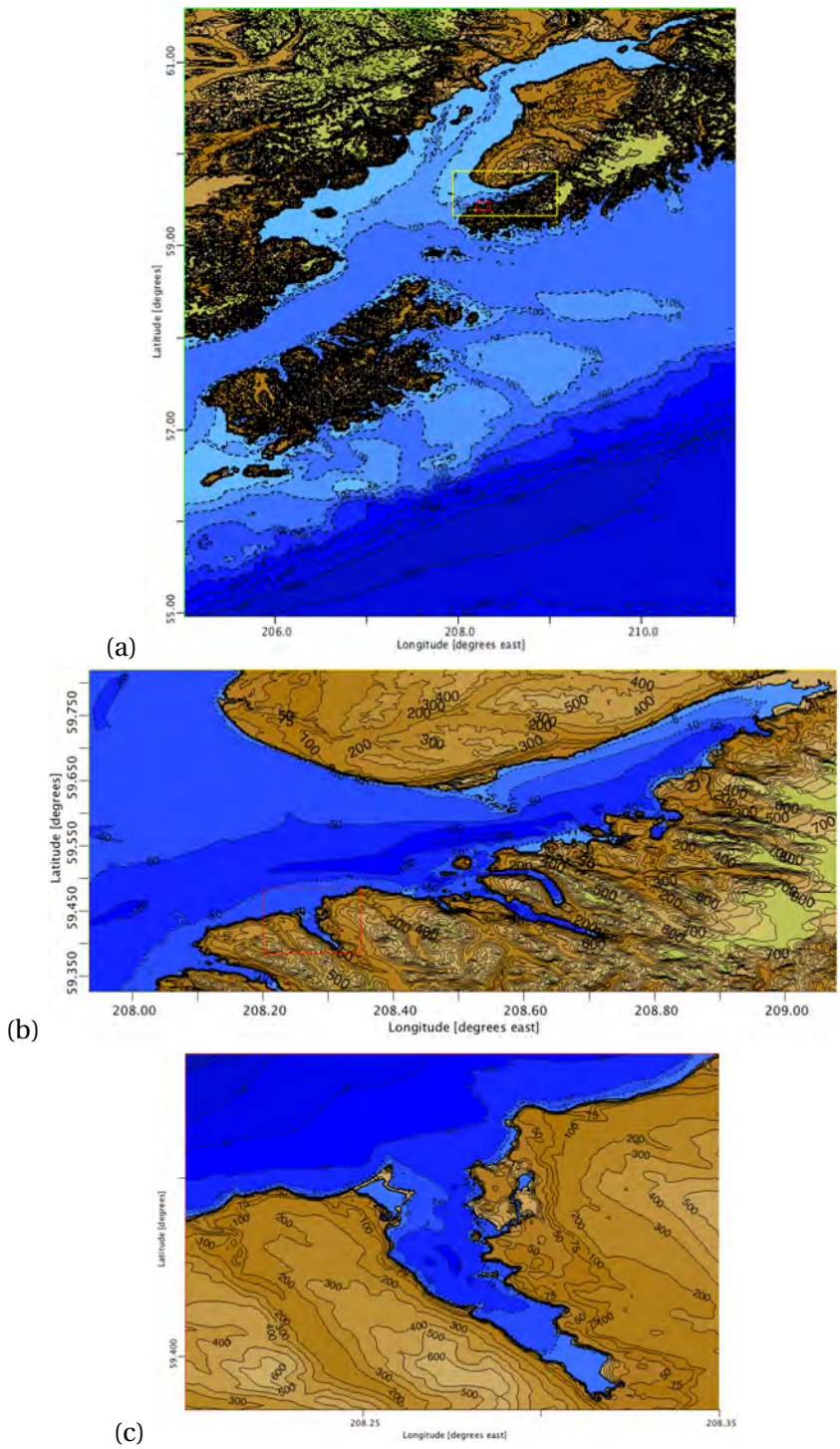

Figure 6: Extent of Seldovia, Alaska FM grids: (a) A-grid, (b) B-grid, (c) C-grid. Yellow and red rectangles in insets show B-grid and C-grid extensions respectively. Seldovia model employs the same A- and B-grids with Homer, Alaska. Grid extents, resolutions and sources used for Seldovia, Alaska FM grids are summarized in Table 1.

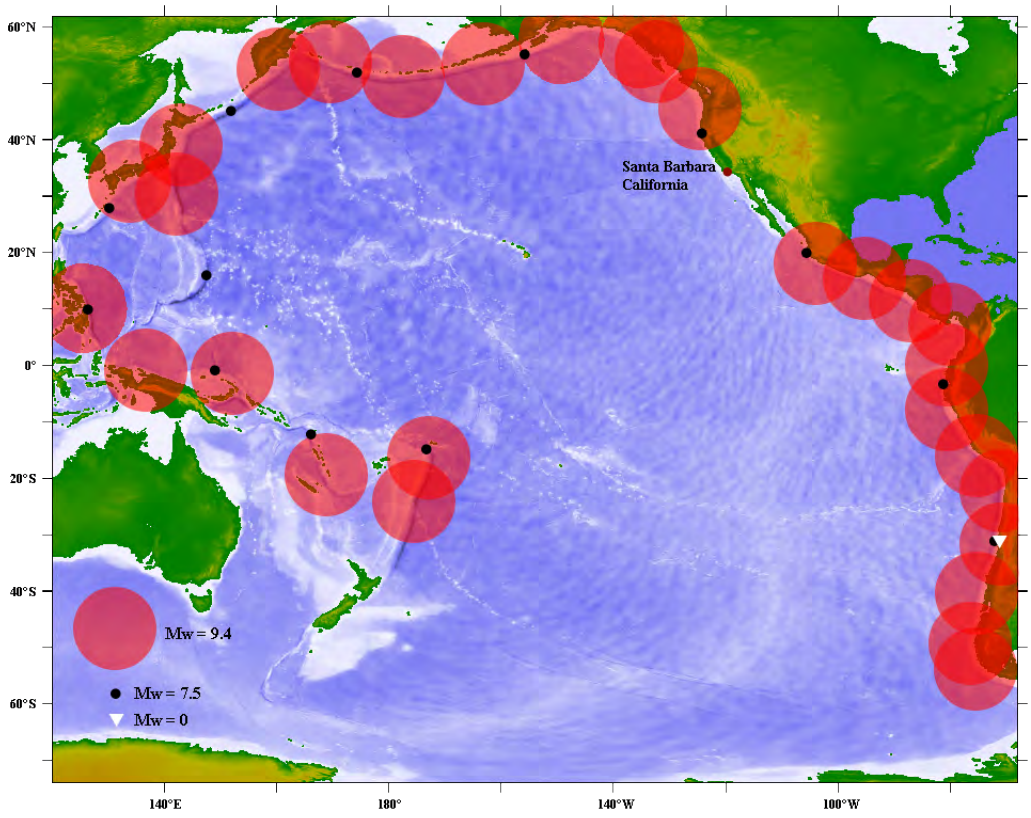

Figure 7: Location maps of synthetic scenarios listed in Table 2 and used in testing the numerical stability and robustness of the Homer, Alaska RM and FM (courtesy of Dr. Edison Gica).

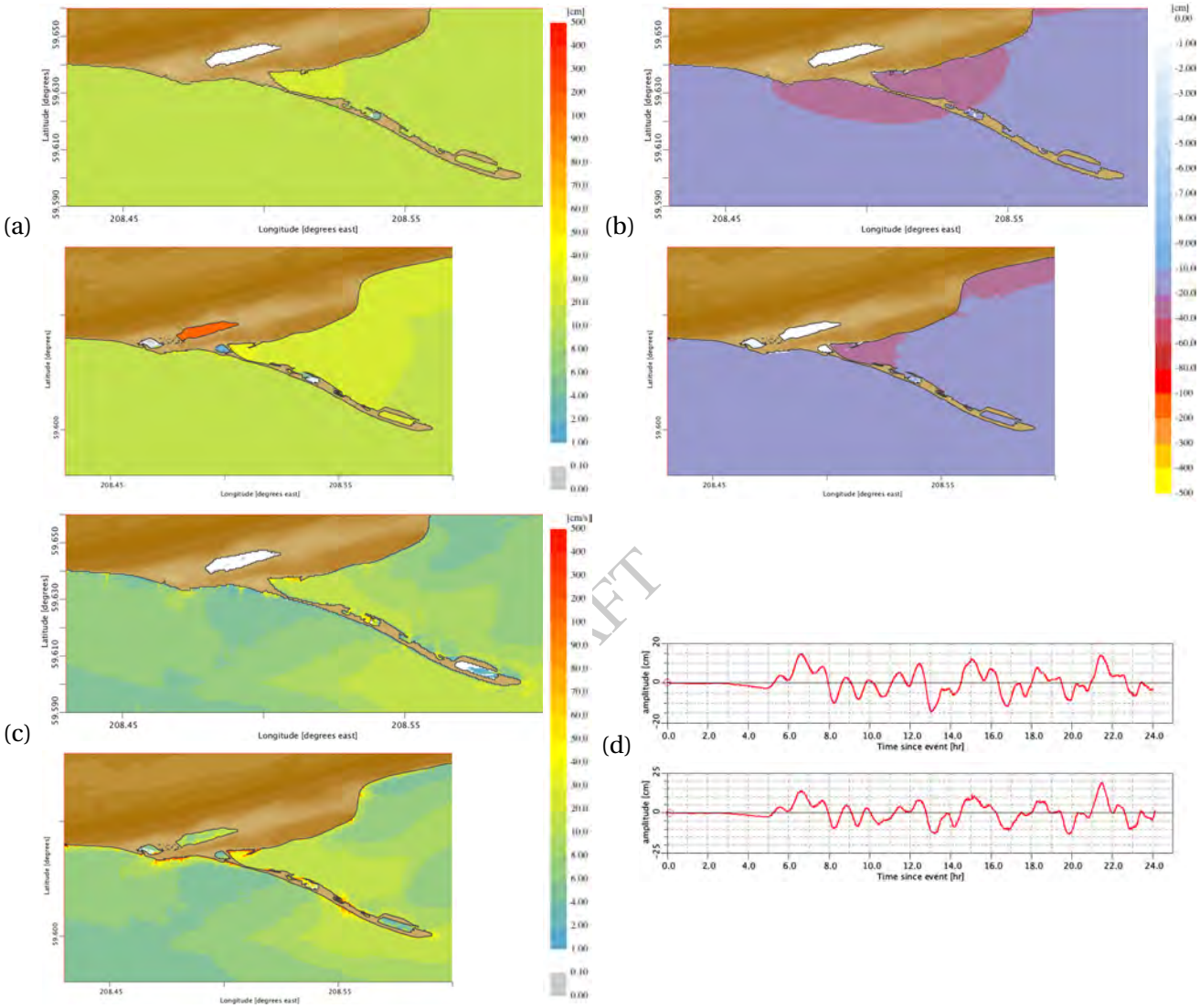

Figure 8: Comparisons for the FM (top insets) and the RM (bottom insets) C-grid results for the magnitude 9.3 synthetic scenario event with the source segment 6–15 on Aleutian–Alaska–Cascadia Subduction Zone (ACSZ) (Figure B.1, Table B.1). (a) Maximum and (b) minimum sea surface elevations, (c) maximum wave speeds at each C-grid point and (d) time histories of water surface elevations at the Homer forecast point.

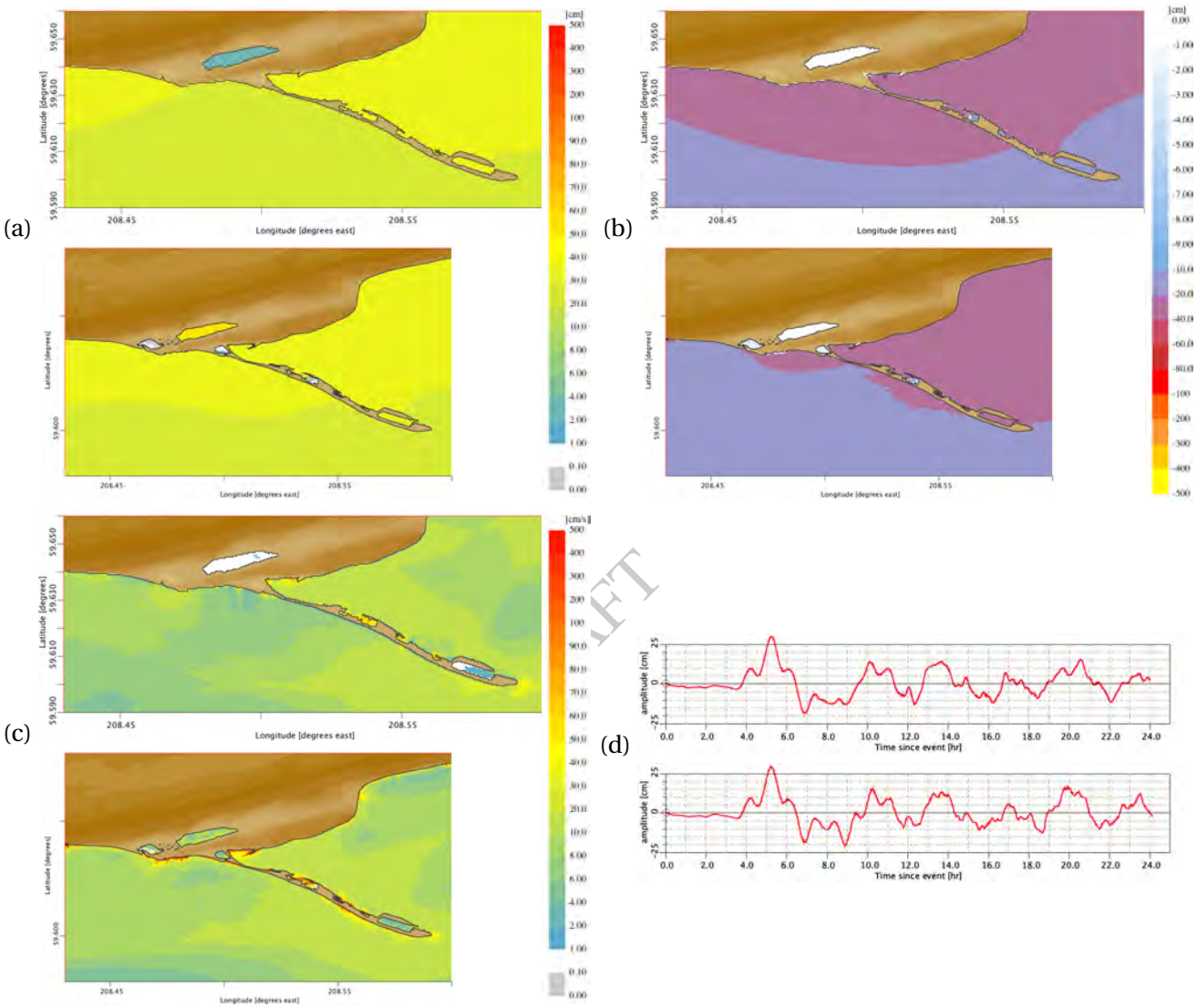

Figure 9: Comparisons for the FM (top insets) and the RM (bottom insets) C-grid results for the magnitude 9.3 synthetic scenario event with the source segment 16–25 on Aleutian–Alaska–Cascadia Subduction Zone (ACSZ) (Figure B.1, Table B.1). (a) Maximum and (b) minimum sea surface elevations, (c) maximum wave speeds at each C-grid point and (d) time histories of water surface elevations at the Homer forecast point.

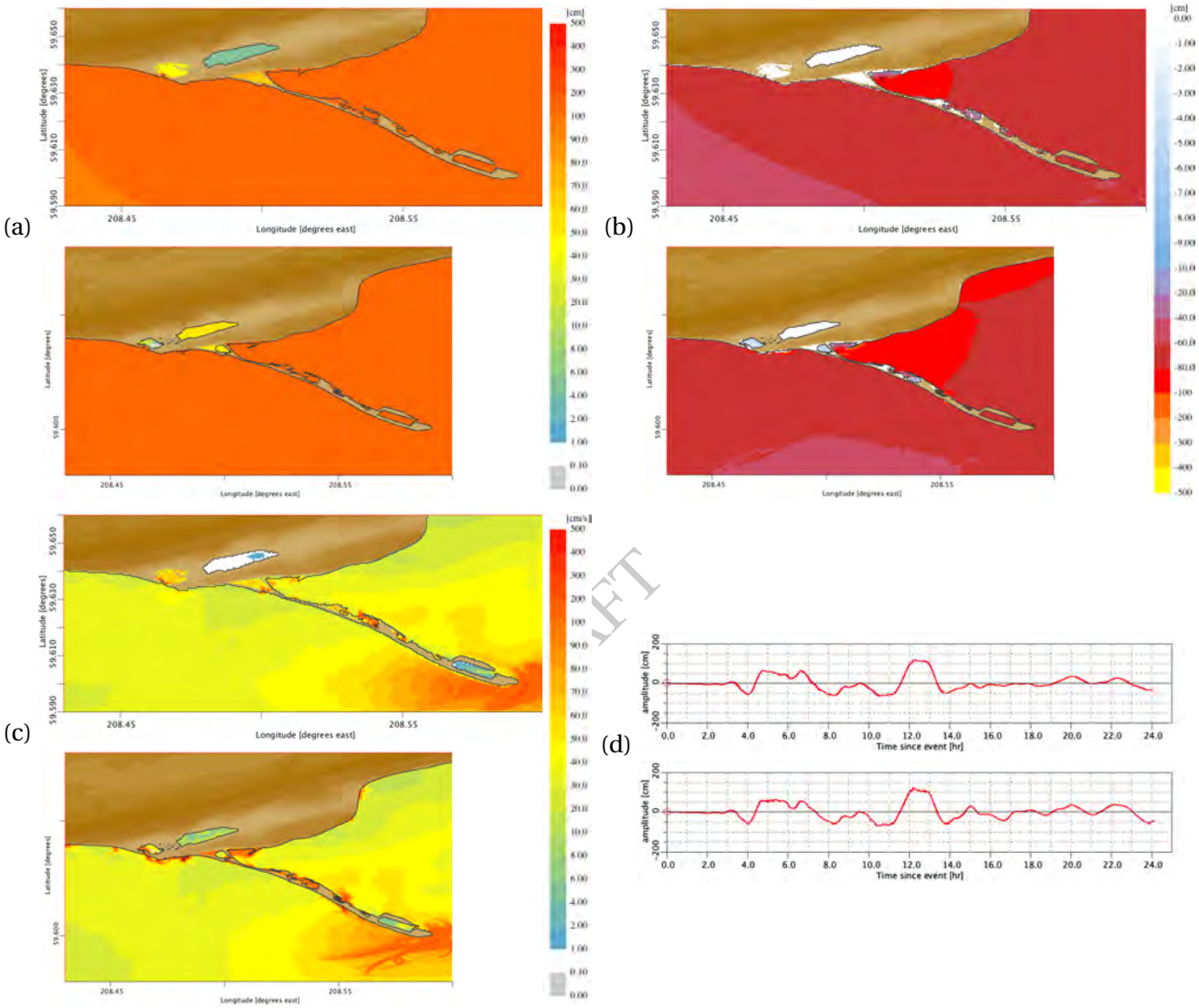

Figure 10: Comparisons for the FM (top insets) and the RM (bottom insets) C-grid results for the magnitude 9.3 synthetic scenario event with the source segment 22–31 on Aleutian–Alaska–Cascadia Subduction Zone (ACSZ) (Figure B.1, Table B.1). (a) Maximum and (b) minimum sea surface elevations, (c) maximum wave speeds at each C-grid point and (d) time histories of water surface elevations at the Homer forecast point.

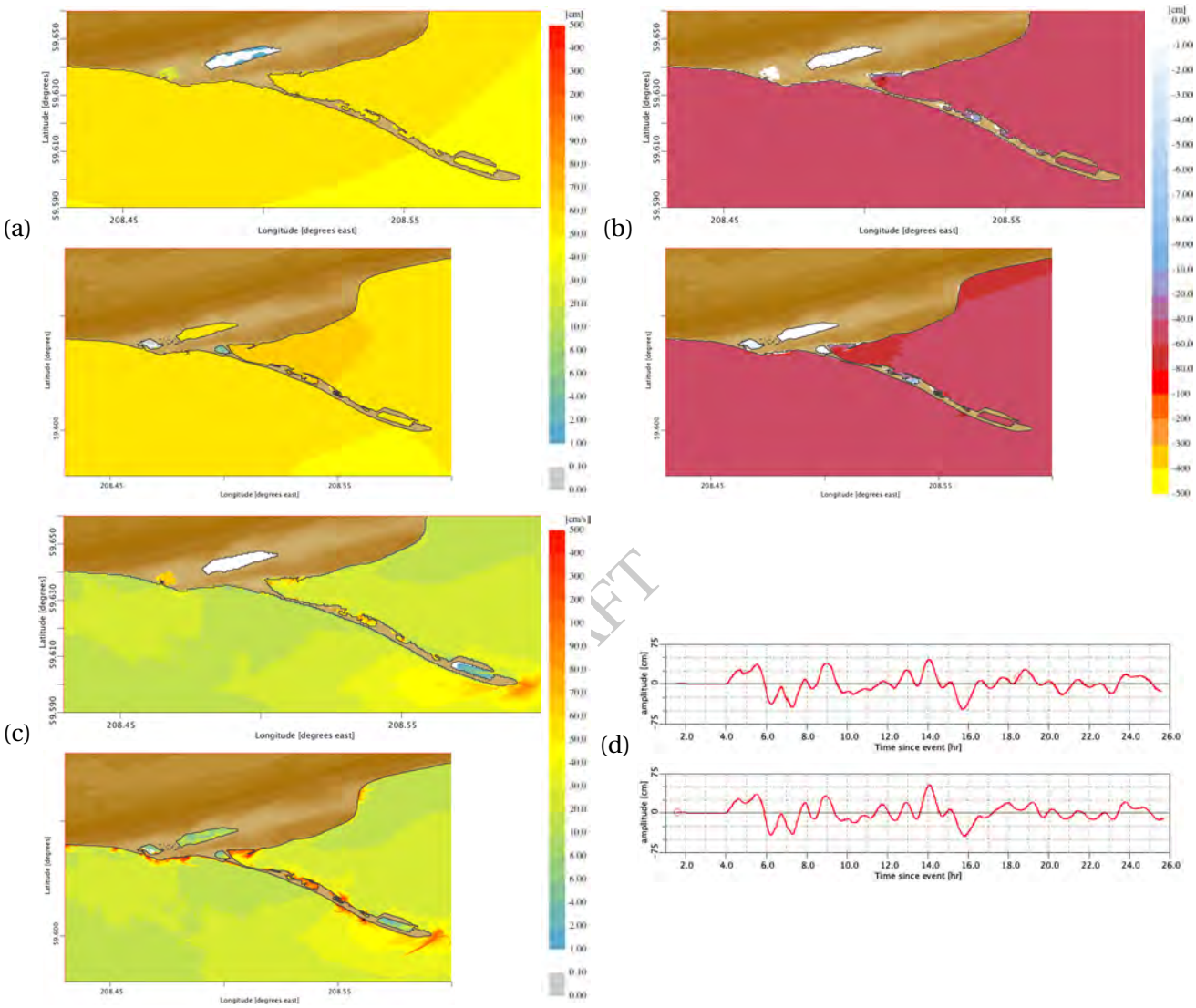

Figure 11: Comparisons for the FM (top insets) and the RM (bottom insets) C-grid results for the magnitude 9.3 synthetic scenario event with the source segment 50–59 on Aleutian–Alaska–Cascadia Subduction Zone (ACSZ) (Figure B.1, Table B.1). (a) Maximum and (b) minimum sea surface elevations, (c) maximum wave speeds at each C-grid point and (d) time histories of water surface elevations at the Homer forecast point.

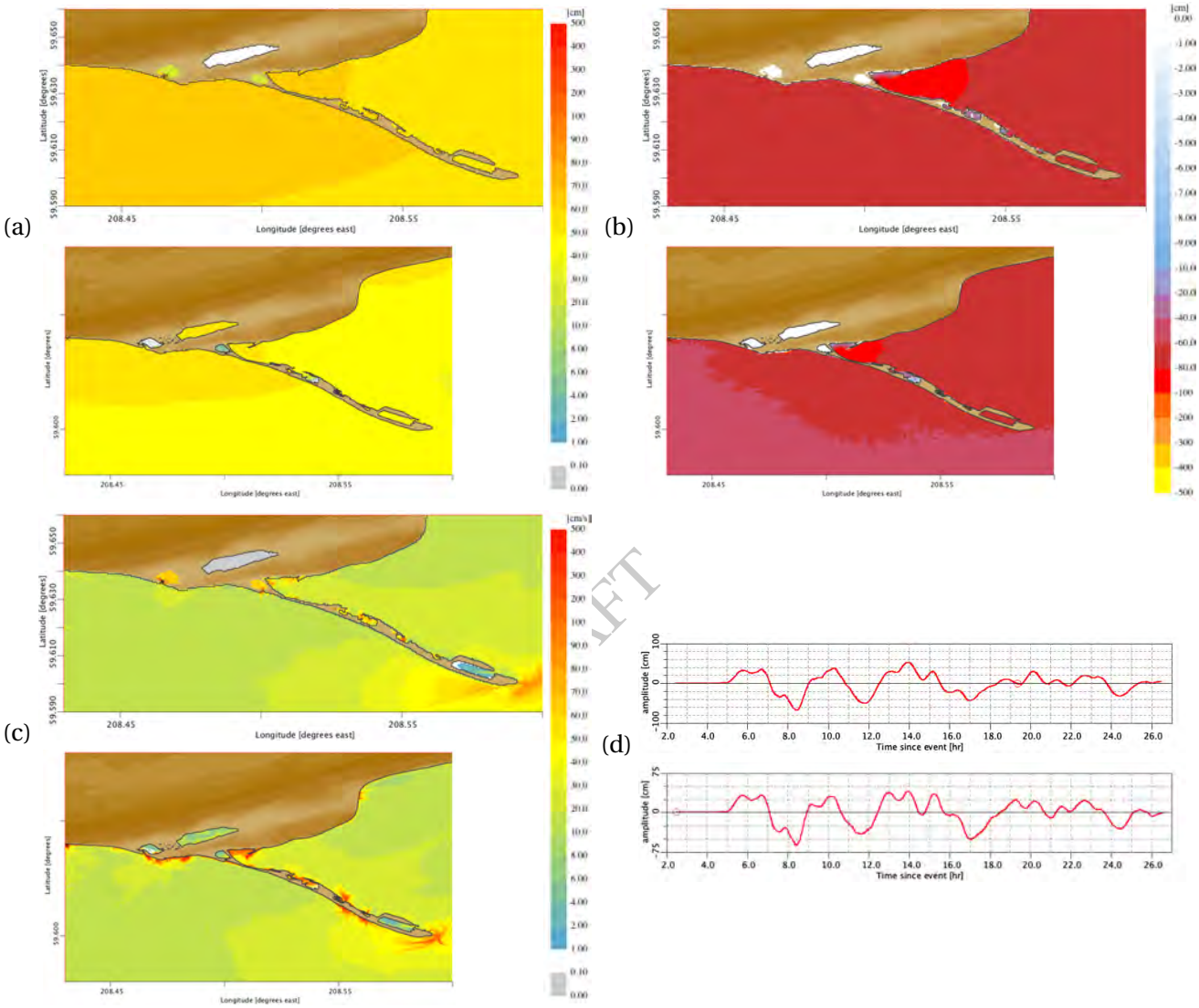

Figure 12: Comparisons for the FM (top insets) and the RM (bottom insets) C-grid results for the magnitude 9.3 synthetic scenario event with the source segment 56–65 on Aleutian–Alaska–Cascadia Subduction Zone (ACSZ) (Figure B.1, Table B.1). (a) Maximum and (b) minimum sea surface elevations, (c) maximum wave speeds at each C-grid point and (d) time histories of water surface elevations at the Homer forecast point.

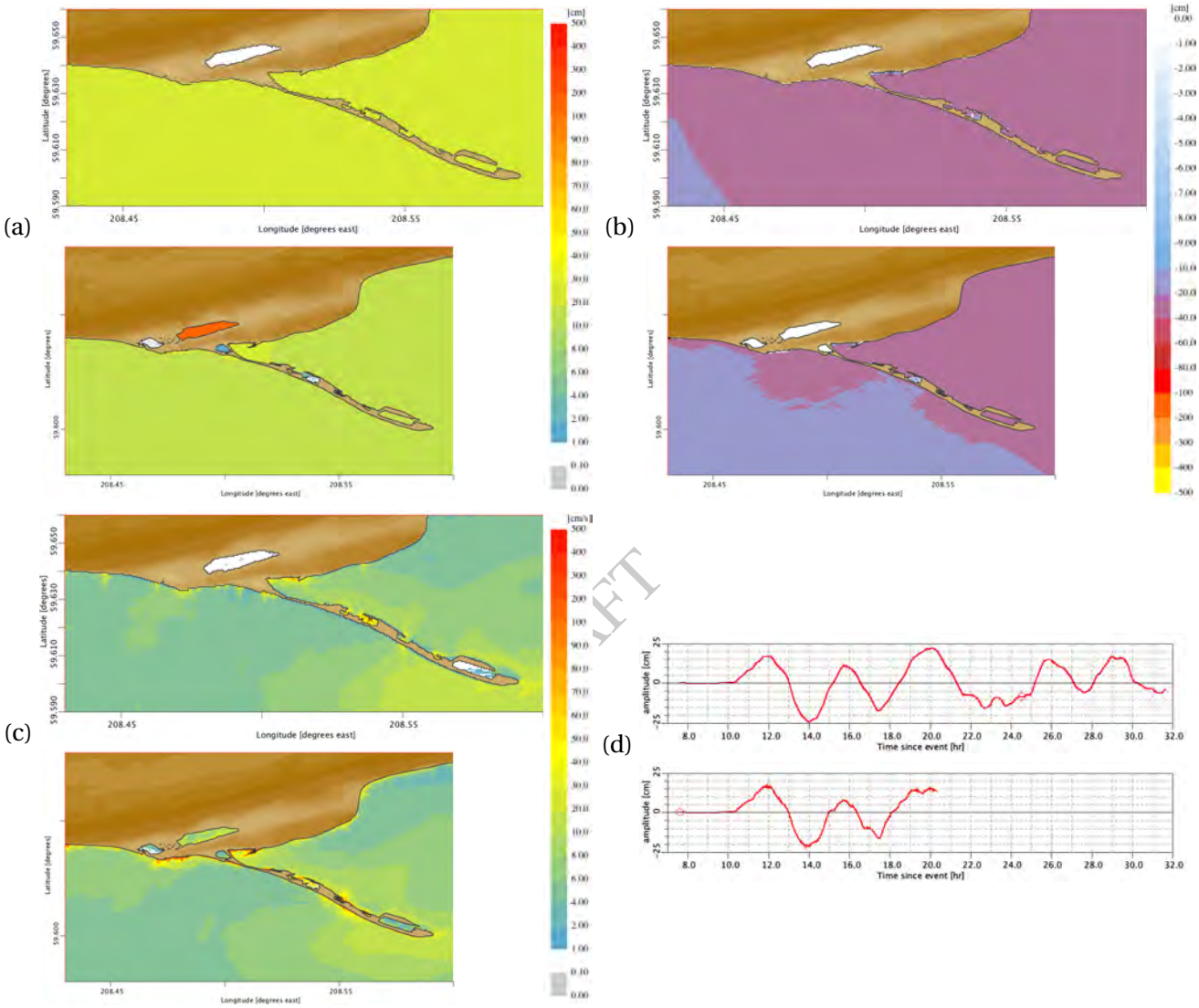

Figure 13: Comparisons for the FM (top insets) and the RM (bottom insets) C-grid results for the magnitude 9.3 synthetic scenario event with the source segment 1–10 on Central and South America Subduction Zone (CSSZ) (Figure B.2, Table B.2). (a) Maximum and (b) minimum sea surface elevations, (c) maximum wave speeds at each C-grid point and (d) time histories of water surface elevations at the Homer forecast point.

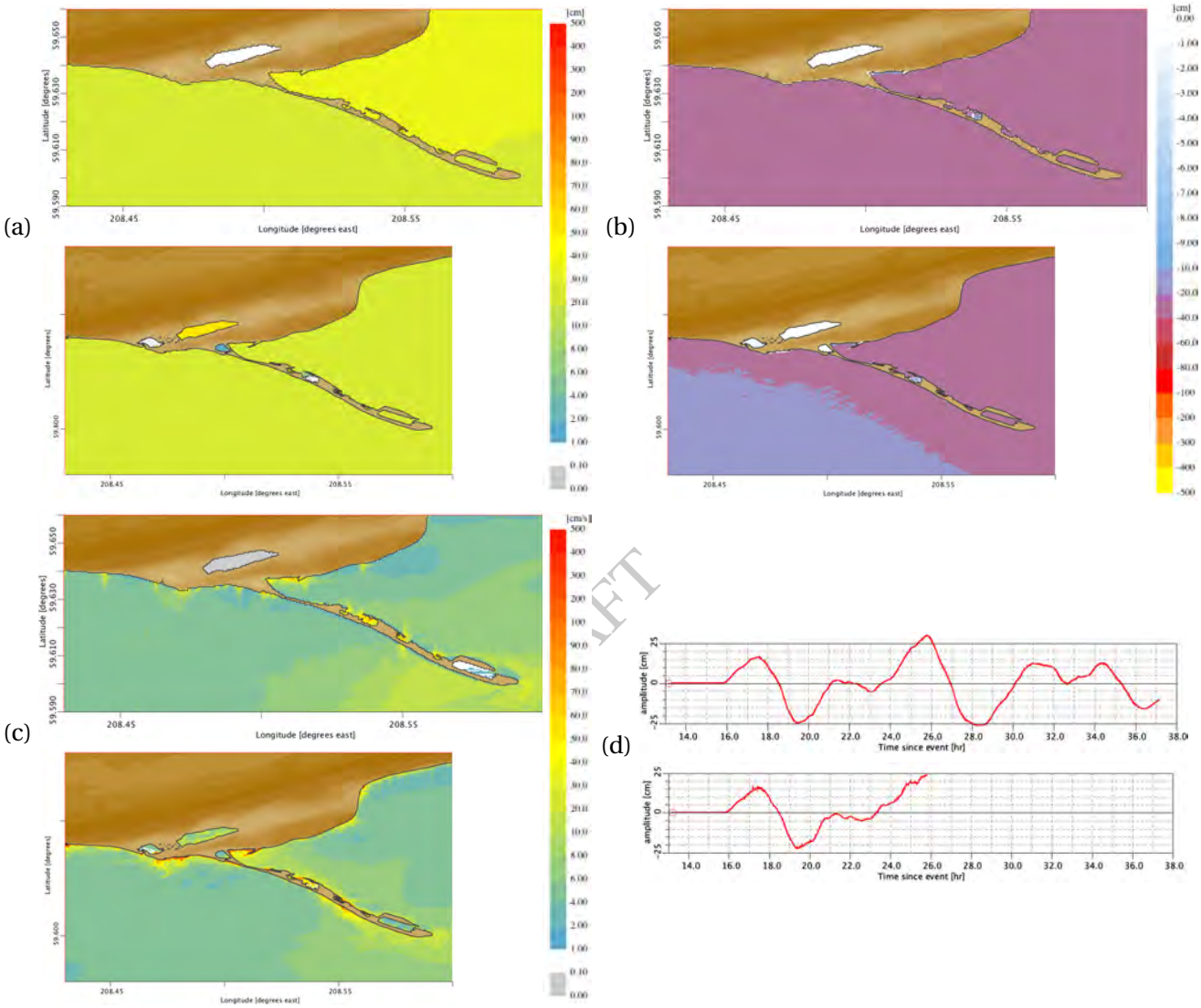

Figure 14: Comparisons for the FM (top insets) and the RM (bottom insets) C-grid results for the magnitude 9.3 synthetic scenario event with the source segment 37–46 on Central and South America Subduction Zone (CSSZ) (Figure B.2, Table B.2). (a) Maximum and (b) minimum sea surface elevations, (c) maximum wave speeds at each C-grid point and (d) time histories of water surface elevations at the Homer forecast point.

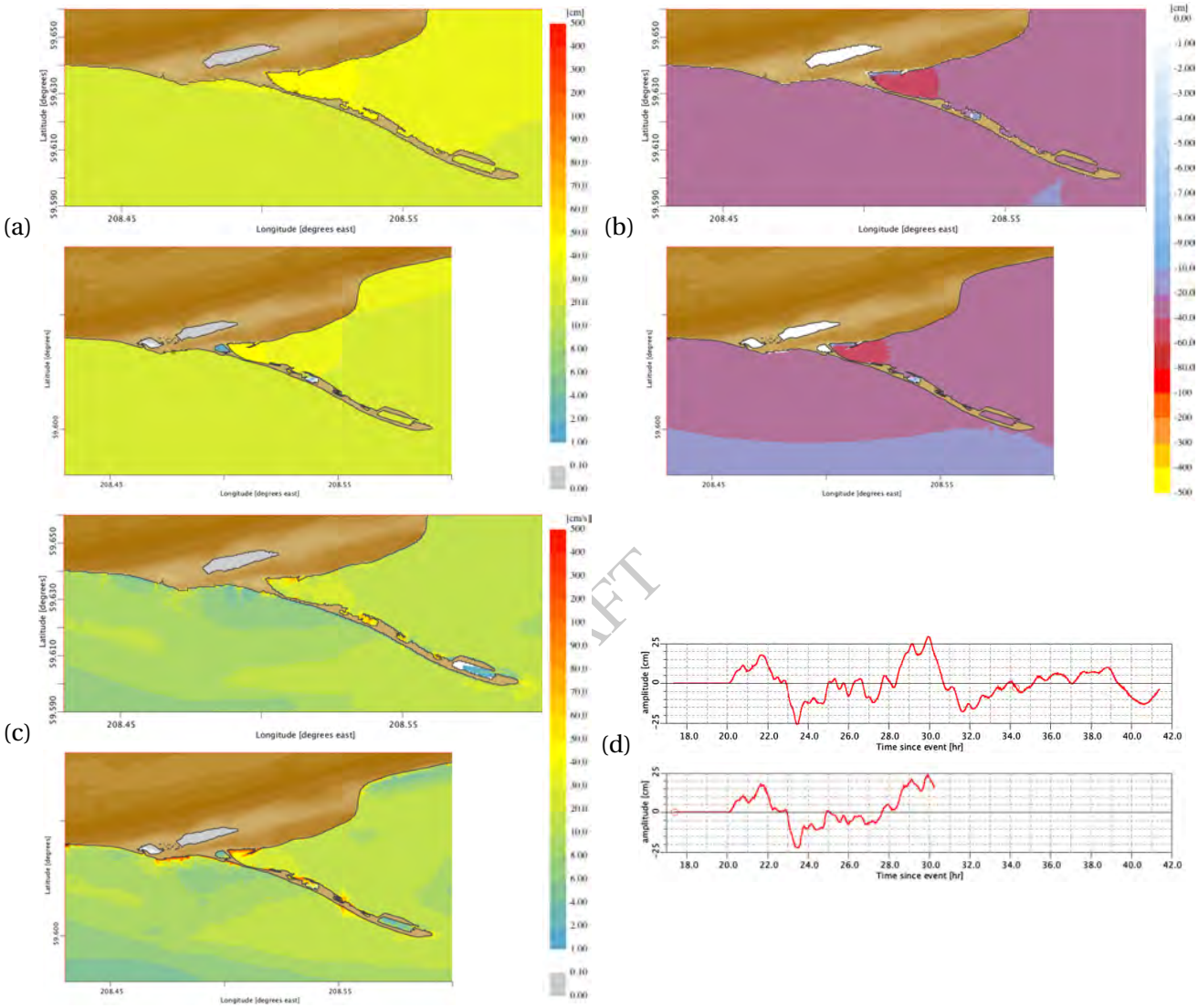

Figure 15: Comparisons for the FM (top insets) and the RM (bottom insets) C-grid results for the magnitude 9.3 synthetic scenario event with the source segment 89–98 on Central and South America Subduction Zone (CSSZ) (Figure B.2, Table B.2). (a) Maximum and (b) minimum sea surface elevations, (c) maximum wave speeds at each C-grid point and (d) time histories of water surface elevations at the Homer forecast point.

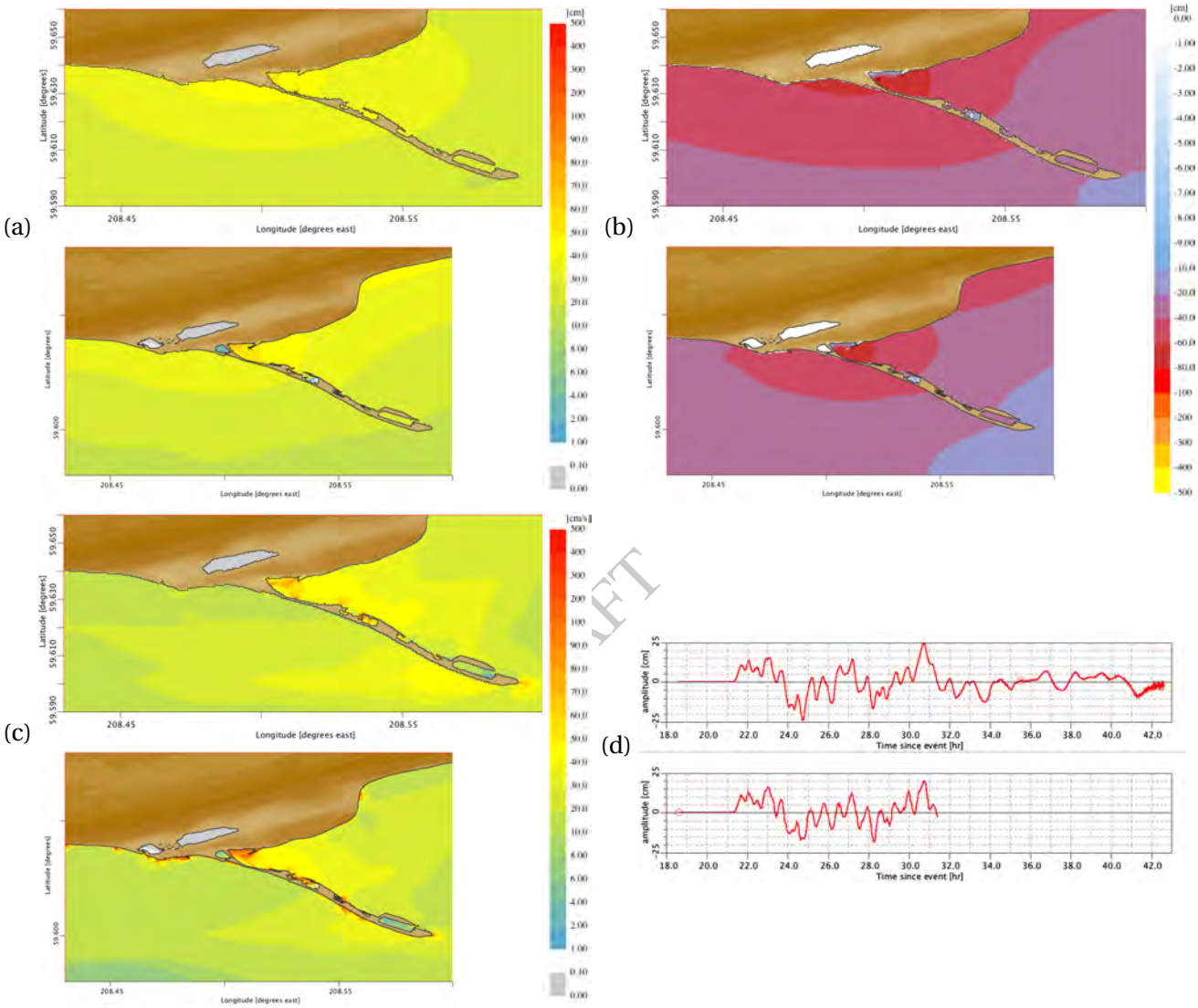

Figure 16: Comparisons for the FM (top insets) and the RM (bottom insets) C-grid results for the magnitude 9.3 synthetic scenario event with the source segment 102–111 on Central and South America Subduction Zone (CSSZ) (Figure B.2, Table B.2). (a) Maximum and (b) minimum sea surface elevations, (c) maximum wave speeds at each C-grid point and (d) time histories of water surface elevations at the Homer forecast point.

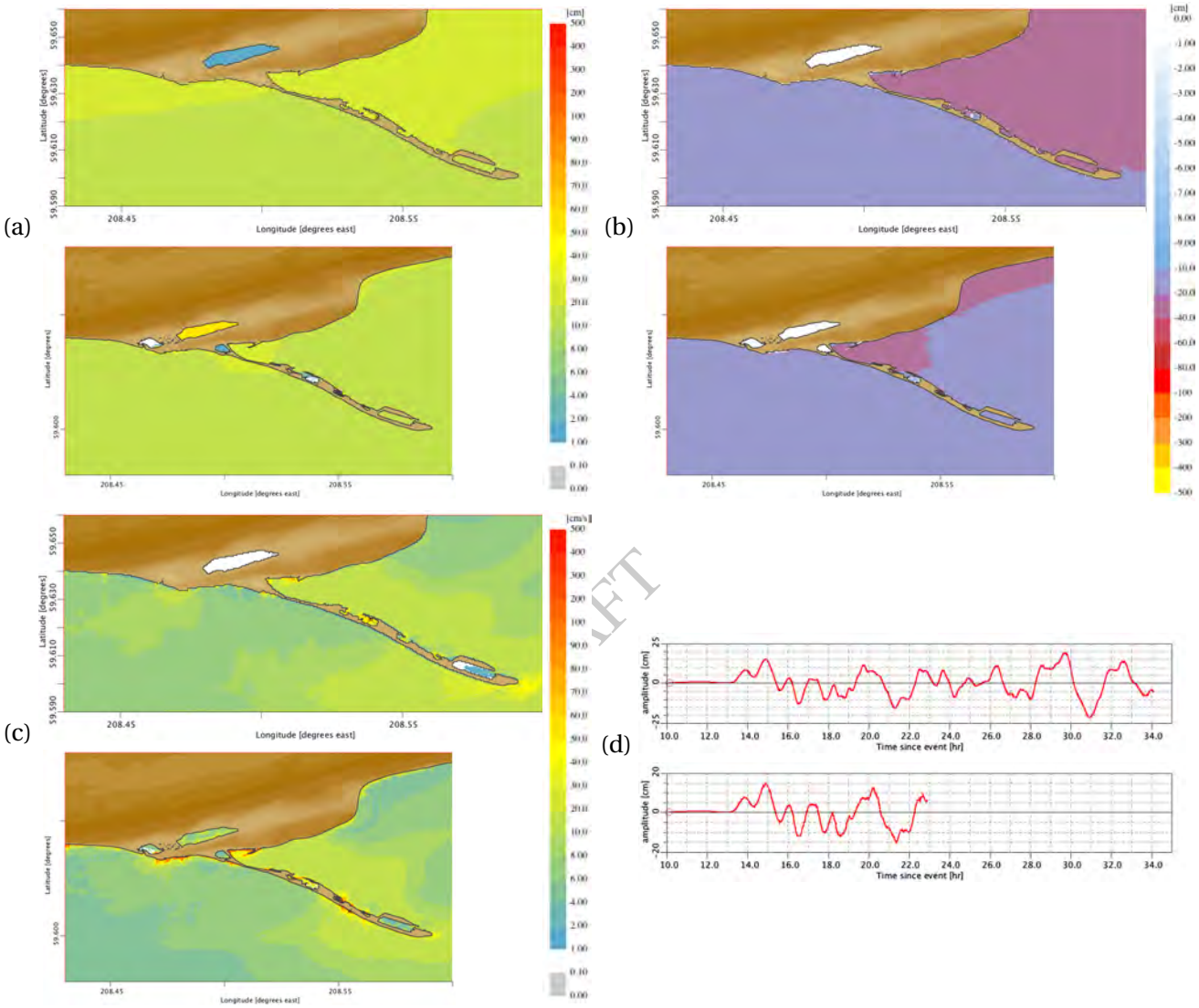

Figure 17: Comparisons for the FM (top insets) and the RM (bottom insets) C-grid results for the magnitude 9.3 synthetic scenario event with the source segment 6–15 on Eastern Philippines Subduction Zone (EPSZ) (Figure B.3, Table B.3). (a) Maximum and (b) minimum sea surface elevations, (c) maximum wave speeds at each C-grid point and (d) time histories of water surface elevations at the Homer forecast point.

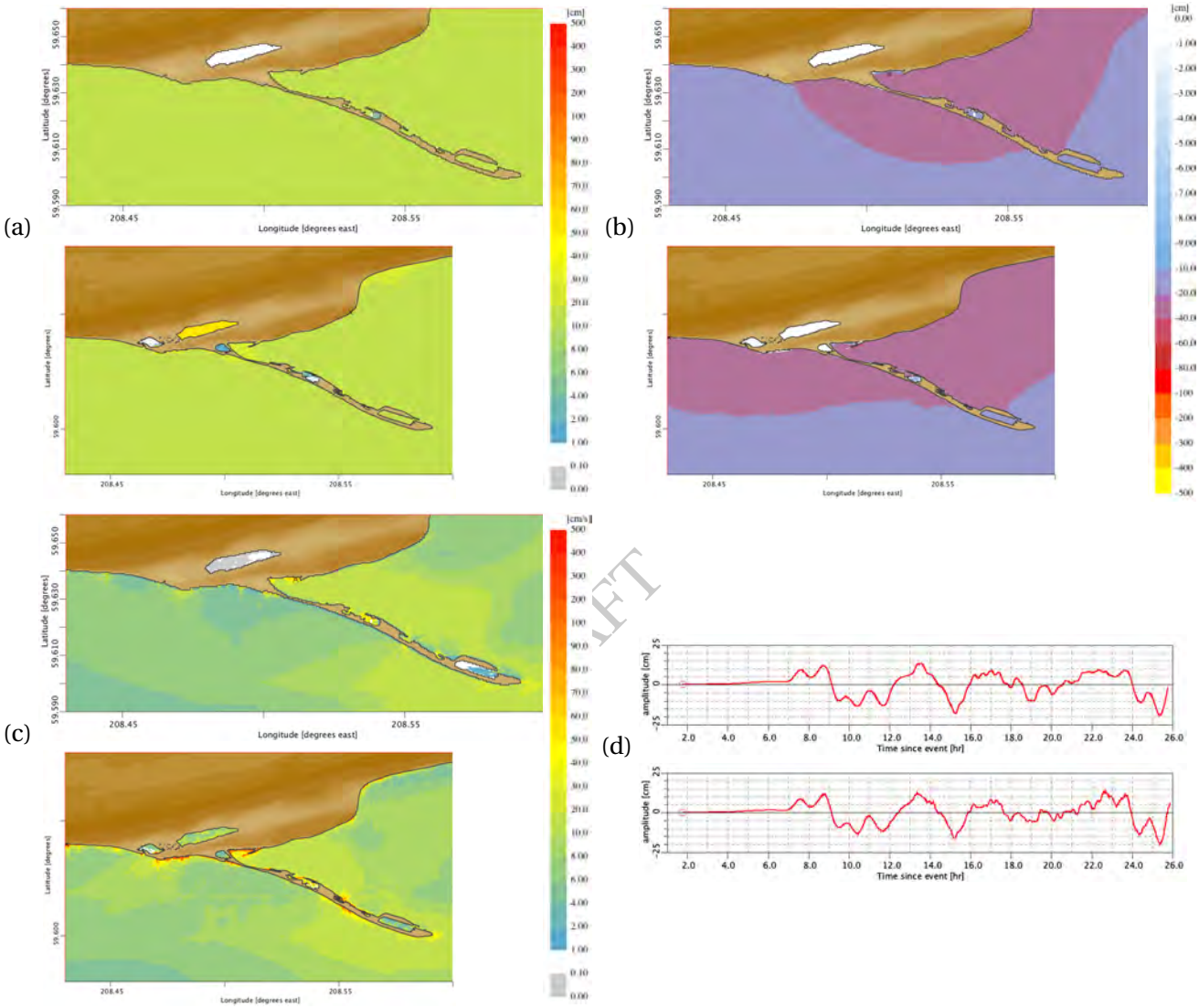

Figure 18: Comparisons for the FM (top insets) and the RM (bottom insets) C-grid results for the magnitude 9.3 synthetic scenario event with the source segment 1–10 on Kamchatka–Yap–Mariana–Izu–Bonin Subduction Zone (KISZ) (Figure B.5, Table B.5). (a) Maximum and (b) minimum sea surface elevations, (c) maximum wave speeds at each C-grid point and (d) time histories of water surface elevations at the Homer forecast point.

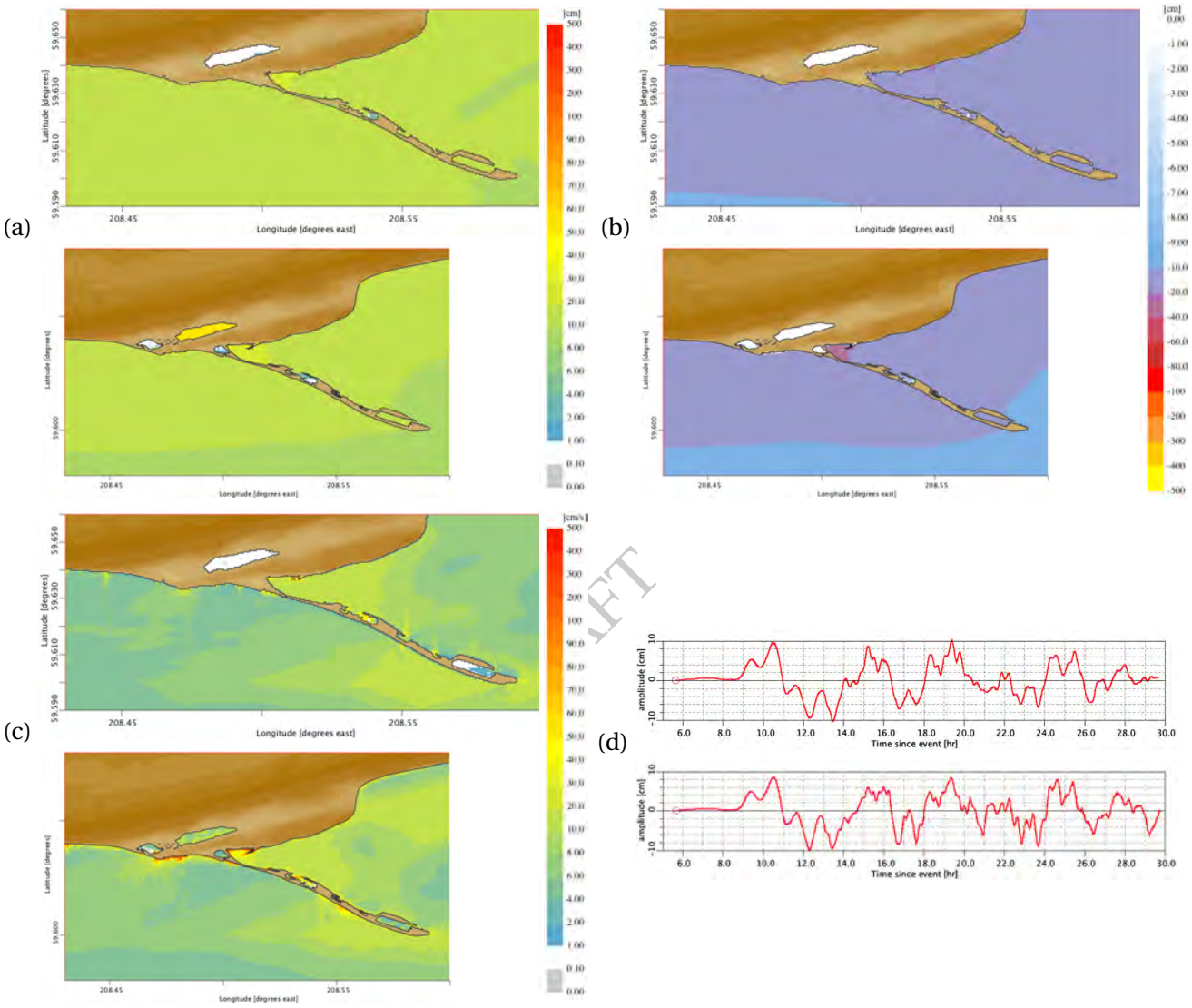

Figure 19: Comparisons for the FM (top insets) and the RM (bottom insets) C-grid results for the magnitude 9.3 synthetic scenario event with the source segment 22–31 on Kamchatka–Yap–Mariana–Izu–Bonin Subduction Zone (KISZ) (Figure B.5, Table B.5). (a) Maximum and (b) minimum sea surface elevations, (c) maximum wave speeds at each C-grid point and (d) time histories of water surface elevations at the Homer forecast point.

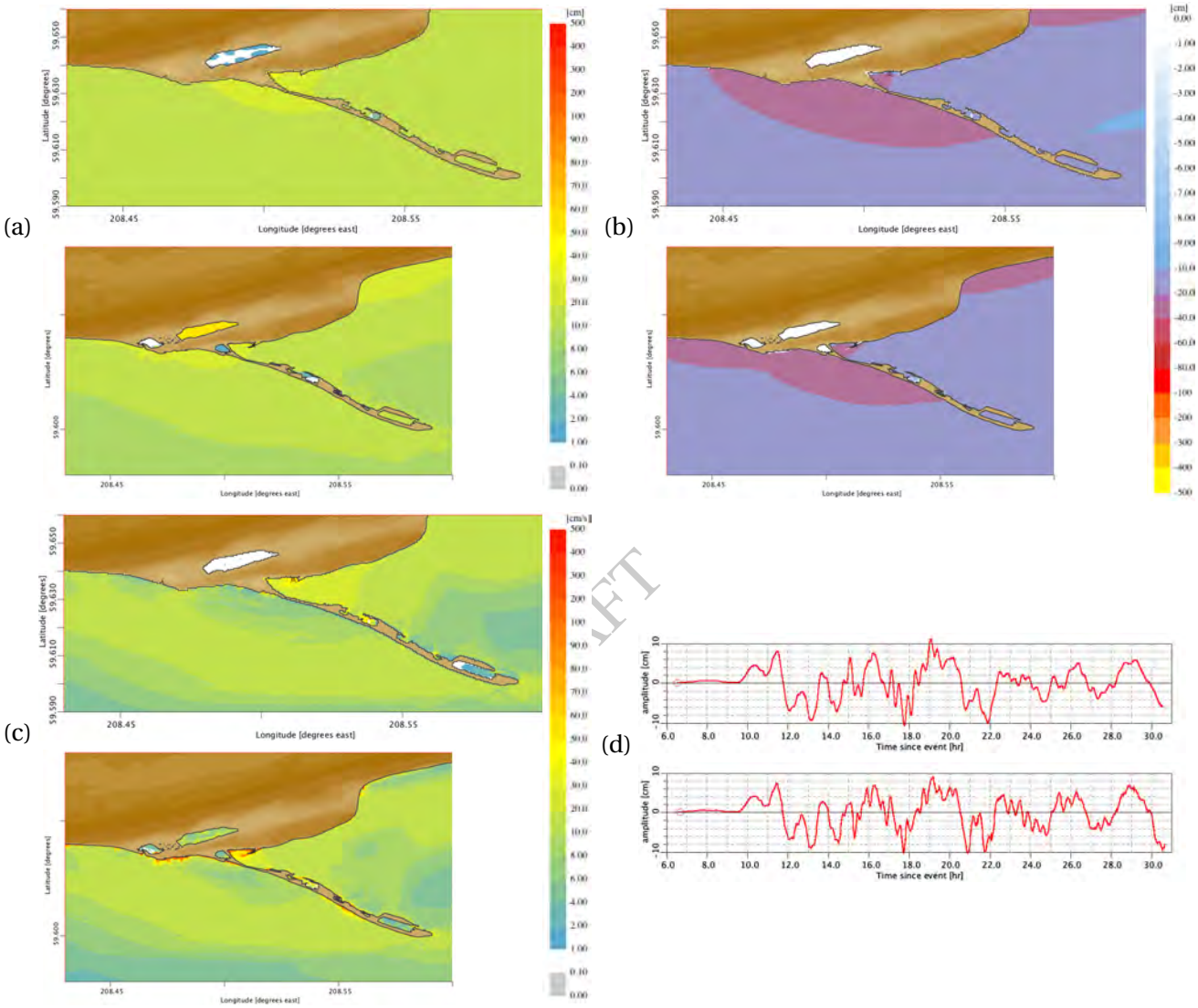

Figure 20: Comparisons for the FM (top insets) and the RM (bottom insets) C-grid results for the magnitude 9.3 synthetic scenario event with the source segment 32–41 on Kamchatka–Yap–Mariana–Izu–Bonin Subduction Zone (KISZ) (Figure B.5, Table B.5). (a) Maximum and (b) minimum sea surface elevations, (c) maximum wave speeds at each C-grid point and (d) time histories of water surface elevations at the Homer forecast point.

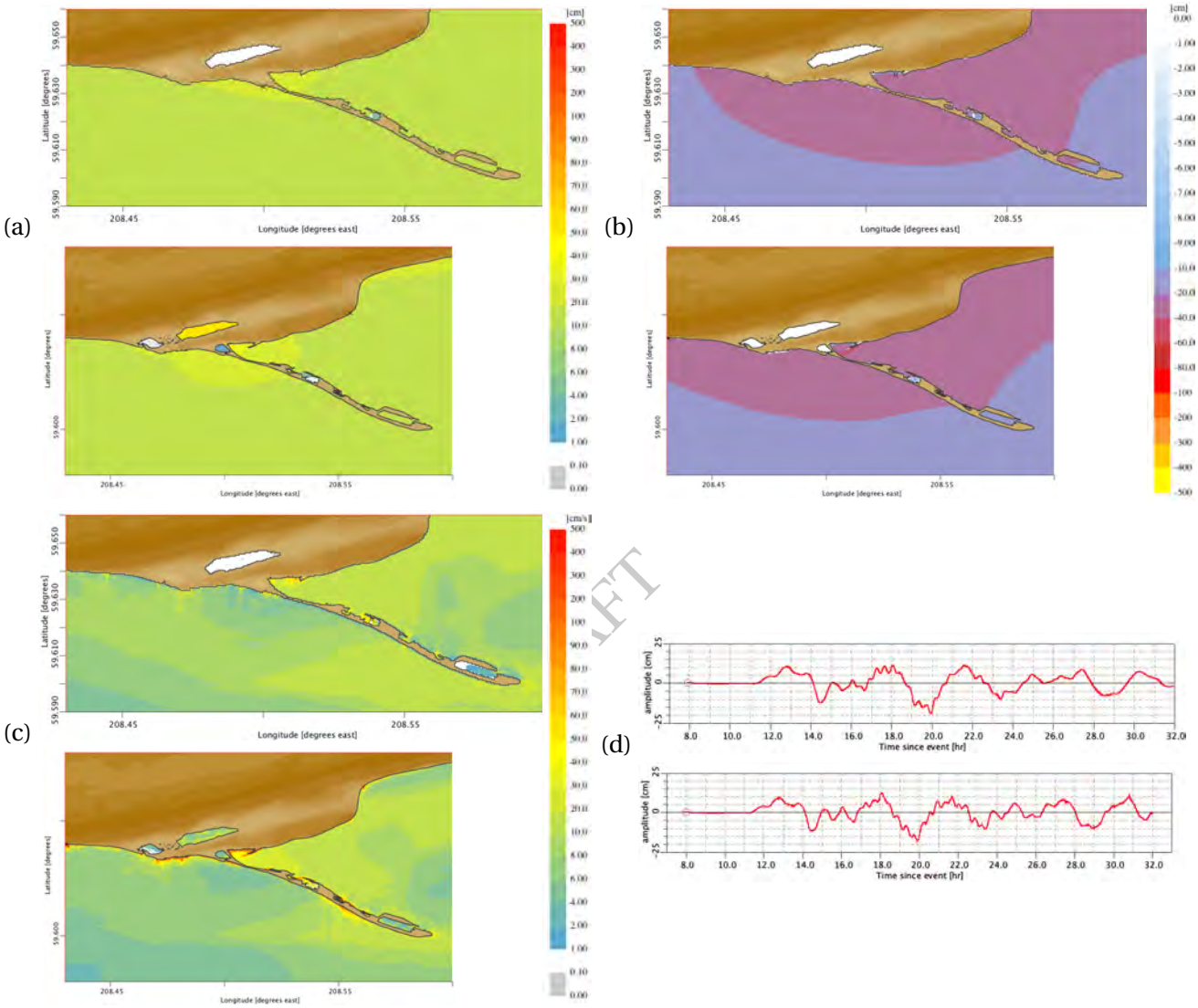

Figure 21: Comparisons for the FM (top insets) and the RM (bottom insets) C-grid results for the magnitude 9.3 synthetic scenario event with the source segment 56–65 on Kamchatka–Yap–Mariana–Izu–Bonin Subduction Zone (KISZ) (Figure B.5, Table B.5). (a) Maximum and (b) minimum sea surface elevations, (c) maximum wave speeds at each C-grid point and (d) time histories of water surface elevations at the Homer forecast point.

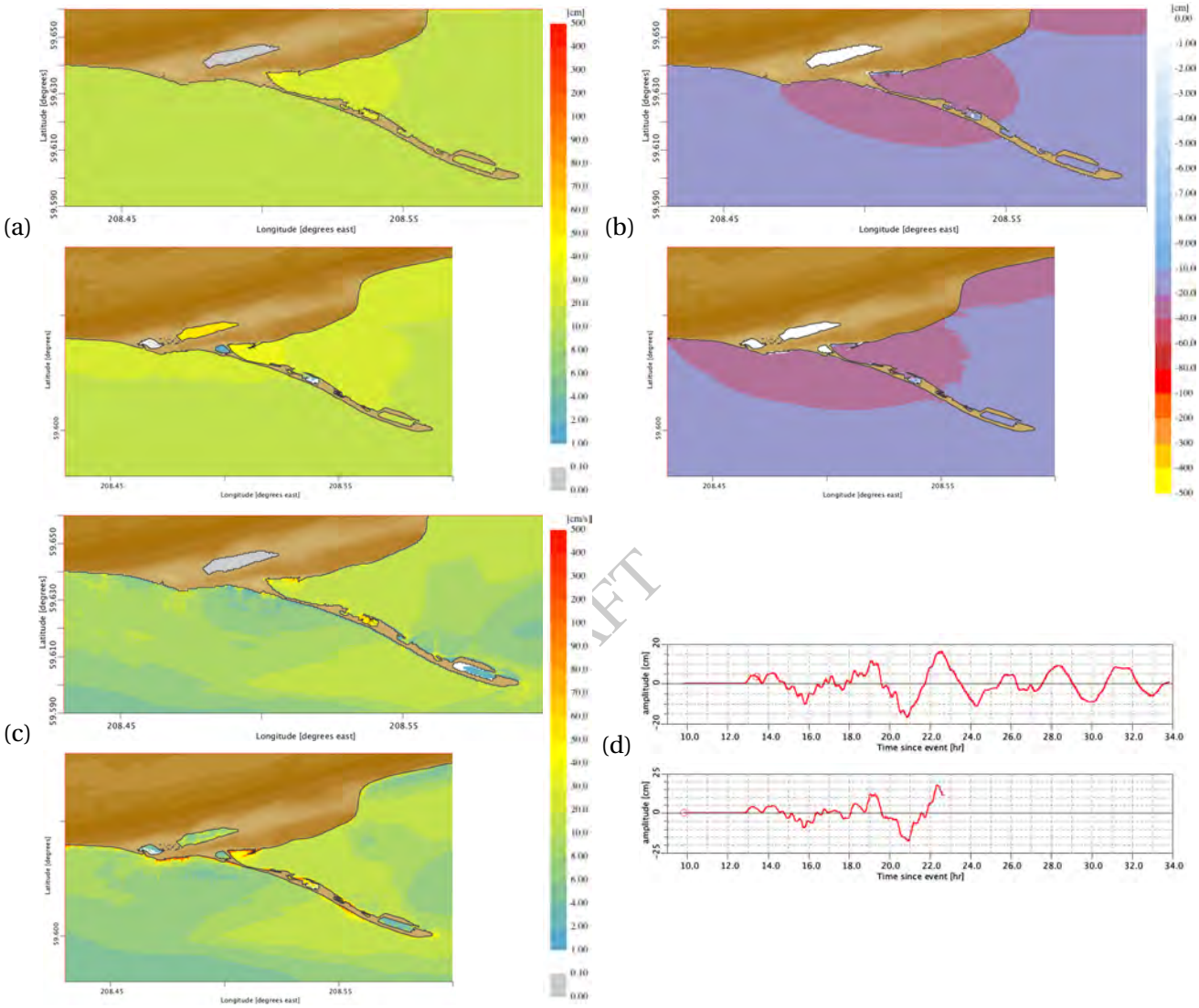

Figure 22: Comparisons for the FM (top insets) and the RM (bottom insets) C-grid results for the magnitude 9.3 synthetic scenario event with the source segment 1–10 on Manus–Oceanic Convergent Boundary Subduction Zone (MOSZ) (Figure B.6, Table B.6). (a) Maximum and (b) minimum sea surface elevations, (c) maximum wave speeds at each C-grid point and (d) time histories of water surface elevations at the Homer forecast point.

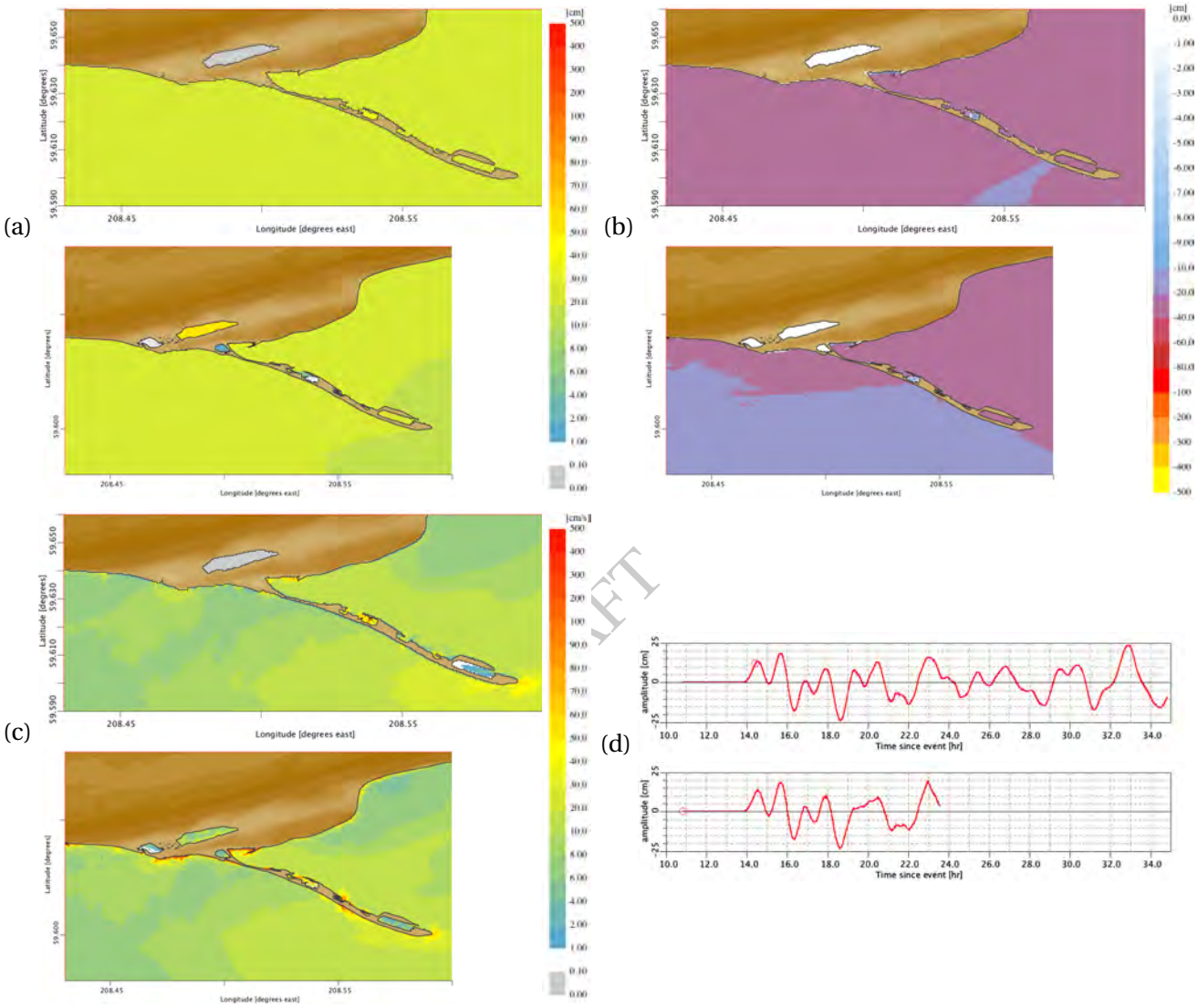

Figure 23: Comparisons for the FM (top insets) and the RM (bottom insets) C-grid results for the magnitude 9.3 synthetic scenario event with the source segment 3–12 on New Guinea Subduction Zone (NGSZ) (Figure B.7, Table B.7). (a) Maximum and (b) minimum sea surface elevations, (c) maximum wave speeds at each C-grid point and (d) time histories of water surface elevations at the Homer forecast point.

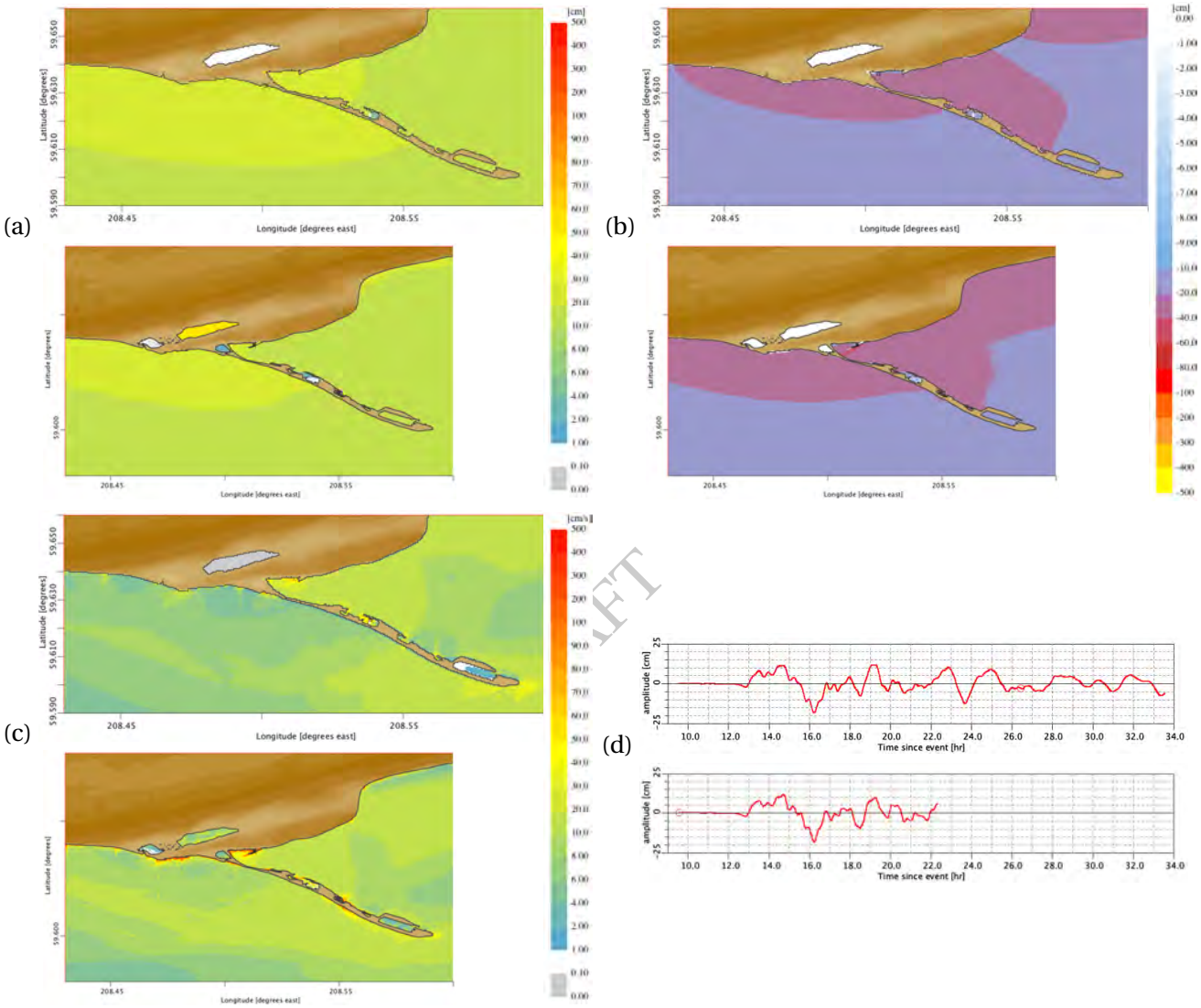

Figure 24: Comparisons for the FM (top insets) and the RM (bottom insets) C-grid results for the magnitude 9.3 synthetic scenario event with the source segment 30–39 on New Zealand–Kermadec–Tonga Subduction Zone (NTSZ) (Figure B.8, Table B.8). (a) Maximum and (b) minimum sea surface elevations, (c) maximum wave speeds at each C-grid point and (d) time histories of water surface elevations at the Homer forecast point.

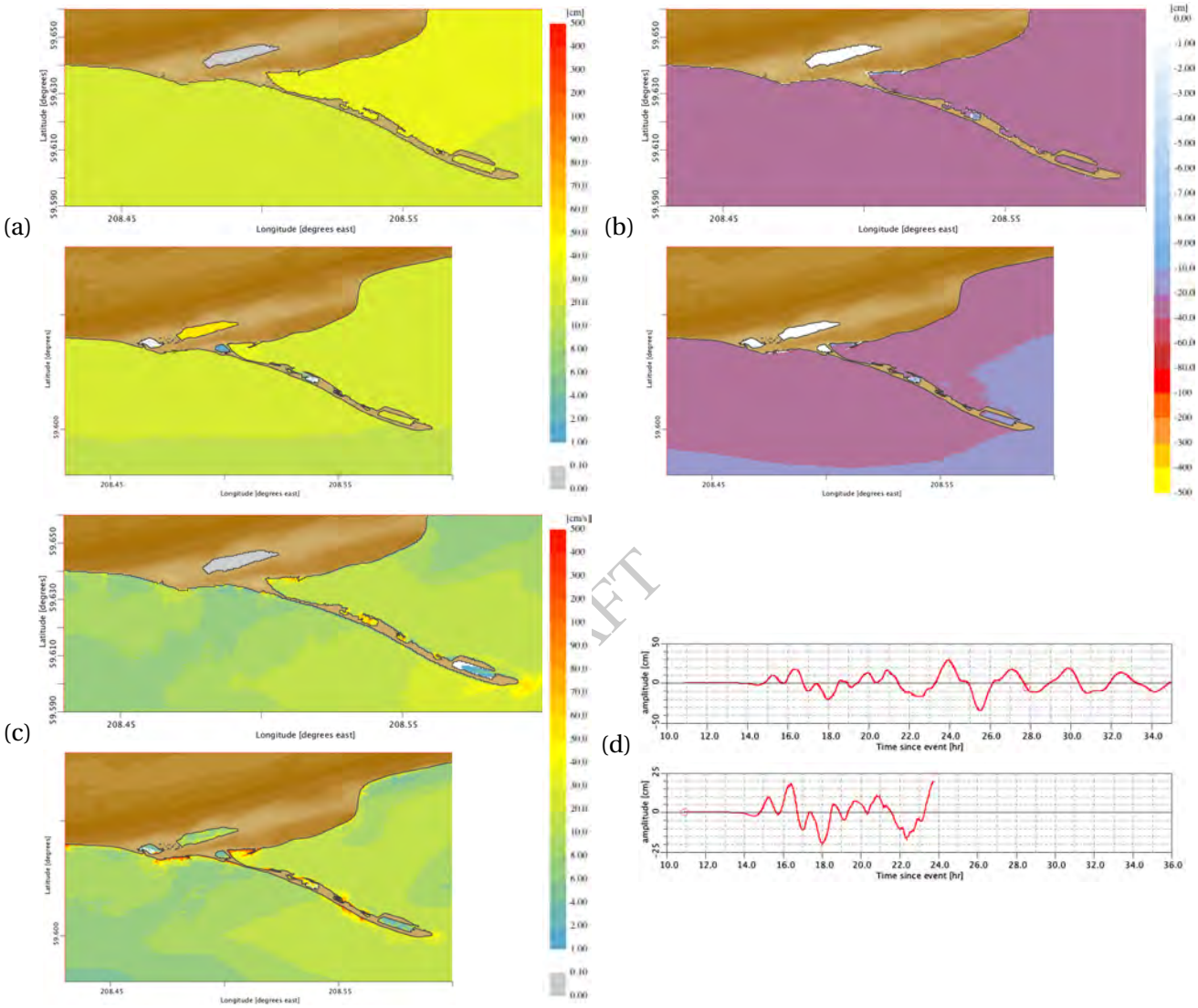

Figure 25: Comparisons for the FM (top insets) and the RM (bottom insets) C-grid results for the magnitude 9.3 synthetic scenario event with the source segment 28–37 on New Britain–Solomons–Vanuatu Subduction Zone (NVSZ) (Figure B.9, Table B.9). (a) Maximum and (b) minimum sea surface elevations, (c) maximum wave speeds at each C-grid point and (d) time histories of water surface elevations at the Homer forecast point.

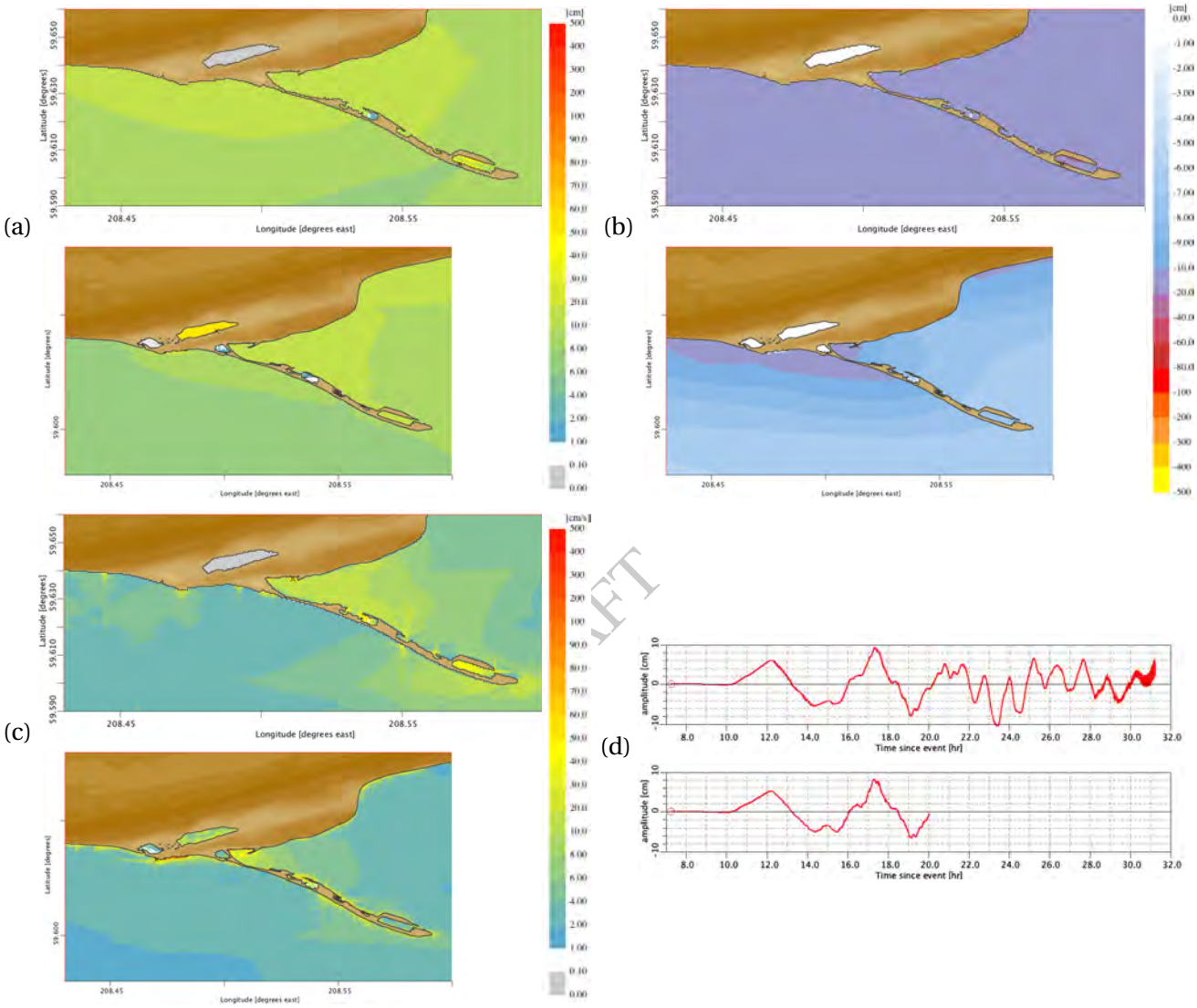

Figure 26: Comparisons for the FM (top insets) and the RM (bottom insets) C-grid results for the magnitude 9.3 synthetic scenario event with the source segment 12–21 on Ryukyu–Kyushu–Nankai Subduction Zone (RNSZ) (Figure B.11, Table B.11). (a) Maximum and (b) minimum sea surface elevations, (c) maximum wave speeds at each C-grid point and (d) time histories of water surface elevations at the Homer forecast point.

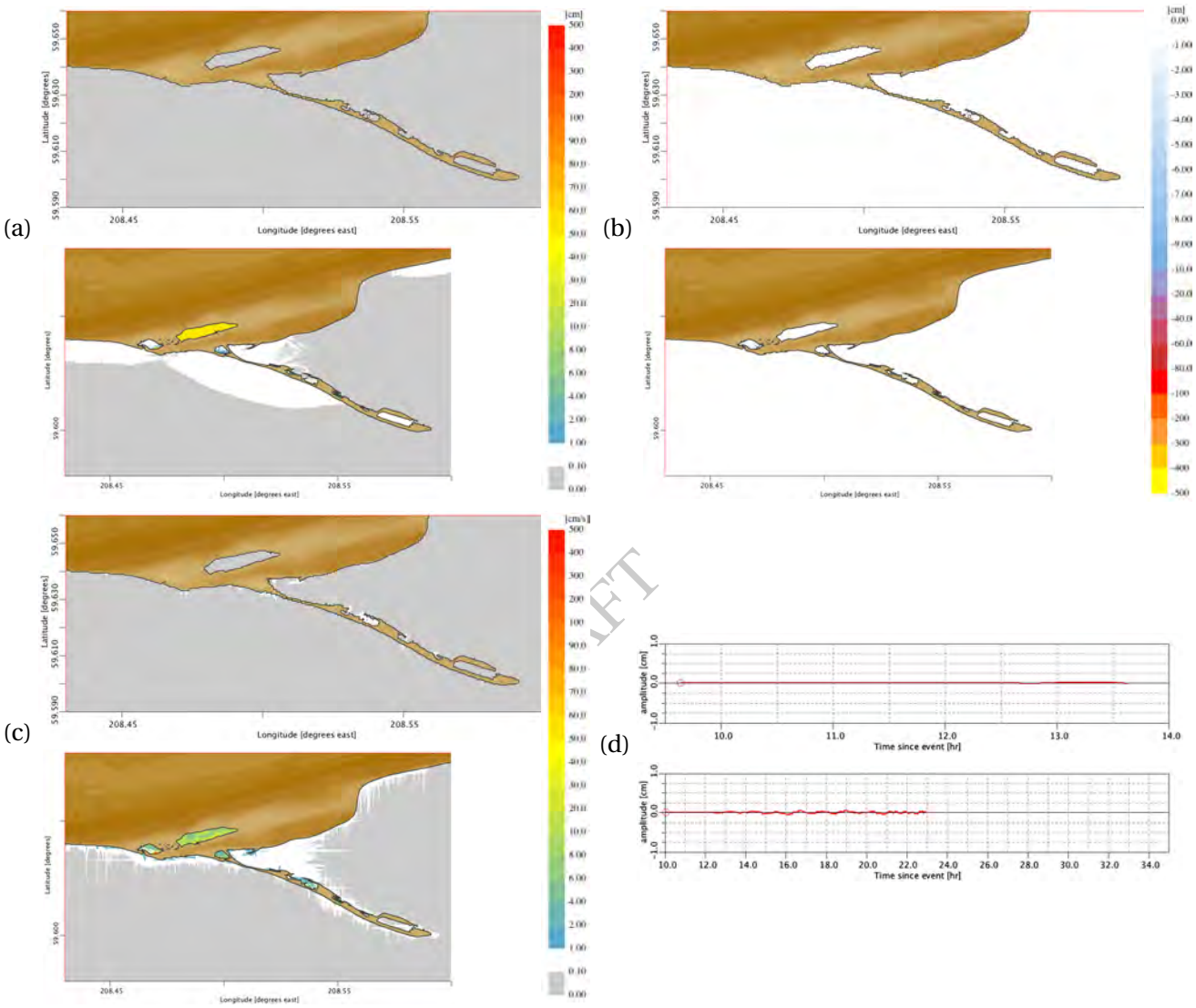

Figure 27: Comparisons for the FM (top insets) and the RM (bottom insets) C-grid results for the magnitude 7.5 synthetic scenario event with the source 36b on New Zealand–Kermadec–Tonga Subduction Zone (NTSZ) (Figure B.8, Table B.8). (a) Maximum and (b) minimum sea surface elevations, (c) maximum wave speeds at each C-grid point and (d) time histories of water surface elevations at the Homer forecast point.

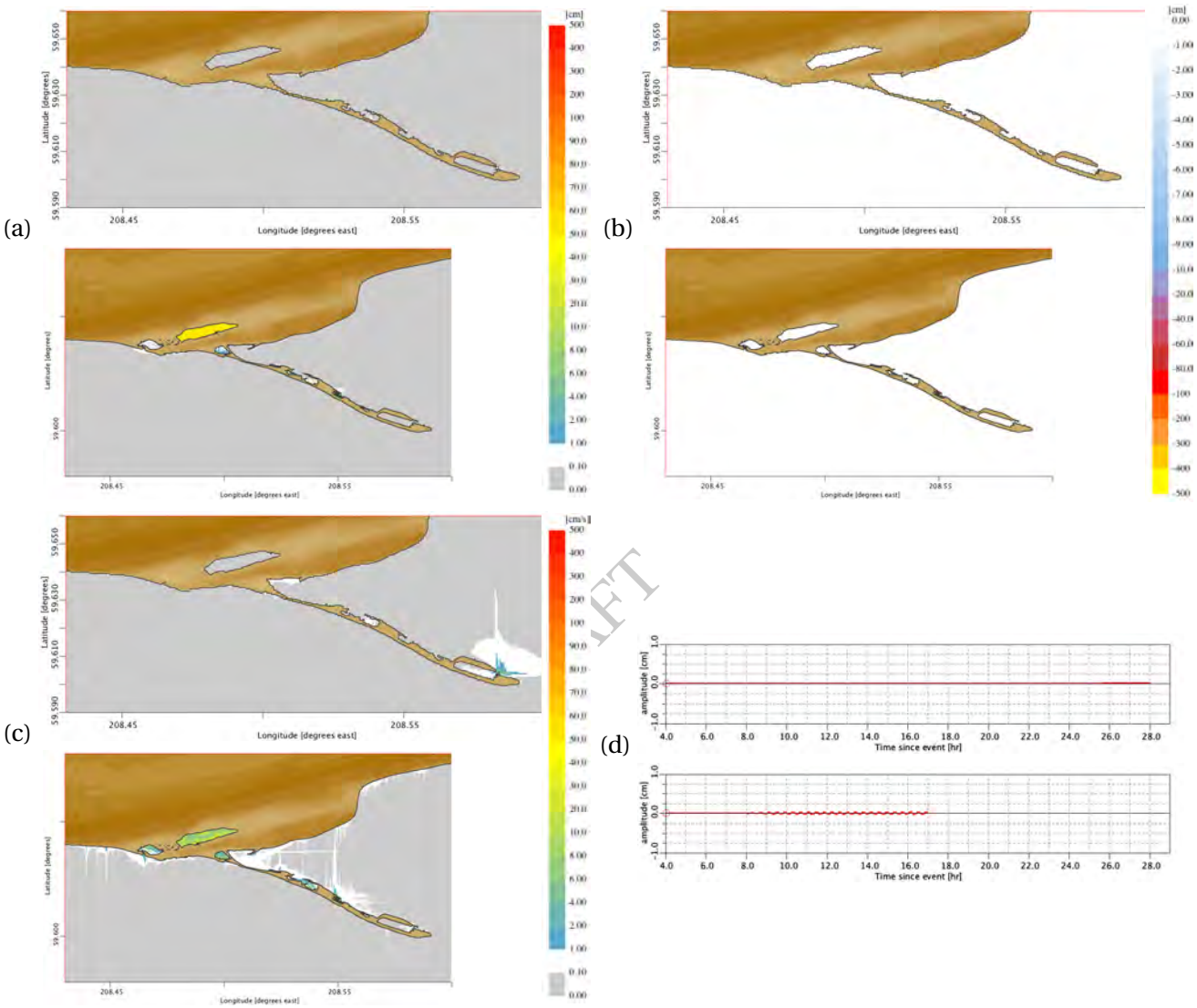

Figure 28: Comparisons for the FM (top insets) and the RM (bottom insets) C-grid results for the micro-tsunami synthetic scenario event with the source 6b on Aleutian–Alaska–Cascadia Subduction Zone (ACSZ) (Figure B.1, Table B.1). (a) Maximum and (b) minimum sea surface elevations, (c) maximum wave speeds at each C-grid point and (d) time histories of water surface elevations at the Homer forecast point.

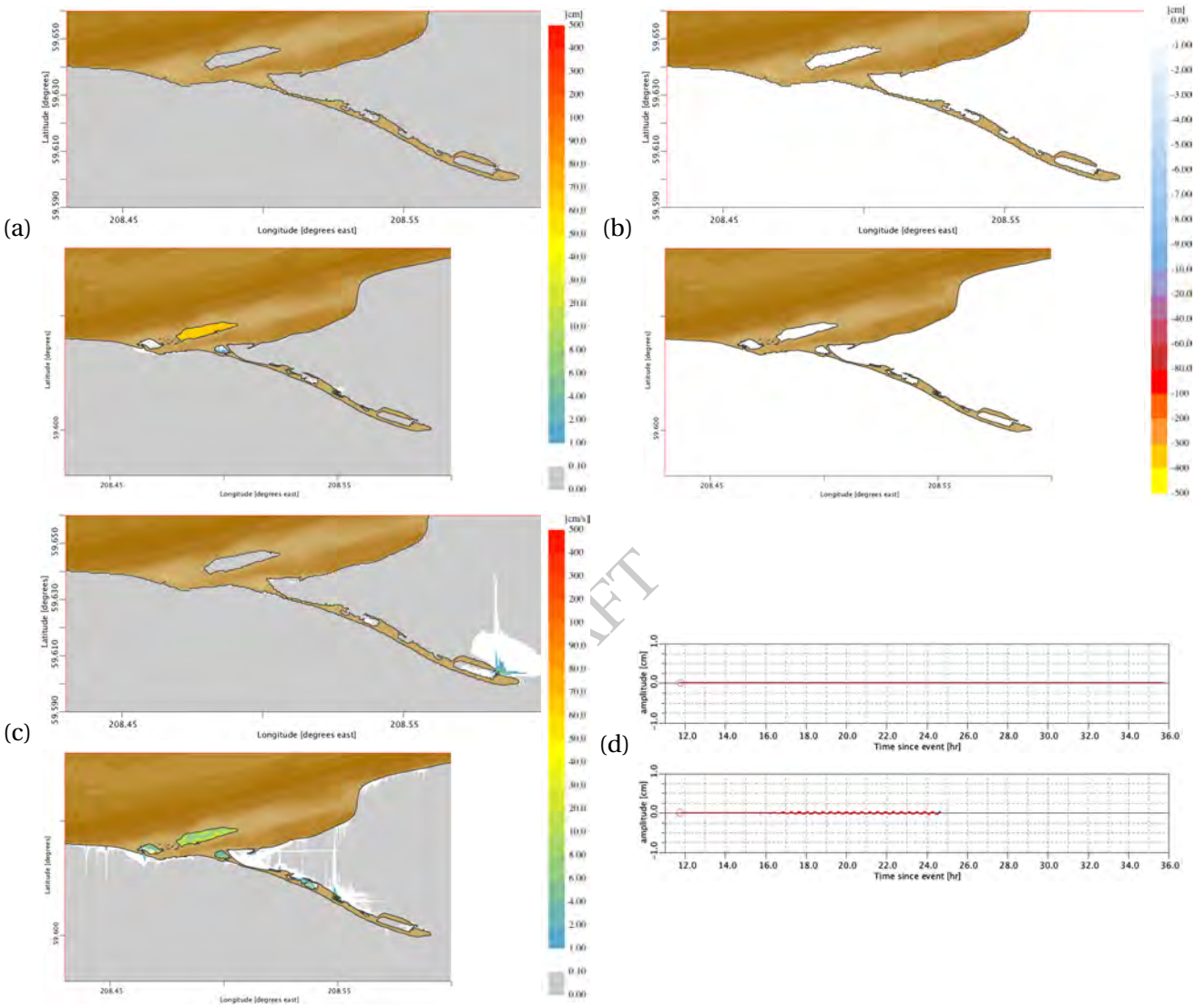

Figure 29: Comparisons for the FM (top insets) and the RM (bottom insets) C-grid results for the micro-tsunami synthetic scenario event with the source 19b on Eastern Philippines Subduction Zone (EPSZ) (Figure B.3, Table B.3). (a) Maximum and (b) minimum sea surface elevations, (c) maximum wave speeds at each C-grid point and (d) time histories of water surface elevations at the Homer forecast point.

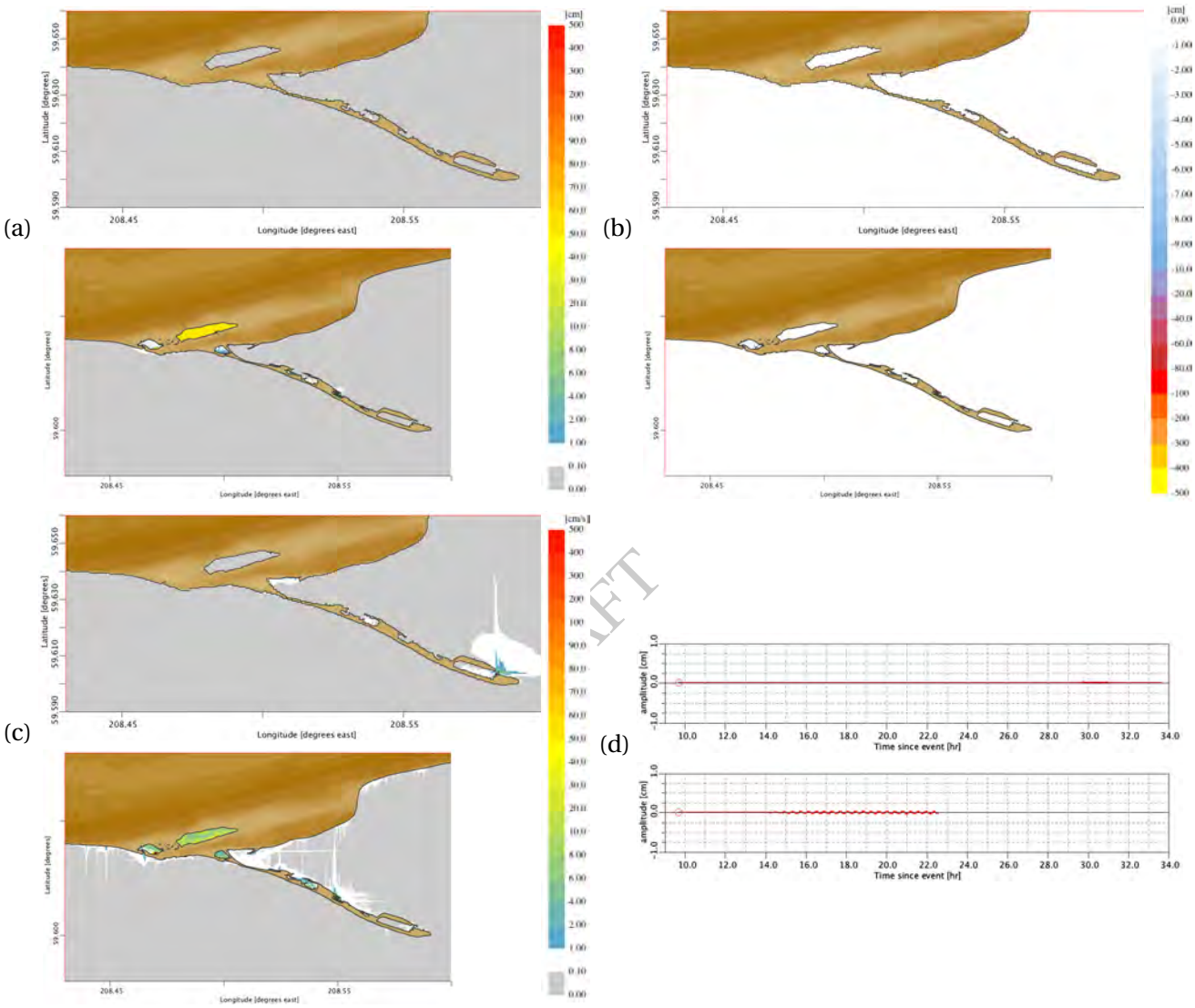

Figure 30: Comparisons for the FM (top insets) and the RM (bottom insets) C-grid results for the micro-tsunami synthetic scenario event with the source 14b on Ryukyu–Kyushu–Nankai Subduction Zone (RNSZ) (Figure B.11, Table B.11). (a) Maximum and (b) minimum sea surface elevations, (c) maximum wave speeds at each C-grid point and (d) time histories of water surface elevations at the Homer forecast point.

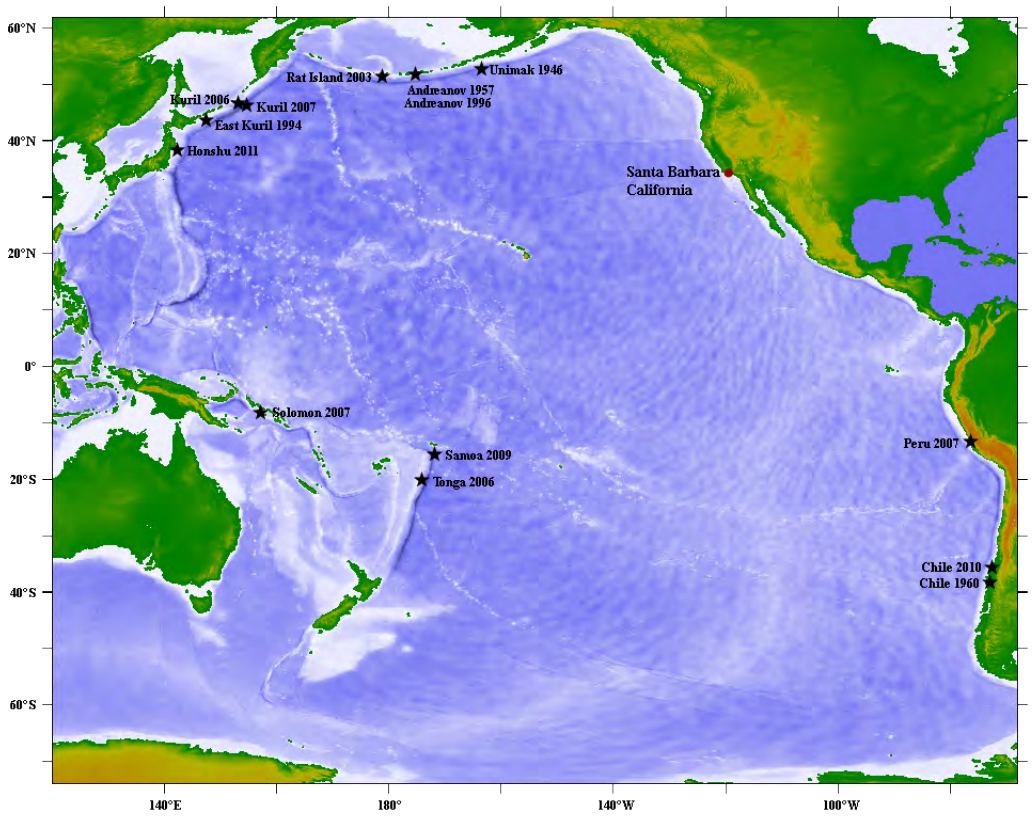

Figure 31: Location maps of historical events listed in Table 3 in testing the numerical stability and robustness of the RMs and FMs. Only 11 March 2011 Japan event is used for Homer, Alaska RM and FM testing (courtesy of Dr. Edison Gica).

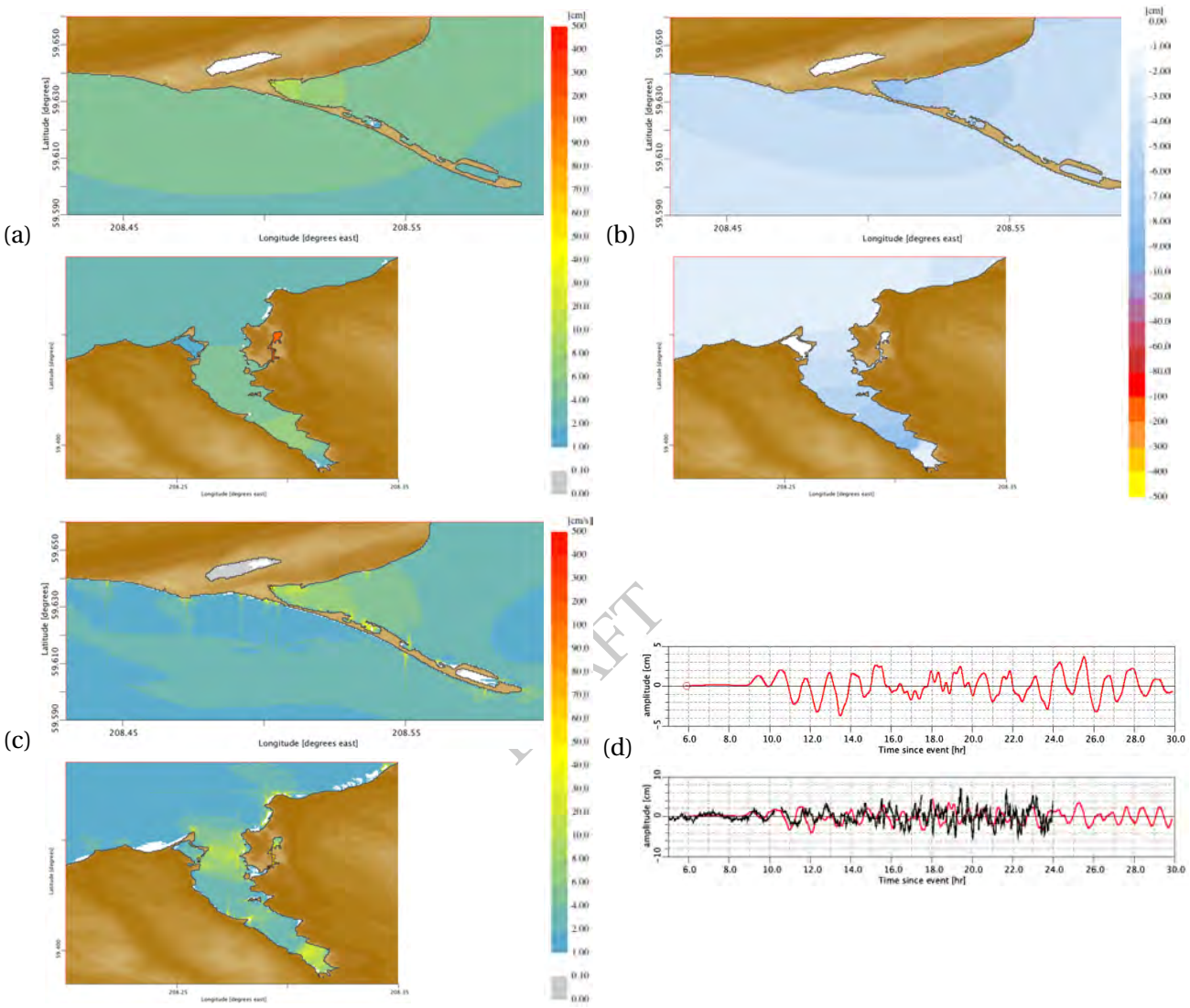

Figure 32: The FM (top insets) results for Homer, Alaska for the 11 March 2011 Japan tsunami. Results of the Seldovia, Alaska model is also given (lover insets) for the 11 March 2011 Japan tsunami. (a) Maximum and (b) minimum sea surface elevations, (c) maximum wave speeds at each C-grid point and (d) time histories of water surface elevations at the Homer forecast point (upper inset) and Seldovia tide gage (lower inset). Time histories of water surface elevations at the Seldovia tide gage is compared with the 11 March 2011 Japan tsunami measurement (black line).

Tables

Table 1: MOST setup of the reference and forecast models for Homer, Alaska.

		Reference Model				Forecast Model			
Grid	**Region**	**Coverage Lat. [°N] Lon. [°W]**	**Cell Size [arc-second]**	**nx × ny**	**Time Step [sec]**	**Coverage Lat. [°N] Lon. [°W]**	**Cell Size [arc-second]**	**nx × ny**	**Time Step [sec]**
A	Southern Alaska Coastal Relief Model	54.9533–61.6000 148.9533–155.0000	24 × 24	908 × 998	1.68	54.9667–61.5867 148.9667–154.9867	72 × 72	302 × 332	5.25
B	Kachemak Bay, Alaska	59.3250–59.8200 150.9203–152.0670	6 × 6	689 × 298	1.68	59.3267–59.8200 150.9203–152.0670	12 × 12	345 × 149	3.75
C (Homer)	Kachemak Bay, Alaska	59.5800–59.6800 151.4000–151.5700	1/3 × 1/3	1837 × 1081	0.14	59.5900–59.6600 151.4000–151.5700	1.5 × 1.5	409 × 169	0.75
C (Seldovia)	Kachemak Bay, Alaska	No reference model was developed	–	–	–	59.3850–59.4850 151.6500–151.8000	1.5 × 1.5	361 × 241	0.75
Minimum offshore depth [m]			1.0				1.0		
Water depth for dry land [m]			0.1				0.1		
Friction coefficient (n^2)			0.0009				0.0009		
CPU time for a 4-hr simulation			1525 min				12.8 min		

Computations were performed on a single Intel Xeon processor at 3.6 GHz, Dell PowerEdge 1850.

Table 2: Synthetic tsunami events used for the development of the Homer, Alaska tsunami forecast model. Unit source combinations used for creating synthetic mega tsunami scenarios of Mw 9.3.

Scenario Name	Subduction Zone	Tsunami Source	α [m]	Reference
Mega-tsunami Scenario				
ACSZ 6–15	Aleutian–Alaska–Cascadia	6a–15a, 6b–15b	25	Figure B.1, Table B.1
ACSZ 16–25	Aleutian–Alaska–Cascadia	16a–25a, 16b–25b	25	Figure B.1, Table B.1
ACSZ 22–31	Aleutian–Alaska–Cascadia	22a–31a, 22b–31b	25	Figure B.1, Table B.1
ACSZ 50–59	Aleutian–Alaska–Cascadia	50a–59a, 50b–59b	25	Figure B.1, Table B.1
ACSZ 56–65	Aleutian–Alaska–Cascadia	56a–65a, 56b–65b	25	Figure B.1, Table B.1
CSSZ 1–10	Central and South America	1a–10a, 1b–10b	25	Figure B.2, Table B.2
CSSZ 37–46	Central and South America	37a–46a, 37b–46b	25	Figure B.2, Table B.2
CSSZ 89–98	Central and South America	89a–98a, 89b–98b	25	Figure B.2, Table B.2
CSSZ 102–111	Central and South America	102a–111a, 102b–111b	25	Figure B.2, Table B.2
EPSZ 6–15	Eastern Philippines	6a–15a, 6b–15b	25	Figure B.3, Table B.3
KISZ 1–10	Kamchatka–Kuril–Japan–Izu–Mariana–Yap	1a–10a, 10b–10b	25	Figure B.5, Table B.5
KISZ 22–31	Kamchatka–Kuril–Japan–Izu–Mariana–Yap	22a–31a, 22b–31b	25	Figure B.5, Table B.5
KISZ 32–41	Kamchatka–Kuril–Japan–Izu–Mariana–Yap	32a–41a, 32b–41b	25	Figure B.5, Table B.5
KISZ 56–65	Kamchatka–Kuril–Japan–Izu–Mariana–Yap	56a–65a, 56b–65b	25	Figure B.5, Table B.5
MOSZ 1–10	Manus–Oceanic Convergent Boundary	1a–10a, 1b–10b	25	Figure B.6, Table B.6
NGSZ 3–12	New Guinea	3a–12a, 3b–12b	25	Figure B.7, Table B.7
NTSZ 30–39	New Zealand–Kermadec-Tonga	30a–39a, 30b–39b	25	Figure B.8, Table B.8
NVSZ 28–37	New Britain–Solomons–Vanuatu	28a–37a, 28b–37b	25	Figure B.9, Table B.9
RNSZ 12–21	Ryukyu–Kyushu–Nankai	12a–21a, 12b–21b	25	Figure B.11, Table B.11
Mw 7.5 Scenario				
NTSZ 36	New Zealand–Kermadec–Tonga	36b	1	Figure B.8, Table B.8
Micro-tsunami Scenario				
ACSZ 6	Aleutian–Alaska–Cascadia	6b	0.01	Figure B.1, Table B.1
EPSZ 19	Eastern Philippines	19b	0.01	Figure B.3, Table B.3
RNSZ 14	Ryukyu–Kyushu–Nankai	14b	0.01	Figure B.11, Table B.11

Table 3: Historical events used for validation of the Homer, Alaska model.

Event	Earthquake Date and Time (UTC)	Latitude	Longitude	Subduction Zone	Seismic Moment Magnitude (Mw)	Tsunami Magnitude[1]	Model Tsunami Source
1946 Unimak	1946-04-01 12:28:56	53.32°N	163.19°W	Aleutian–Alaska–Cascadia (ACSZ)	[2]8.5	8.5	7.5 × 23b + 19.7 × 24b + 3.7 × 25b
1994 East Kuril	1994-10-04 13:23:28.5	43.60°N	147.63°E	Kamchatka–Kuril–Japan–Izu–Mariana–Yap (KISZ)	[3]8.3	8.1	9.0 × 20a
1996 Andreanov	1996-06-10 04:04:03.4	51.10°N	177.410°W	Aleutian–Alaska–Cascadia (ACSZ)	[3]7.9	7.8	2.40 × 15a + 0.80 × 16b
2001 Peru	2001-06-23 20:34:23.3	17.28°S	72.71°W	South America (SASZ)	[3]8.4	8.2	5.70 × 15a + 2.90 × 16b + 1.98 × 16a
2003 Rat Island	2003-11-17 06:43:31.0	51.14°N	177.86°E	Aleutian–Alaska–Cascadia (ACSZ)	[3]7.7	7.8	[4]2.81 × 11b
2006 Tonga	2006-05-03 15:27:03.7	20.39°S	173.47°W	New Zealand–Kermadec–Tonga (NTSZ)	[3]8.0	8.0	8.44 × 29b
2006 Kuril	2006-11-15 11:15:08.0	46.71°N	154.33°E	Kamchatka–Kuril–Japan–Izu–Mariana–Yap (KISZ)	[3]8.3	8.1	[4]4.0 × 12a + 0.5 × 12b + 2 × 13a + 1.5 × 13b
2007 Kuril	2007-01-13 04:23:48.1	46.17°N	154.80°E	Kamchatka–Kuril–Japan–Izu–Mariana–Yap (KISZ)	[3]8.1	7.9	−3.64 × 13b
2007 Solomon	2007-04-01 20:40:38.9	7.79°S	156.34°E	New Britain–Solomons–Vanuatu (NVSZ)	8.1	8.2	12.0 × 10b
2007 Peru	2007-08-15 23:41:57.9	13.73°S	77.04°W	South America (SASZ)	[3]8.0	8.1	[4]4.1 × 9a + 4.32 × 9b
2007 Chile	2011-03-11 15:41:11.2	22.64°S	70.62°W	South America (SASZ)	[3]7.7	7.6	0.81 × 22a + 0.3 × 23a + 0.11 × 23b
2011 Tohoku	2007-11-14 05:46:23.82	38.308°N	142.383°E	Kamchatka–Kuril–Japan–Izu–Mariana–Yap (KISZ)	[3]9.0	8.8	4.66 × 24b + 12.23 × 25b + 26.31 × 26a + 21.27 × 26b + 22.75 × 27a + 4.98 × 27b

[1]Equivalent tsunami source moment magnitude from model source constrained by tsunami observations.
[2]Lopez and Okal (2006)
[3]Centroid Moment Tensor
[4]The tsunami source was obtained during real time and applied to the forecast

Appendix A

Development of the Homer, Alaska tsunami forecast model occurred prior to parameter changes that were made to reflect modifications to the MOST model code. As a result, the input file for running both the tsunami forecast model and the high-resolution reference inundation model in MOST have been updated accordingly. Appendix A1 and A2 provide the updated files for Homer, Alaska.

A.1 Reference Model ⋆.in File for Homer, Alaska

0.001 Minimum amplitude of input offshore wave (m)
1.0 Minimum depth of offshore (m)
0.1 Dry land depth of inundation (m)
0.0009 Friction coefficient (n^2)
Let A-grid and B-grid runup
300.0 Maximum eta before blow-up (m)
0.14 Time step (sec)
620000 Total number of time steps in run
12 Time steps between A-grid computations
12 Time steps between B-grid computations
540 Time steps between output steps
0 Time steps before saving first output step
1 Save output every n-th point

A.2 Forecast Model ⋆.in File for Homer, Alaska

0.0001 Minimum amplitude of input offshore wave (m)
1.0 Minimum depth of offshore (m)
0.1 Dry land depth of inundation (m)
0.0009 Friction coefficient (n^2)
Let A-grid and B-grid runup
300.0 Maximum eta before blow-up (m)
0.75 Time step (sec)
115200 Total number of time steps in run
7 Time steps between A-grid computations

5 Time steps between B-grid computations
35 Time steps between output steps
0 Time steps before saving first output step
1 Save output every n-th point

Appendix B

Propagation Database: Pacific Ocean Unit Sources

NOAA Propagation Database presented in this section is the representation of the database as of March, 2013. This database may have been updated since March, 2013.

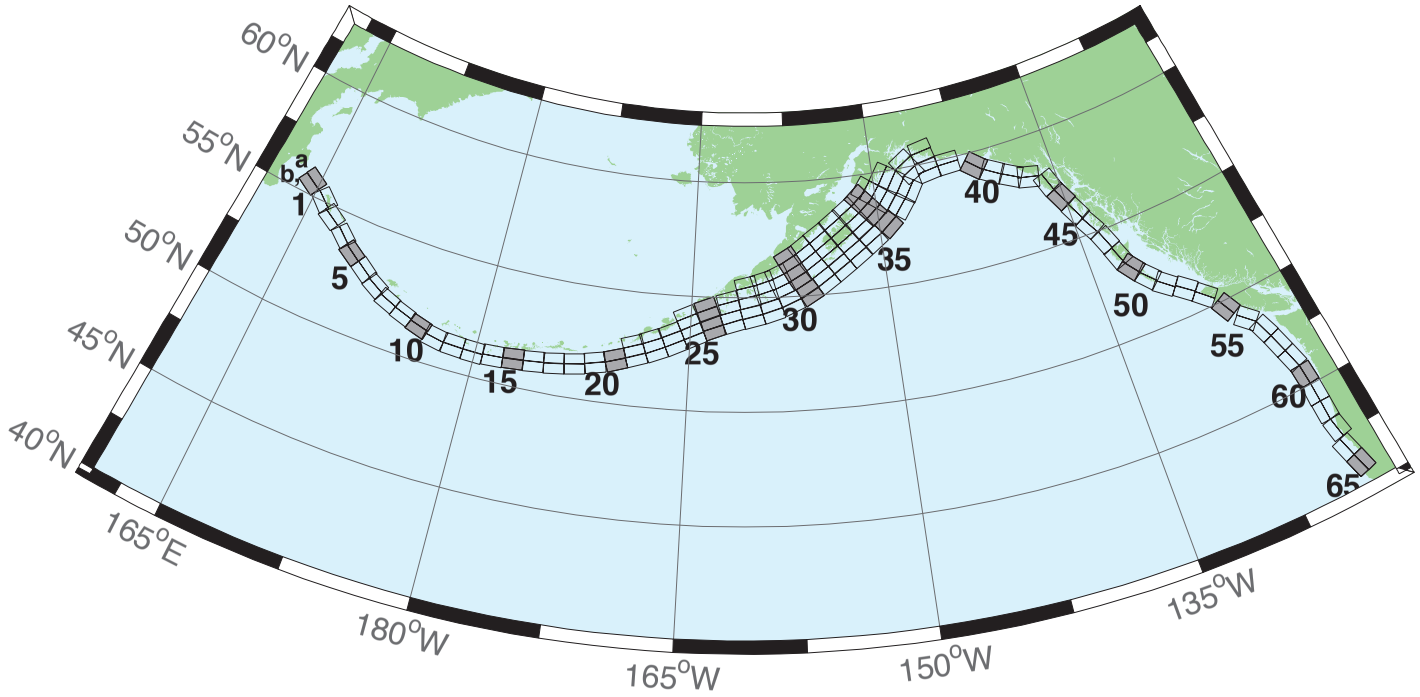

Figure B.1: Aleutian–Alaska–Cascadia Subduction Zone (ACSZ) unit sources.

Table B.1: Earthquake parameters for Aleutian–Alaska–Cascadia Subduction Zone (ACSZ) unit sources.

Segment	Description	Longitude (°E)	Latitude (°N)	Strike (°)	Dip (°)	Depth (km)
ACSZ–1a	Aleutian–Alaska–Cascadia	164.7994	55.9606	299	17	19.61
ACSZ–1b	Aleutian–Alaska–Cascadia	164.4310	55.5849	299	17	5
ACSZ–2a	Aleutian–Alaska–Cascadia	166.3418	55.4016	310.2	17	19.61
ACSZ–2b	Aleutian–Alaska–Cascadia	165.8578	55.0734	310.2	17	5
ACSZ–3a	Aleutian–Alaska–Cascadia	167.2939	54.8919	300.2	23.36	24.82
ACSZ–3b	Aleutian–Alaska–Cascadia	166.9362	54.5356	300.2	23.36	5
ACSZ–4a	Aleutian–Alaska–Cascadia	168.7131	54.2852	310.2	38.51	25.33
ACSZ–4b	Aleutian–Alaska–Cascadia	168.3269	54.0168	310.2	24	5
ACSZ–5a	Aleutian–Alaska–Cascadia	169.7447	53.7808	302.8	37.02	23.54
ACSZ–5b	Aleutian–Alaska–Cascadia	169.4185	53.4793	302.8	21.77	5
ACSZ–6a	Aleutian–Alaska–Cascadia	171.0144	53.3054	303.2	35.31	22.92
ACSZ–6b	Aleutian–Alaska–Cascadia	170.6813	52.9986	303.2	21	5
ACSZ–7a	Aleutian–Alaska–Cascadia	172.1500	52.8528	298.2	35.56	20.16
ACSZ–7b	Aleutian–Alaska–Cascadia	171.8665	52.5307	298.2	17.65	5
ACSZ–8a	Aleutian–Alaska–Cascadia	173.2726	52.4579	290.8	37.92	20.35
ACSZ–8b	Aleutian–Alaska–Cascadia	173.0681	52.1266	290.8	17.88	5
ACSZ–9a	Aleutian–Alaska–Cascadia	174.5866	52.1434	289	39.09	21.05
ACSZ–9b	Aleutian–Alaska–Cascadia	174.4027	51.8138	289	18.73	5
ACSZ–10a	Aleutian–Alaska–Cascadia	175.8784	51.8526	286.1	40.51	20.87
ACSZ–10b	Aleutian–Alaska–Cascadia	175.7265	51.5245	286.1	18.51	5
ACSZ–11a	Aleutian–Alaska–Cascadia	177.1140	51.6488	280	15	17.94
ACSZ–11b	Aleutian–Alaska–Cascadia	176.9937	51.2215	280	15	5
ACSZ–12a	Aleutian–Alaska–Cascadia	178.4500	51.5690	273	15	17.94
ACSZ–12b	Aleutian–Alaska–Cascadia	178.4130	51.1200	273	15	5
ACSZ–13a	Aleutian–Alaska–Cascadia	179.8550	51.5340	271	15	17.94
ACSZ–13b	Aleutian–Alaska–Cascadia	179.8420	51.0850	271	15	5
ACSZ–14a	Aleutian–Alaska–Cascadia	181.2340	51.5780	267	15	17.94
ACSZ–14b	Aleutian–Alaska–Cascadia	181.2720	51.1290	267	15	5
ACSZ–15a	Aleutian–Alaska–Cascadia	182.6380	51.6470	265	15	17.94
ACSZ–15b	Aleutian–Alaska–Cascadia	182.7000	51.2000	265	15	5
ACSZ–16a	Aleutian–Alaska–Cascadia	184.0550	51.7250	264	15	17.94
ACSZ–16b	Aleutian–Alaska–Cascadia	184.1280	51.2780	264	15	5
ACSZ–17a	Aleutian–Alaska–Cascadia	185.4560	51.8170	262	15	17.94
ACSZ–17b	Aleutian–Alaska–Cascadia	185.5560	51.3720	262	15	5
ACSZ–18a	Aleutian–Alaska–Cascadia	186.8680	51.9410	261	15	17.94
ACSZ–18b	Aleutian–Alaska–Cascadia	186.9810	51.4970	261	15	5
ACSZ–19a	Aleutian–Alaska–Cascadia	188.2430	52.1280	257	15	17.94
ACSZ–19b	Aleutian–Alaska–Cascadia	188.4060	51.6900	257	15	5
ACSZ–20a	Aleutian–Alaska–Cascadia	189.5810	52.3550	251	15	17.94
ACSZ–20b	Aleutian–Alaska–Cascadia	189.8180	51.9300	251	15	5
ACSZ–21a	Aleutian–Alaska–Cascadia	190.9570	52.6470	251	15	17.94
ACSZ–21b	Aleutian–Alaska–Cascadia	191.1960	52.2220	251	15	5
ACSZ–21z	Aleutian–Alaska–Cascadia	190.7399	53.0443	250.8	15	30.88
ACSZ–22a	Aleutian–Alaska–Cascadia	192.2940	52.9430	247	15	17.94
ACSZ–22b	Aleutian–Alaska–Cascadia	192.5820	52.5300	247	15	5
ACSZ–22z	Aleutian–Alaska–Cascadia	192.0074	53.3347	247.8	15	30.88
ACSZ–23a	Aleutian–Alaska–Cascadia	193.6270	53.3070	245	15	17.94
ACSZ–23b	Aleutian–Alaska–Cascadia	193.9410	52.9000	245	15	5
ACSZ–23z	Aleutian–Alaska–Cascadia	193.2991	53.6768	244.6	15	30.88
ACSZ–24a	Aleutian–Alaska–Cascadia	194.9740	53.6870	245	15	17.94
ACSZ–24b	Aleutian–Alaska–Cascadia	195.2910	53.2800	245	15	5
ACSZ–24y	Aleutian–Alaska–Cascadia	194.3645	54.4604	244.4	15	43.82
ACSZ–24z	Aleutian–Alaska–Cascadia	194.6793	54.0674	244.6	15	30.88
ACSZ–25a	Aleutian–Alaska–Cascadia	196.4340	54.0760	250	15	17.94
ACSZ–25b	Aleutian–Alaska–Cascadia	196.6930	53.6543	250	15	5
ACSZ–25y	Aleutian–Alaska–Cascadia	195.9009	54.8572	247.9	15	43.82
ACSZ–25z	Aleutian–Alaska–Cascadia	196.1761	54.4536	248.1	15	30.88
ACSZ–26a	Aleutian–Alaska–Cascadia	197.8970	54.3600	253	15	17.94
ACSZ–26b	Aleutian–Alaska–Cascadia	198.1200	53.9300	253	15	5
ACSZ–26y	Aleutian–Alaska–Cascadia	197.5498	55.1934	253.1	15	43.82

Continued on next page

Table B.1 – continued

Segment	Description	Longitude (°E)	Latitude (°N)	Strike (°)	Dip (°)	Depth (km)
ACSZ–26z	Aleutian–Alaska–Cascadia	197.7620	54.7770	253.3	15	30.88
ACSZ–27a	Aleutian–Alaska–Cascadia	199.4340	54.5960	256	15	17.94
ACSZ–27b	Aleutian–Alaska–Cascadia	199.6200	54.1600	256	15	5
ACSZ–27x	Aleutian–Alaska–Cascadia	198.9736	55.8631	256.5	15	56.24
ACSZ–27y	Aleutian–Alaska–Cascadia	199.1454	55.4401	256.6	15	43.82
ACSZ–27z	Aleutian–Alaska–Cascadia	199.3135	55.0170	256.8	15	30.88
ACSZ–28a	Aleutian–Alaska–Cascadia	200.8820	54.8300	253	15	17.94
ACSZ–28b	Aleutian–Alaska–Cascadia	201.1080	54.4000	253	15	5
ACSZ–28x	Aleutian–Alaska–Cascadia	200.1929	56.0559	252.5	15	56.24
ACSZ–28y	Aleutian–Alaska–Cascadia	200.4167	55.6406	252.7	15	43.82
ACSZ–28z	Aleutian–Alaska–Cascadia	200.6360	55.2249	252.9	15	30.88
ACSZ–29a	Aleutian–Alaska–Cascadia	202.2610	55.1330	247	15	17.94
ACSZ–29b	Aleutian–Alaska–Cascadia	202.5650	54.7200	247	15	5
ACSZ–29x	Aleutian–Alaska–Cascadia	201.2606	56.2861	245.7	15	56.24
ACSZ–29y	Aleutian–Alaska–Cascadia	201.5733	55.8888	246	15	43.82
ACSZ–29z	Aleutian–Alaska–Cascadia	201.8797	55.4908	246.2	15	30.88
ACSZ–30a	Aleutian–Alaska–Cascadia	203.6040	55.5090	240	15	17.94
ACSZ–30b	Aleutian–Alaska–Cascadia	203.9970	55.1200	240	15	5
ACSZ–30w	Aleutian–Alaska–Cascadia	201.9901	56.9855	239.5	15	69.12
ACSZ–30x	Aleutian–Alaska–Cascadia	202.3851	56.6094	239.8	15	56.24
ACSZ–30y	Aleutian–Alaska–Cascadia	202.7724	56.2320	240.2	15	43.82
ACSZ–30z	Aleutian–Alaska–Cascadia	203.1521	55.8534	240.5	15	30.88
ACSZ–31a	Aleutian–Alaska–Cascadia	204.8950	55.9700	236	15	17.94
ACSZ–31b	Aleutian–Alaska–Cascadia	205.3400	55.5980	236	15	5
ACSZ–31w	Aleutian–Alaska–Cascadia	203.0825	57.3740	234.5	15	69.12
ACSZ–31x	Aleutian–Alaska–Cascadia	203.5408	57.0182	234.9	15	56.24
ACSZ–31y	Aleutian–Alaska–Cascadia	203.9904	56.6607	235.3	15	43.82
ACSZ–31z	Aleutian–Alaska–Cascadia	204.4315	56.3016	235.7	15	30.88
ACSZ–32a	Aleutian–Alaska–Cascadia	206.2080	56.4730	236	15	17.94
ACSZ–32b	Aleutian–Alaska–Cascadia	206.6580	56.1000	236	15	5
ACSZ–32w	Aleutian–Alaska–Cascadia	204.4129	57.8908	234.3	15	69.12
ACSZ–32x	Aleutian–Alaska–Cascadia	204.8802	57.5358	234.7	15	56.24
ACSZ–32y	Aleutian–Alaska–Cascadia	205.3385	57.1792	235.1	15	43.82
ACSZ–32z	Aleutian–Alaska–Cascadia	205.7880	56.8210	235.5	15	30.88
ACSZ–33a	Aleutian–Alaska–Cascadia	207.5370	56.9750	236	15	17.94
ACSZ–33b	Aleutian–Alaska–Cascadia	207.9930	56.6030	236	15	5
ACSZ–33w	Aleutian–Alaska–Cascadia	205.7126	58.3917	234.2	15	69.12
ACSZ–33x	Aleutian–Alaska–Cascadia	206.1873	58.0371	234.6	15	56.24
ACSZ–33y	Aleutian–Alaska–Cascadia	206.6527	57.6808	235	15	43.82
ACSZ–33z	Aleutian–Alaska–Cascadia	207.1091	57.3227	235.4	15	30.88
ACSZ–34a	Aleutian–Alaska–Cascadia	208.9371	57.5124	236	15	17.94
ACSZ–34b	Aleutian–Alaska–Cascadia	209.4000	57.1400	236	15	5
ACSZ–34w	Aleutian–Alaska–Cascadia	206.9772	58.8804	233.5	15	69.12
ACSZ–34x	Aleutian–Alaska–Cascadia	207.4677	58.5291	233.9	15	56.24
ACSZ–34y	Aleutian–Alaska–Cascadia	207.9485	58.1760	234.3	15	43.82
ACSZ–34z	Aleutian–Alaska–Cascadia	208.4198	57.8213	234.7	15	30.88
ACSZ–35a	Aleutian–Alaska–Cascadia	210.2597	58.0441	230	15	17.94
ACSZ–35b	Aleutian–Alaska–Cascadia	210.8000	57.7000	230	15	5
ACSZ–35w	Aleutian–Alaska–Cascadia	208.0204	59.3199	228.8	15	69.12
ACSZ–35x	Aleutian–Alaska–Cascadia	208.5715	58.9906	229.3	15	56.24
ACSZ–35y	Aleutian–Alaska–Cascadia	209.1122	58.6590	229.7	15	43.82
ACSZ–35z	Aleutian–Alaska–Cascadia	209.6425	58.3252	230.2	15	30.88
ACSZ–36a	Aleutian–Alaska–Cascadia	211.3249	58.6565	218	15	17.94
ACSZ–36b	Aleutian–Alaska–Cascadia	212.0000	58.3800	218	15	5
ACSZ–36w	Aleutian–Alaska–Cascadia	208.5003	59.5894	215.6	15	69.12
ACSZ–36x	Aleutian–Alaska–Cascadia	209.1909	59.3342	216.2	15	56.24
ACSZ–36y	Aleutian–Alaska–Cascadia	209.8711	59.0753	216.8	15	43.82
ACSZ–36z	Aleutian–Alaska–Cascadia	210.5412	58.8129	217.3	15	30.88
ACSZ–37a	Aleutian–Alaska–Cascadia	212.2505	59.2720	213.7	15	17.94
ACSZ–37b	Aleutian–Alaska–Cascadia	212.9519	59.0312	213.7	15	5
ACSZ–37x	Aleutian–Alaska–Cascadia	210.1726	60.0644	213	15	56.24
ACSZ–37y	Aleutian–Alaska–Cascadia	210.8955	59.8251	213.7	15	43.82

Continued on next page

Table B.1 – continued

Segment	Description	Longitude (°E)	Latitude (°N)	Strike (°)	Dip (°)	Depth (km)
ACSZ–37z	Aleutian–Alaska–Cascadia	211.6079	59.5820	214.3	15	30.88
ACSZ–38a	Aleutian–Alaska–Cascadia	214.6555	60.1351	260.1	0	15
ACSZ–38b	Aleutian–Alaska–Cascadia	214.8088	59.6927	260.1	0	15
ACSZ–38y	Aleutian–Alaska–Cascadia	214.3737	60.9838	259	0	15
ACSZ–38z	Aleutian–Alaska–Cascadia	214.5362	60.5429	259	0	15
ACSZ–39a	Aleutian–Alaska–Cascadia	216.5607	60.2480	267	0	15
ACSZ–39b	Aleutian–Alaska–Cascadia	216.6068	59.7994	267	0	15
ACSZ–40a	Aleutian–Alaska–Cascadia	219.3069	59.7574	310.9	0	15
ACSZ–40b	Aleutian–Alaska–Cascadia	218.7288	59.4180	310.9	0	15
ACSZ–41a	Aleutian–Alaska–Cascadia	220.4832	59.3390	300.7	0	15
ACSZ–41b	Aleutian–Alaska–Cascadia	220.0382	58.9529	300.7	0	15
ACSZ–42a	Aleutian–Alaska–Cascadia	221.8835	58.9310	298.9	0	15
ACSZ–42b	Aleutian–Alaska–Cascadia	221.4671	58.5379	298.9	0	15
ACSZ–43a	Aleutian–Alaska–Cascadia	222.9711	58.6934	282.3	0	15
ACSZ–43b	Aleutian–Alaska–Cascadia	222.7887	58.2546	282.3	0	15
ACSZ–44a	Aleutian–Alaska–Cascadia	224.9379	57.9054	340.9	12	11.09
ACSZ–44b	Aleutian–Alaska–Cascadia	224.1596	57.7617	340.9	7	5
ACSZ–45a	Aleutian–Alaska–Cascadia	225.4994	57.1634	334.1	12	11.09
ACSZ–45b	Aleutian–Alaska–Cascadia	224.7740	56.9718	334.1	7	5
ACSZ–46a	Aleutian–Alaska–Cascadia	226.1459	56.3552	334.1	12	11.09
ACSZ–46b	Aleutian–Alaska–Cascadia	225.4358	56.1636	334.1	7	5
ACSZ–47a	Aleutian–Alaska–Cascadia	226.7731	55.5830	332.3	12	11.09
ACSZ–47b	Aleutian–Alaska–Cascadia	226.0887	55.3785	332.3	7	5
ACSZ–48a	Aleutian–Alaska–Cascadia	227.4799	54.6763	339.4	12	11.09
ACSZ–48b	Aleutian–Alaska–Cascadia	226.7713	54.5217	339.4	7	5
ACSZ–49a	Aleutian–Alaska–Cascadia	227.9482	53.8155	341.2	12	11.09
ACSZ–49b	Aleutian–Alaska–Cascadia	227.2462	53.6737	341.2	7	5
ACSZ–50a	Aleutian–Alaska–Cascadia	228.3970	53.2509	324.5	12	11.09
ACSZ–50b	Aleutian–Alaska–Cascadia	227.8027	52.9958	324.5	7	5
ACSZ–51a	Aleutian–Alaska–Cascadia	229.1844	52.6297	318.4	12	11.09
ACSZ–51b	Aleutian–Alaska–Cascadia	228.6470	52.3378	318.4	7	5
ACSZ–52a	Aleutian–Alaska–Cascadia	230.0306	52.0768	310.9	12	11.09
ACSZ–52b	Aleutian–Alaska–Cascadia	229.5665	51.7445	310.9	7	5
ACSZ–53a	Aleutian–Alaska–Cascadia	231.1735	51.5258	310.9	12	11.09
ACSZ–53b	Aleutian–Alaska–Cascadia	230.7150	51.1935	310.9	7	5
ACSZ–54a	Aleutian–Alaska–Cascadia	232.2453	50.8809	314.1	12	11.09
ACSZ–54b	Aleutian–Alaska–Cascadia	231.7639	50.5655	314.1	7	5
ACSZ–55a	Aleutian–Alaska–Cascadia	233.3066	49.9032	333.7	12	11.09
ACSZ–55b	Aleutian–Alaska–Cascadia	232.6975	49.7086	333.7	7	5
ACSZ–56a	Aleutian–Alaska–Cascadia	234.0588	49.1702	315	11	12.82
ACSZ–56b	Aleutian–Alaska–Cascadia	233.5849	48.8584	315	9	5
ACSZ–57a	Aleutian–Alaska–Cascadia	234.9041	48.2596	341	11	12.82
ACSZ–57b	Aleutian–Alaska–Cascadia	234.2797	48.1161	341	9	5
ACSZ–58a	Aleutian–Alaska–Cascadia	235.3021	47.3812	344	11	12.82
ACSZ–58b	Aleutian–Alaska–Cascadia	234.6776	47.2597	344	9	5
ACSZ–59a	Aleutian–Alaska–Cascadia	235.6432	46.5082	345	11	12.82
ACSZ–59b	Aleutian–Alaska–Cascadia	235.0257	46.3941	345	9	5
ACSZ–60a	Aleutian–Alaska–Cascadia	235.8640	45.5429	356	11	12.82
ACSZ–60b	Aleutian–Alaska–Cascadia	235.2363	45.5121	356	9	5
ACSZ–61a	Aleutian–Alaska–Cascadia	235.9106	44.6227	359	11	12.82
ACSZ–61b	Aleutian–Alaska–Cascadia	235.2913	44.6150	359	9	5
ACSZ–62a	Aleutian–Alaska–Cascadia	235.9229	43.7245	359	11	12.82
ACSZ–62b	Aleutian–Alaska–Cascadia	235.3130	43.7168	359	9	5
ACSZ–63a	Aleutian–Alaska–Cascadia	236.0220	42.9020	350	11	12.82
ACSZ–63b	Aleutian–Alaska–Cascadia	235.4300	42.8254	350	9	5
ACSZ–64a	Aleutian–Alaska–Cascadia	235.9638	41.9818	345	11	12.82
ACSZ–64b	Aleutian–Alaska–Cascadia	235.3919	41.8677	345	9	5
ACSZ–65a	Aleutian–Alaska–Cascadia	236.2643	41.1141	345	11	12.82
ACSZ–65b	Aleutian–Alaska–Cascadia	235.7000	41.0000	345	9	5
ACSZ–238a	Aleutian–Alaska–Cascadia	213.2878	59.8406	236.8	15	17.94
ACSZ–238y	Aleutian–Alaska–Cascadia	212.3424	60.5664	236.8	15	43.82
ACSZ–238z	Aleutian–Alaska–Cascadia	212.8119	60.2035	236.8	15	30.88

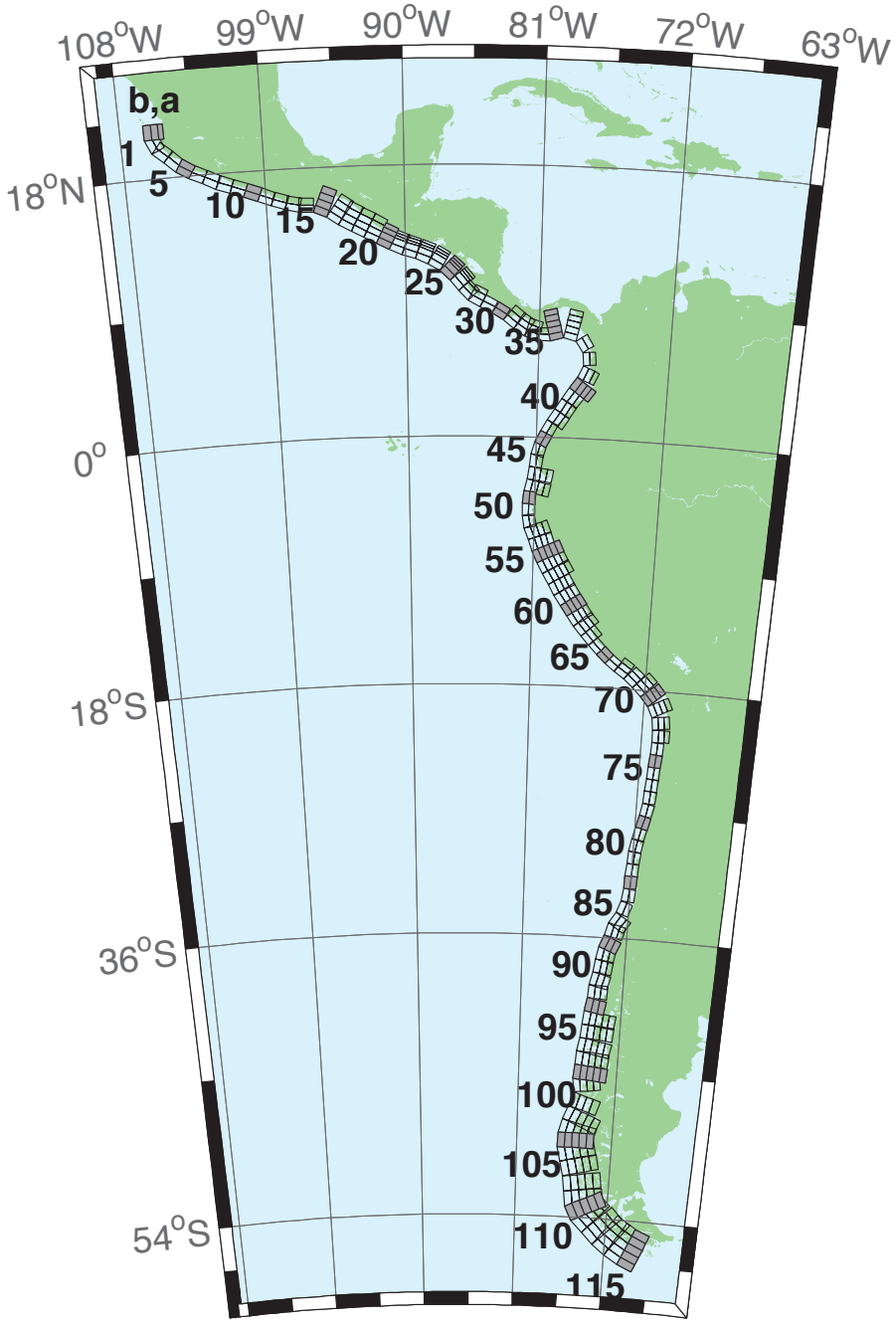

Figure B.2: Central and South America Subduction Zone (CSSZ) unit sources.

Table B.2: Earthquake parameters for Central and South America Subduction Zone (CSSZ) unit sources.

Segment	Description	Longitude (°E)	Latitude (°N)	Strike (°)	Dip (°)	Depth (km)
CSSZ–1a	Central and South America	254.4573	20.8170	359	19	15.4
CSSZ–1b	Central and South America	254.0035	20.8094	359	12	5
CSSZ–1z	Central and South America	254.7664	20.8222	359	50	31.67
CSSZ–2a	Central and South America	254.5765	20.2806	336.8	19	15.4
CSSZ–2b	Central and South America	254.1607	20.1130	336.8	12	5
CSSZ–3a	Central and South America	254.8789	19.8923	310.6	18.31	15.27
CSSZ–3b	Central and South America	254.5841	19.5685	310.6	11.85	5
CSSZ–4a	Central and South America	255.6167	19.2649	313.4	17.62	15.12
CSSZ–4b	Central and South America	255.3056	18.9537	313.4	11.68	5
CSSZ–5a	Central and South America	256.2240	18.8148	302.7	16.92	15
CSSZ–5b	Central and South America	255.9790	18.4532	302.7	11.54	5
CSSZ–6a	Central and South America	256.9425	18.4383	295.1	16.23	14.87
CSSZ–6b	Central and South America	256.7495	18.0479	295.1	11.38	5
CSSZ–7a	Central and South America	257.8137	18.0339	296.9	15.54	14.74
CSSZ–7b	Central and South America	257.6079	17.6480	296.9	11.23	5
CSSZ–8a	Central and South America	258.5779	17.7151	290.4	14.85	14.61
CSSZ–8b	Central and South America	258.4191	17.3082	290.4	11.08	5
CSSZ–9a	Central and South America	259.4578	17.4024	290.5	14.15	14.47
CSSZ–9b	Central and South America	259.2983	16.9944	290.5	10.92	5
CSSZ–10a	Central and South America	260.3385	17.0861	290.8	13.46	14.34
CSSZ–10b	Central and South America	260.1768	16.6776	290.8	10.77	5
CSSZ–11a	Central and South America	261.2255	16.7554	291.8	12.77	14.21
CSSZ–11b	Central and South America	261.0556	16.3487	291.8	10.62	5
CSSZ–12a	Central and South America	262.0561	16.4603	288.9	12.08	14.08
CSSZ–12b	Central and South America	261.9082	16.0447	288.9	10.46	5
CSSZ–13a	Central and South America	262.8638	16.2381	283.2	11.38	13.95
CSSZ–13b	Central and South America	262.7593	15.8094	283.2	10.31	5
CSSZ–14a	Central and South America	263.6066	16.1435	272.1	10.69	13.81
CSSZ–14b	Central and South America	263.5901	15.7024	272.1	10.15	5
CSSZ–15a	Central and South America	264.8259	15.8829	293	10	13.68
CSSZ–15b	Central and South America	264.6462	15.4758	293	10	5
CSSZ–15y	Central and South America	265.1865	16.6971	293	10	31.05
CSSZ–15z	Central and South America	265.0060	16.2900	293	10	22.36
CSSZ–16a	Central and South America	265.7928	15.3507	304.9	15	15.82
CSSZ–16b	Central and South America	265.5353	14.9951	304.9	12.5	5
CSSZ–16y	Central and South America	266.3092	16.0619	304.9	15	41.7
CSSZ–16z	Central and South America	266.0508	15.7063	304.9	15	28.76
CSSZ–17a	Central and South America	266.4947	14.9019	299.5	20	17.94
CSSZ–17b	Central and South America	266.2797	14.5346	299.5	15	5
CSSZ–17y	Central and South America	266.9259	15.6365	299.5	20	52.14
CSSZ–17z	Central and South America	266.7101	15.2692	299.5	20	35.04
CSSZ–18a	Central and South America	267.2827	14.4768	298	21.5	17.94
CSSZ–18b	Central and South America	267.0802	14.1078	298	15	5
CSSZ–18y	Central and South America	267.6888	15.2148	298	21.5	54.59
CSSZ–18z	Central and South America	267.4856	14.8458	298	21.5	36.27
CSSZ–19a	Central and South America	268.0919	14.0560	297.6	23	17.94
CSSZ–19b	Central and South America	267.8943	13.6897	297.6	15	5
CSSZ–19y	Central and South America	268.4880	14.7886	297.6	23	57.01
CSSZ–19z	Central and South America	268.2898	14.4223	297.6	23	37.48
CSSZ–20a	Central and South America	268.8929	13.6558	296.2	24	17.94
CSSZ–20b	Central and South America	268.7064	13.2877	296.2	15	5
CSSZ–20y	Central and South America	269.1796	14.2206	296.2	45.5	73.94
CSSZ–20z	Central and South America	269.0362	13.9382	296.2	45.5	38.28
CSSZ–21a	Central and South America	269.6797	13.3031	292.6	25	17.94
CSSZ–21b	Central and South America	269.5187	12.9274	292.6	15	5
CSSZ–21x	Central and South America	269.8797	13.7690	292.6	68	131.8
CSSZ–21y	Central and South America	269.8130	13.6137	292.6	68	85.43
CSSZ–21z	Central and South America	269.7463	13.4584	292.6	68	39.07
CSSZ–22a	Central and South America	270.4823	13.0079	288.6	25	17.94
CSSZ–22b	Central and South America	270.3492	12.6221	288.6	15	5

Continued on next page

Table B.2 – continued

Segment	Description	Longitude (°E)	Latitude (°N)	Strike (°)	Dip (°)	Depth (km)
CSSZ–22x	Central and South America	270.6476	13.4864	288.6	68	131.8
CSSZ–22y	Central and South America	270.5925	13.3269	288.6	68	85.43
CSSZ–22z	Central and South America	270.5374	13.1674	288.6	68	39.07
CSSZ–23a	Central and South America	271.3961	12.6734	292.4	25	17.94
CSSZ–23b	Central and South America	271.2369	12.2972	292.4	15	5
CSSZ–23x	Central and South America	271.5938	13.1399	292.4	68	131.8
CSSZ–23y	Central and South America	271.5279	12.9844	292.4	68	85.43
CSSZ–23z	Central and South America	271.4620	12.8289	292.4	68	39.07
CSSZ–24a	Central and South America	272.3203	12.2251	300.2	25	17.94
CSSZ–24b	Central and South America	272.1107	11.8734	300.2	15	5
CSSZ–24x	Central and South America	272.5917	12.6799	300.2	67	131.1
CSSZ–24y	Central and South America	272.5012	12.5283	300.2	67	85.1
CSSZ–24z	Central and South America	272.4107	12.3767	300.2	67	39.07
CSSZ–25a	Central and South America	273.2075	11.5684	313.8	25	17.94
CSSZ–25b	Central and South America	272.9200	11.2746	313.8	15	5
CSSZ–25x	Central and South America	273.5950	11.9641	313.8	66	130.4
CSSZ–25y	Central and South America	273.4658	11.8322	313.8	66	84.75
CSSZ–25z	Central and South America	273.3366	11.7003	313.8	66	39.07
CSSZ–26a	Central and South America	273.8943	10.8402	320.4	25	17.94
CSSZ–26b	Central and South America	273.5750	10.5808	320.4	15	5
CSSZ–26x	Central and South America	274.3246	11.1894	320.4	66	130.4
CSSZ–26y	Central and South America	274.1811	11.0730	320.4	66	84.75
CSSZ–26z	Central and South America	274.0377	10.9566	320.4	66	39.07
CSSZ–27a	Central and South America	274.4569	10.2177	316.1	25	17.94
CSSZ–27b	Central and South America	274.1590	9.9354	316.1	15	5
CSSZ–27z	Central and South America	274.5907	10.3444	316.1	66	39.07
CSSZ–28a	Central and South America	274.9586	9.8695	297.1	22	14.54
CSSZ–28b	Central and South America	274.7661	9.4988	297.1	11	5
CSSZ–28z	Central and South America	275.1118	10.1643	297.1	42.5	33.27
CSSZ–29a	Central and South America	275.7686	9.4789	296.6	19	11.09
CSSZ–29b	Central and South America	275.5759	9.0992	296.6	7	5
CSSZ–30a	Central and South America	276.6346	8.9973	302.2	19	9.36
CSSZ–30b	Central and South America	276.4053	8.6381	302.2	5	5
CSSZ–31a	Central and South America	277.4554	8.4152	309.1	19	7.62
CSSZ–31b	Central and South America	277.1851	8.0854	309.1	3	5
CSSZ–31z	Central and South America	277.7260	8.7450	309.1	19	23.9
CSSZ–32a	Central and South America	278.1112	7.9425	303	18.67	8.49
CSSZ–32b	Central and South America	277.8775	7.5855	303	4	5
CSSZ–32z	Central and South America	278.3407	8.2927	303	21.67	24.49
CSSZ–33a	Central and South America	278.7082	7.6620	287.6	18.33	10.23
CSSZ–33b	Central and South America	278.5785	7.2555	287.6	6	5
CSSZ–33z	Central and South America	278.8328	8.0522	287.6	24.33	25.95
CSSZ–34a	Central and South America	279.3184	7.5592	269.5	18	17.94
CSSZ–34b	Central and South America	279.3223	7.1320	269.5	15	5
CSSZ–35a	Central and South America	280.0039	7.6543	255.9	17.67	14.54
CSSZ–35b	Central and South America	280.1090	7.2392	255.9	11	5
CSSZ–35x	Central and South America	279.7156	8.7898	255.9	29.67	79.22
CSSZ–35y	Central and South America	279.8118	8.4113	255.9	29.67	54.47
CSSZ–35z	Central and South America	279.9079	8.0328	255.9	29.67	29.72
CSSZ–36a	Central and South America	281.2882	7.6778	282.5	17.33	11.09
CSSZ–36b	Central and South America	281.1948	7.2592	282.5	7	5
CSSZ–36x	Central and South America	281.5368	8.7896	282.5	32.33	79.47
CSSZ–36y	Central and South America	281.4539	8.4190	282.5	32.33	52.73
CSSZ–36z	Central and South America	281.3710	8.0484	282.5	32.33	25.99
CSSZ–37a	Central and South America	282.5252	6.8289	326.9	17	10.23
CSSZ–37b	Central and South America	282.1629	6.5944	326.9	6	5
CSSZ–38a	Central and South America	282.9469	5.5973	355.4	17	10.23
CSSZ–38b	Central and South America	282.5167	5.5626	355.4	6	5
CSSZ–39a	Central and South America	282.7236	4.3108	24.13	17	10.23
CSSZ–39b	Central and South America	282.3305	4.4864	24.13	6	5
CSSZ–39z	Central and South America	283.0603	4.1604	24.13	35	24.85
CSSZ–40a	Central and South America	282.1940	3.3863	35.28	17	10.23

Continued on next page

Table B.2 – continued

Segment	Description	Longitude (°E)	Latitude (°N)	Strike (°)	Dip (°)	Depth (km)
CSSZ–40b	Central and South America	281.8427	3.6344	35.28	6	5
CSSZ–40y	Central and South America	282.7956	2.9613	35.28	35	53.52
CSSZ–40z	Central and South America	282.4948	3.1738	35.28	35	24.85
CSSZ–41a	Central and South America	281.6890	2.6611	34.27	17	10.23
CSSZ–41b	Central and South America	281.3336	2.9030	34.27	6	5
CSSZ–41z	Central and South America	281.9933	2.4539	34.27	35	24.85
CSSZ–42a	Central and South America	281.2266	1.9444	31.29	17	10.23
CSSZ–42b	Central and South America	280.8593	2.1675	31.29	6	5
CSSZ–42z	Central and South America	281.5411	1.7533	31.29	35	24.85
CSSZ–43a	Central and South America	280.7297	1.1593	33.3	17	10.23
CSSZ–43b	Central and South America	280.3706	1.3951	33.3	6	5
CSSZ–43z	Central and South America	281.0373	0.9573	33.3	35	24.85
CSSZ–44a	Central and South America	280.3018	0.4491	28.8	17	10.23
CSSZ–44b	Central and South America	279.9254	0.6560	28.8	6	5
CSSZ–45a	Central and South America	279.9083	-0.3259	26.91	10	8.49
CSSZ–45b	Central and South America	279.5139	-0.1257	26.91	4	5
CSSZ–46a	Central and South America	279.6461	-0.9975	15.76	10	8.49
CSSZ–46b	Central and South America	279.2203	-0.8774	15.76	4	5
CSSZ–47a	Central and South America	279.4972	-1.7407	6.9	10	8.49
CSSZ–47b	Central and South America	279.0579	-1.6876	6.9	4	5
CSSZ–48a	Central and South America	279.3695	-2.6622	8.96	10	8.49
CSSZ–48b	Central and South America	278.9321	-2.5933	8.96	4	5
CSSZ–48y	Central and South America	280.2444	-2.8000	8.96	10	25.85
CSSZ–48z	Central and South America	279.8070	-2.7311	8.96	10	17.17
CSSZ–49a	Central and South America	279.1852	-3.6070	13.15	10	8.49
CSSZ–49b	Central and South America	278.7536	-3.5064	13.15	4	5
CSSZ–49y	Central and South America	280.0486	-3.8082	13.15	10	25.85
CSSZ–49z	Central and South America	279.6169	-3.7076	13.15	10	17.17
CSSZ–50a	Central and South America	279.0652	-4.3635	4.78	10.33	9.64
CSSZ–50b	Central and South America	278.6235	-4.3267	4.78	5.33	5
CSSZ–51a	Central and South America	279.0349	-5.1773	359.4	10.67	10.81
CSSZ–51b	Central and South America	278.5915	-5.1817	359.4	6.67	5
CSSZ–52a	Central and South America	279.1047	-5.9196	349.8	11	11.96
CSSZ–52b	Central and South America	278.6685	-5.9981	349.8	8	5
CSSZ–53a	Central and South America	279.3044	-6.6242	339.2	10.25	11.74
CSSZ–53b	Central and South America	278.8884	-6.7811	339.2	7.75	5
CSSZ–53y	Central and South America	280.1024	-6.3232	339.2	19.25	37.12
CSSZ–53z	Central and South America	279.7035	-6.4737	339.2	19.25	20.64
CSSZ–54a	Central and South America	279.6256	-7.4907	340.8	9.5	11.53
CSSZ–54b	Central and South America	279.2036	-7.6365	340.8	7.5	5
CSSZ–54y	Central and South America	280.4267	-7.2137	340.8	20.5	37.29
CSSZ–54z	Central and South America	280.0262	-7.3522	340.8	20.5	19.78
CSSZ–55a	Central and South America	279.9348	-8.2452	335.4	8.75	11.74
CSSZ–55b	Central and South America	279.5269	-8.4301	335.4	7.75	5
CSSZ–55x	Central and South America	281.0837	-7.7238	335.4	21.75	56.4
CSSZ–55y	Central and South America	280.7009	-7.8976	335.4	21.75	37.88
CSSZ–55z	Central and South America	280.3180	-8.0714	335.4	21.75	19.35
CSSZ–56a	Central and South America	280.3172	-8.9958	331.6	8	11.09
CSSZ–56b	Central and South America	279.9209	-9.2072	331.6	7	5
CSSZ–56x	Central and South America	281.4212	-8.4063	331.6	23	57.13
CSSZ–56y	Central and South America	281.0534	-8.6028	331.6	23	37.59
CSSZ–56z	Central and South America	280.6854	-8.7993	331.6	23	18.05
CSSZ–57a	Central and South America	280.7492	-9.7356	328.7	8.6	10.75
CSSZ–57b	Central and South America	280.3640	-9.9663	328.7	6.6	5
CSSZ–57x	Central and South America	281.8205	-9.0933	328.7	23.4	57.94
CSSZ–57y	Central and South America	281.4636	-9.3074	328.7	23.4	38.08
CSSZ–57z	Central and South America	281.1065	-9.5215	328.7	23.4	18.22
CSSZ–58a	Central and South America	281.2275	-10.5350	330.5	9.2	10.4
CSSZ–58b	Central and South America	280.8348	-10.7532	330.5	6.2	5
CSSZ–58y	Central and South America	281.9548	-10.1306	330.5	23.8	38.57
CSSZ–58z	Central and South America	281.5913	-10.3328	330.5	23.8	18.39
CSSZ–59a	Central and South America	281.6735	-11.2430	326.2	9.8	10.05

Continued on next page

Table B.2 – continued

Segment	Description	Longitude (°E)	Latitude (°N)	Strike (°)	Dip (°)	Depth (km)
CSSZ–59b	Central and South America	281.2982	-11.4890	326.2	5.8	5
CSSZ–59y	Central and South America	282.3675	-10.7876	326.2	24.2	39.06
CSSZ–59z	Central and South America	282.0206	-11.0153	326.2	24.2	18.56
CSSZ–60a	Central and South America	282.1864	-11.9946	326.5	10.4	9.71
CSSZ–60b	Central and South America	281.8096	-12.2384	326.5	5.4	5
CSSZ–60y	Central and South America	282.8821	-11.5438	326.5	24.6	39.55
CSSZ–60z	Central and South America	282.5344	-11.7692	326.5	24.6	18.73
CSSZ–61a	Central and South America	282.6944	-12.7263	325.5	11	9.36
CSSZ–61b	Central and South America	282.3218	-12.9762	325.5	5	5
CSSZ–61y	Central and South America	283.3814	-12.2649	325.5	25	40.03
CSSZ–61z	Central and South America	283.0381	-12.4956	325.5	25	18.9
CSSZ–62a	Central and South America	283.1980	-13.3556	319	11	9.79
CSSZ–62b	Central and South America	282.8560	-13.6451	319	5.5	5
CSSZ–62y	Central and South America	283.8178	-12.8300	319	27	42.03
CSSZ–62z	Central and South America	283.5081	-13.0928	319	27	19.33
CSSZ–63a	Central and South America	283.8032	-14.0147	317.9	11	10.23
CSSZ–63b	Central and South America	283.4661	-14.3106	317.9	6	5
CSSZ–63z	Central and South America	284.1032	-13.7511	317.9	29	19.77
CSSZ–64a	Central and South America	284.4144	-14.6482	315.7	13	11.96
CSSZ–64b	Central and South America	284.0905	-14.9540	315.7	8	5
CSSZ–65a	Central and South America	285.0493	-15.2554	313.2	15	13.68
CSSZ–65b	Central and South America	284.7411	-15.5715	313.2	10	5
CSSZ–66a	Central and South America	285.6954	-15.7816	307.7	14.5	13.68
CSSZ–66b	Central and South America	285.4190	-16.1258	307.7	10	5
CSSZ–67a	Central and South America	286.4127	-16.2781	304.3	14	13.68
CSSZ–67b	Central and South America	286.1566	-16.6381	304.3	10	5
CSSZ–67z	Central and South America	286.6552	-15.9365	304.3	23	25.78
CSSZ–68a	Central and South America	287.2481	-16.9016	311.8	14	13.68
CSSZ–68b	Central and South America	286.9442	-17.2264	311.8	10	5
CSSZ–68z	Central and South America	287.5291	-16.6007	311.8	26	25.78
CSSZ–69a	Central and South America	287.9724	-17.5502	314.9	14	13.68
CSSZ–69b	Central and South America	287.6496	-17.8590	314.9	10	5
CSSZ–69y	Central and South America	288.5530	-16.9934	314.9	29	50.02
CSSZ–69z	Central and South America	288.2629	-17.2718	314.9	29	25.78
CSSZ–70a	Central and South America	288.6731	-18.2747	320.4	14	13.25
CSSZ–70b	Central and South America	288.3193	-18.5527	320.4	9.5	5
CSSZ–70y	Central and South America	289.3032	-17.7785	320.4	30	50.35
CSSZ–70z	Central and South America	288.9884	-18.0266	320.4	30	25.35
CSSZ–71a	Central and South America	289.3089	-19.1854	333.2	14	12.82
CSSZ–71b	Central and South America	288.8968	-19.3820	333.2	9	5
CSSZ–71y	Central and South America	290.0357	-18.8382	333.2	31	50.67
CSSZ–71z	Central and South America	289.6725	-19.0118	333.2	31	24.92
CSSZ–72a	Central and South America	289.6857	-20.3117	352.4	14	12.54
CSSZ–72b	Central and South America	289.2250	-20.3694	352.4	8.67	5
CSSZ–72z	Central and South America	290.0882	-20.2613	352.4	32	24.63
CSSZ–73a	Central and South America	289.7731	-21.3061	358.9	14	12.24
CSSZ–73b	Central and South America	289.3053	-21.3142	358.9	8.33	5
CSSZ–73z	Central and South America	290.1768	-21.2991	358.9	33	24.34
CSSZ–74a	Central and South America	289.7610	-22.2671	3.06	14	11.96
CSSZ–74b	Central and South America	289.2909	-22.2438	3.06	8	5
CSSZ–75a	Central and South America	289.6982	-23.1903	4.83	14.09	11.96
CSSZ–75b	Central and South America	289.2261	-23.1536	4.83	8	5
CSSZ–76a	Central and South America	289.6237	-24.0831	4.67	14.18	11.96
CSSZ–76b	Central and South America	289.1484	-24.0476	4.67	8	5
CSSZ–77a	Central and South America	289.5538	-24.9729	4.3	14.27	11.96
CSSZ–77b	Central and South America	289.0750	-24.9403	4.3	8	5
CSSZ–78a	Central and South America	289.4904	-25.8621	3.86	14.36	11.96
CSSZ–78b	Central and South America	289.0081	-25.8328	3.86	8	5
CSSZ–79a	Central and South America	289.3491	-26.8644	11.34	14.45	11.96
CSSZ–79b	Central and South America	288.8712	-26.7789	11.34	8	5
CSSZ–80a	Central and South America	289.1231	-27.7826	14.16	14.54	11.96
CSSZ–80b	Central and South America	288.6469	-27.6762	14.16	8	5

Continued on next page

Table B.2 – continued

Segment	Description	Longitude (°E)	Latitude (°N)	Strike (°)	Dip (°)	Depth (km)
CSSZ–81a	Central and South America	288.8943	-28.6409	13.19	14.63	11.96
CSSZ–81b	Central and South America	288.4124	-28.5417	13.19	8	5
CSSZ–82a	Central and South America	288.7113	-29.4680	9.68	14.72	11.96
CSSZ–82b	Central and South America	288.2196	-29.3950	9.68	8	5
CSSZ–83a	Central and South America	288.5944	-30.2923	5.36	14.81	11.96
CSSZ–83b	Central and South America	288.0938	-30.2517	5.36	8	5
CSSZ–84a	Central and South America	288.5223	-31.1639	3.8	14.9	11.96
CSSZ–84b	Central and South America	288.0163	-31.1351	3.8	8	5
CSSZ–85a	Central and South America	288.4748	-32.0416	2.55	15	11.96
CSSZ–85b	Central and South America	287.9635	-32.0223	2.55	8	5
CSSZ–86a	Central and South America	288.3901	-33.0041	7.01	15	11.96
CSSZ–86b	Central and South America	287.8768	-32.9512	7.01	8	5
CSSZ–87a	Central and South America	288.1050	-34.0583	19.4	15	11.96
CSSZ–87b	Central and South America	287.6115	-33.9142	19.4	8	5
CSSZ–88a	Central and South America	287.5309	-35.0437	32.81	15	11.96
CSSZ–88b	Central and South America	287.0862	-34.8086	32.81	8	5
CSSZ–88z	Central and South America	287.9308	-35.2545	32.81	30	24.9
CSSZ–89a	Central and South America	287.2380	-35.5993	14.52	16.67	11.96
CSSZ–89b	Central and South America	286.7261	-35.4914	14.52	8	5
CSSZ–89z	Central and South America	287.7014	-35.6968	14.52	30	26.3
CSSZ–90a	Central and South America	286.8442	-36.5645	22.64	18.33	11.96
CSSZ–90b	Central and South America	286.3548	-36.4004	22.64	8	5
CSSZ–90z	Central and South America	287.2916	-36.7142	22.64	30	27.68
CSSZ–91a	Central and South America	286.5925	-37.2488	10.9	20	11.96
CSSZ–91b	Central and South America	286.0721	-37.1690	10.9	8	5
CSSZ–91z	Central and South America	287.0726	-37.3224	10.9	30	29.06
CSSZ–92a	Central and South America	286.4254	-38.0945	8.23	20	11.96
CSSZ–92b	Central and South America	285.8948	-38.0341	8.23	8	5
CSSZ–92z	Central and South America	286.9303	-38.1520	8.23	26.67	29.06
CSSZ–93a	Central and South America	286.2047	-39.0535	13.46	20	11.96
CSSZ–93b	Central and South America	285.6765	-38.9553	13.46	8	5
CSSZ–93z	Central and South America	286.7216	-39.1495	13.46	23.33	29.06
CSSZ–94a	Central and South America	286.0772	-39.7883	3.4	20	11.96
CSSZ–94b	Central and South America	285.5290	-39.7633	3.4	8	5
CSSZ–94z	Central and South America	286.6255	-39.8133	3.4	20	29.06
CSSZ–95a	Central and South America	285.9426	-40.7760	9.84	20	11.96
CSSZ–95b	Central and South America	285.3937	-40.7039	9.84	8	5
CSSZ–95z	Central and South America	286.4921	-40.8481	9.84	20	29.06
CSSZ–96a	Central and South America	285.7839	-41.6303	7.6	20	11.96
CSSZ–96b	Central and South America	285.2245	-41.5745	7.6	8	5
CSSZ–96x	Central and South America	287.4652	-41.7977	7.6	20	63.26
CSSZ–96y	Central and South America	286.9043	-41.7419	7.6	20	46.16
CSSZ–96z	Central and South America	286.3439	-41.6861	7.6	20	29.06
CSSZ–97a	Central and South America	285.6695	-42.4882	5.3	20	11.96
CSSZ–97b	Central and South America	285.0998	-42.4492	5.3	8	5
CSSZ–97x	Central and South America	287.3809	-42.6052	5.3	20	63.26
CSSZ–97y	Central and South America	286.8101	-42.5662	5.3	20	46.16
CSSZ–97z	Central and South America	286.2396	-42.5272	5.3	20	29.06
CSSZ–98a	Central and South America	285.5035	-43.4553	10.53	20	11.96
CSSZ–98b	Central and South America	284.9322	-43.3782	10.53	8	5
CSSZ–98x	Central and South America	287.2218	-43.6866	10.53	20	63.26
CSSZ–98y	Central and South America	286.6483	-43.6095	10.53	20	46.16
CSSZ–98z	Central and South America	286.0755	-43.5324	10.53	20	29.06
CSSZ–99a	Central and South America	285.3700	-44.2595	4.86	20	11.96
CSSZ–99b	Central and South America	284.7830	-44.2237	4.86	8	5
CSSZ–99x	Central and South America	287.1332	-44.3669	4.86	20	63.26
CSSZ–99y	Central and South America	286.5451	-44.3311	4.86	20	46.16
CSSZ–99z	Central and South America	285.9574	-44.2953	4.86	20	29.06
CSSZ–100a	Central and South America	285.2713	-45.1664	5.68	20	11.96
CSSZ–100b	Central and South America	284.6758	-45.1246	5.68	8	5
CSSZ–100x	Central and South America	287.0603	-45.2918	5.68	20	63.26
CSSZ–100y	Central and South America	286.4635	-45.2500	5.68	20	46.16

Continued on next page

Table B.2 – continued

Segment	Description	Longitude (°E)	Latitude (°N)	Strike (°)	Dip (°)	Depth (km)
CSSZ–100z	Central and South America	285.8672	-45.2082	5.68	20	29.06
CSSZ–101a	Central and South America	285.3080	-45.8607	352.6	20	9.36
CSSZ–101b	Central and South America	284.7067	-45.9152	352.6	5	5
CSSZ–101y	Central and South America	286.5089	-45.7517	352.6	20	43.56
CSSZ–101z	Central and South America	285.9088	-45.8062	352.6	20	26.46
CSSZ–102a	Central and South America	285.2028	-47.1185	17.72	5	9.36
CSSZ–102b	Central and South America	284.5772	-46.9823	17.72	5	5
CSSZ–102y	Central and South America	286.4588	-47.3909	17.72	5	18.07
CSSZ–102z	Central and South America	285.8300	-47.2547	17.72	5	13.72
CSSZ–103a	Central and South America	284.7075	-48.0396	23.37	7.5	11.53
CSSZ–103b	Central and South America	284.0972	-47.8630	23.37	7.5	5
CSSZ–103x	Central and South America	286.5511	-48.5694	23.37	7.5	31.11
CSSZ–103y	Central and South America	285.9344	-48.3928	23.37	7.5	24.58
CSSZ–103z	Central and South America	285.3199	-48.2162	23.37	7.5	18.05
CSSZ–104a	Central and South America	284.3440	-48.7597	14.87	10	13.68
CSSZ–104b	Central and South America	283.6962	-48.6462	14.87	10	5
CSSZ–104x	Central and South America	286.2962	-49.1002	14.87	10	39.73
CSSZ–104y	Central and South America	285.6440	-48.9867	14.87	10	31.05
CSSZ–104z	Central and South America	284.9933	-48.8732	14.87	10	22.36
CSSZ–105a	Central and South America	284.2312	-49.4198	0.25	9.67	13.4
CSSZ–105b	Central and South America	283.5518	-49.4179	0.25	9.67	5
CSSZ–105x	Central and South America	286.2718	-49.4255	0.25	9.67	38.59
CSSZ–105y	Central and South America	285.5908	-49.4236	0.25	9.67	30.2
CSSZ–105z	Central and South America	284.9114	-49.4217	0.25	9.67	21.8
CSSZ–106a	Central and South America	284.3730	-50.1117	347.5	9.25	13.04
CSSZ–106b	Central and South America	283.6974	-50.2077	347.5	9.25	5
CSSZ–106x	Central and South America	286.3916	-49.8238	347.5	9.25	37.15
CSSZ–106y	Central and South America	285.7201	-49.9198	347.5	9.25	29.11
CSSZ–106z	Central and South America	285.0472	-50.0157	347.5	9.25	21.07
CSSZ–107a	Central and South America	284.7130	-50.9714	346.5	9	12.82
CSSZ–107b	Central and South America	284.0273	-51.0751	346.5	9	5
CSSZ–107x	Central and South America	286.7611	-50.6603	346.5	9	36.29
CSSZ–107y	Central and South America	286.0799	-50.7640	346.5	9	28.47
CSSZ–107z	Central and South America	285.3972	-50.8677	346.5	9	20.64
CSSZ–108a	Central and South America	285.0378	-51.9370	352	8.67	12.54
CSSZ–108b	Central and South America	284.3241	-51.9987	352	8.67	5
CSSZ–108x	Central and South America	287.1729	-51.7519	352	8.67	35.15
CSSZ–108y	Central and South America	286.4622	-51.8136	352	8.67	27.61
CSSZ–108z	Central and South America	285.7505	-51.8753	352	8.67	20.07
CSSZ–109a	Central and South America	285.2635	-52.8439	353.1	8.33	12.24
CSSZ–109b	Central and South America	284.5326	-52.8974	353.1	8.33	5
CSSZ–109x	Central and South America	287.4508	-52.6834	353.1	8.33	33.97
CSSZ–109y	Central and South America	286.7226	-52.7369	353.1	8.33	26.73
CSSZ–109z	Central and South America	285.9935	-52.7904	353.1	8.33	19.49
CSSZ–110a	Central and South America	285.5705	-53.4139	334.2	8	11.96
CSSZ–110b	Central and South America	284.8972	-53.6076	334.2	8	5
CSSZ–110x	Central and South America	287.5724	-52.8328	334.2	8	32.83
CSSZ–110y	Central and South America	286.9081	-53.0265	334.2	8	25.88
CSSZ–110z	Central and South America	286.2408	-53.2202	334.2	8	18.92
CSSZ–111a	Central and South America	286.1627	-53.8749	313.8	8	11.96
CSSZ–111b	Central and South America	285.6382	-54.1958	313.8	8	5
CSSZ–111x	Central and South America	287.7124	-52.9122	313.8	8	32.83
CSSZ–111y	Central and South America	287.1997	-53.2331	313.8	8	25.88
CSSZ–111z	Central and South America	286.6832	-53.5540	313.8	8	18.92
CSSZ–112a	Central and South America	287.3287	-54.5394	316.4	8	11.96
CSSZ–112b	Central and South America	286.7715	-54.8462	316.4	8	5
CSSZ–112x	Central and South America	288.9756	-53.6190	316.4	8	32.83
CSSZ–112y	Central and South America	288.4307	-53.9258	316.4	8	25.88
CSSZ–112z	Central and South America	287.8817	-54.2326	316.4	8	18.92
CSSZ–113a	Central and South America	288.3409	-55.0480	307.6	8	11.96
CSSZ–113b	Central and South America	287.8647	-55.4002	307.6	8	5
CSSZ–113x	Central and South America	289.7450	-53.9914	307.6	8	32.83
CSSZ–113y	Central and South America	289.2810	-54.3436	307.6	8	25.88
CSSZ–113z	Central and South America	288.8130	-54.6958	307.6	8	18.92
CSSZ–114a	Central and South America	289.5342	-55.5026	301.5	8	11.96

Continued on next page

Table B.2 – continued

Segment	Description	Longitude (°E)	Latitude (°N)	Strike (°)	Dip (°)	Depth (km)
CSSZ–114b	Central and South America	289.1221	-55.8819	301.5	8	5
CSSZ–114x	Central and South America	290.7472	-54.3647	301.5	8	32.83
CSSZ–114y	Central and South America	290.3467	-54.7440	301.5	8	25.88
CSSZ–114z	Central and South America	289.9424	-55.1233	301.5	8	18.92
CSSZ–115a	Central and South America	290.7682	-55.8485	292.7	8	11.96
CSSZ–115b	Central and South America	290.4608	-56.2588	292.7	8	5
CSSZ–115x	Central and South America	291.6714	-54.6176	292.7	8	32.83
CSSZ–115y	Central and South America	291.3734	-55.0279	292.7	8	25.88
CSSZ–115z	Central and South America	291.0724	-55.4382	292.7	8	18.92

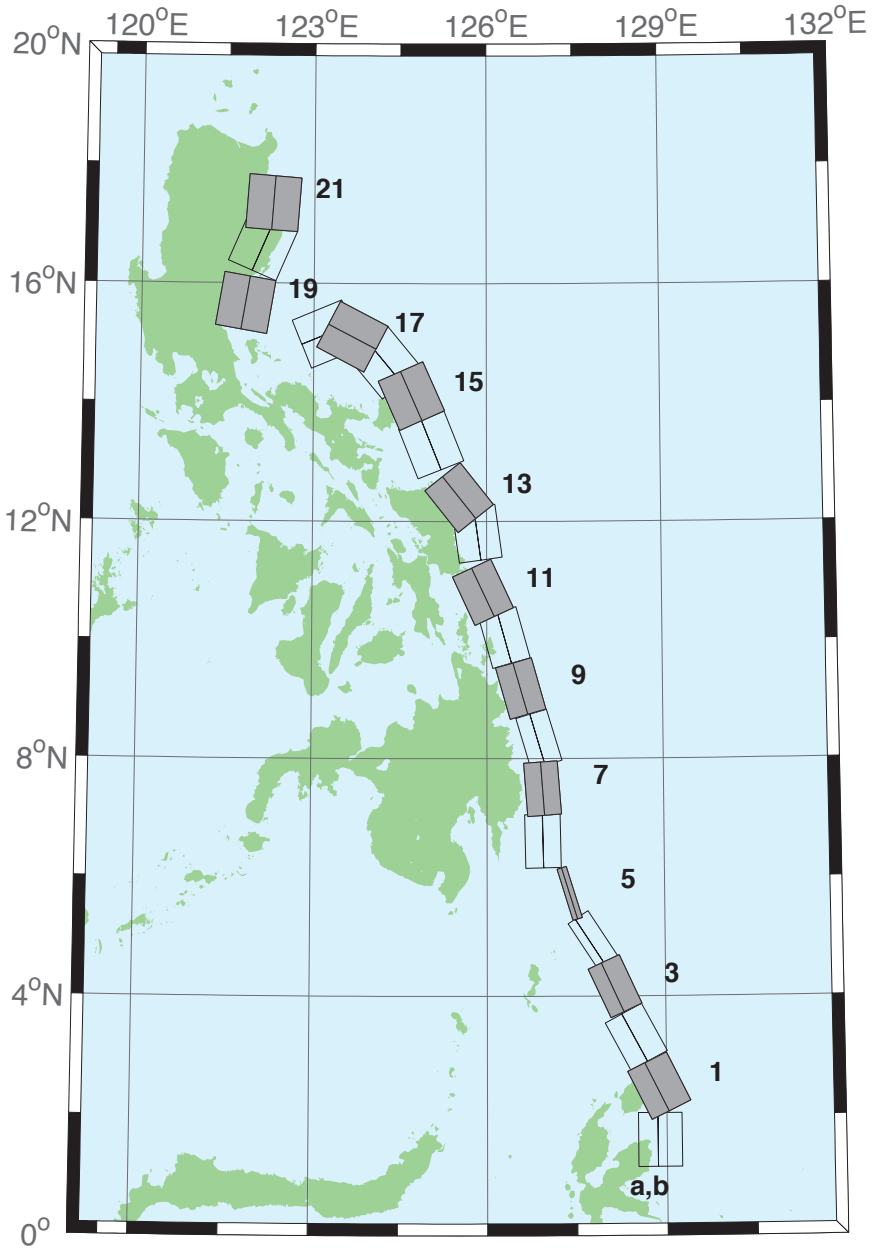

Figure B.3: Eastern Philippines Subduction Zone (EPSZ) unit sources.

Table B.3: Earthquake parameters for Eastern Philippines Subduction Zone (EPSZ) unit sources.

Segment	Description	Longitude (°E)	Latitude (°N)	Strike (°)	Dip (°)	Depth (km)
EPSZ–0a	Eastern Philippines	128.5264	1.5930	180	44	26.92
EPSZ–0b	Eastern Philippines	128.8496	1.5930	180	26	5
EPSZ–1a	Eastern Philippines	128.5521	2.3289	153.6	44.2	27.62
EPSZ–1b	Eastern Philippines	128.8408	2.4720	153.6	26.9	5
EPSZ–2a	Eastern Philippines	128.1943	3.1508	151.9	45.9	32.44
EPSZ–2b	Eastern Philippines	128.4706	3.2979	151.9	32.8	5.35
EPSZ–3a	Eastern Philippines	127.8899	4.0428	155.2	57.3	40.22
EPSZ–3b	Eastern Philippines	128.1108	4.1445	155.2	42.7	6.31
EPSZ–4a	Eastern Philippines	127.6120	4.8371	146.8	71.4	48.25
EPSZ–4b	Eastern Philippines	127.7324	4.9155	146.8	54.8	7.39
EPSZ–5a	Eastern Philippines	127.3173	5.7040	162.9	79.9	57.4
EPSZ–5b	Eastern Philippines	127.3930	5.7272	162.9	79.4	8.25
EPSZ–6a	Eastern Philippines	126.6488	6.6027	178.9	48.6	45.09
EPSZ–6b	Eastern Philippines	126.9478	6.6085	178.9	48.6	7.58
EPSZ–7a	Eastern Philippines	126.6578	7.4711	175.8	50.7	45.52
EPSZ–7b	Eastern Philippines	126.9439	7.4921	175.8	50.7	6.83
EPSZ–8a	Eastern Philippines	126.6227	8.2456	163.3	56.7	45.6
EPSZ–8b	Eastern Philippines	126.8614	8.3164	163.3	48.9	7.92
EPSZ–9a	Eastern Philippines	126.2751	9.0961	164.1	47	43.59
EPSZ–9b	Eastern Philippines	126.5735	9.1801	164.1	44.9	8.3
EPSZ–10a	Eastern Philippines	125.9798	9.9559	164.5	43.1	42.25
EPSZ–10b	Eastern Philippines	126.3007	10.0438	164.5	43.1	8.09
EPSZ–11a	Eastern Philippines	125.6079	10.6557	155	37.8	38.29
EPSZ–11b	Eastern Philippines	125.9353	10.8059	155	37.8	7.64
EPSZ–12a	Eastern Philippines	125.4697	11.7452	172.1	36	37.01
EPSZ–12b	Eastern Philippines	125.8374	11.7949	172.1	36	7.62
EPSZ–13a	Eastern Philippines	125.2238	12.1670	141.5	32.4	33.87
EPSZ–13b	Eastern Philippines	125.5278	12.4029	141.5	32.4	7.08
EPSZ–14a	Eastern Philippines	124.6476	13.1365	158.2	23	25.92
EPSZ–14b	Eastern Philippines	125.0421	13.2898	158.2	23	6.38
EPSZ–15a	Eastern Philippines	124.3107	13.9453	156.1	24.1	26.51
EPSZ–15b	Eastern Philippines	124.6973	14.1113	156.1	24.1	6.09
EPSZ–16a	Eastern Philippines	123.8998	14.4025	140.3	19.5	21.69
EPSZ–16b	Eastern Philippines	124.2366	14.6728	140.3	19.5	5
EPSZ–17a	Eastern Philippines	123.4604	14.7222	117.6	15.3	18.19
EPSZ–17b	Eastern Philippines	123.6682	15.1062	117.6	15.3	5
EPSZ–18a	Eastern Philippines	123.3946	14.7462	67.4	15	17.94
EPSZ–18b	Eastern Philippines	123.2219	15.1467	67.4	15	5
EPSZ–19a	Eastern Philippines	121.3638	15.7400	189.6	15	17.94
EPSZ–19b	Eastern Philippines	121.8082	15.6674	189.6	15	5
EPSZ–20a	Eastern Philippines	121.6833	16.7930	203.3	15	17.94
EPSZ–20b	Eastern Philippines	122.0994	16.6216	203.3	15	5
EPSZ–21a	Eastern Philippines	121.8279	17.3742	184.2	15	17.94
EPSZ–21b	Eastern Philippines	122.2814	17.3425	184.2	15	5

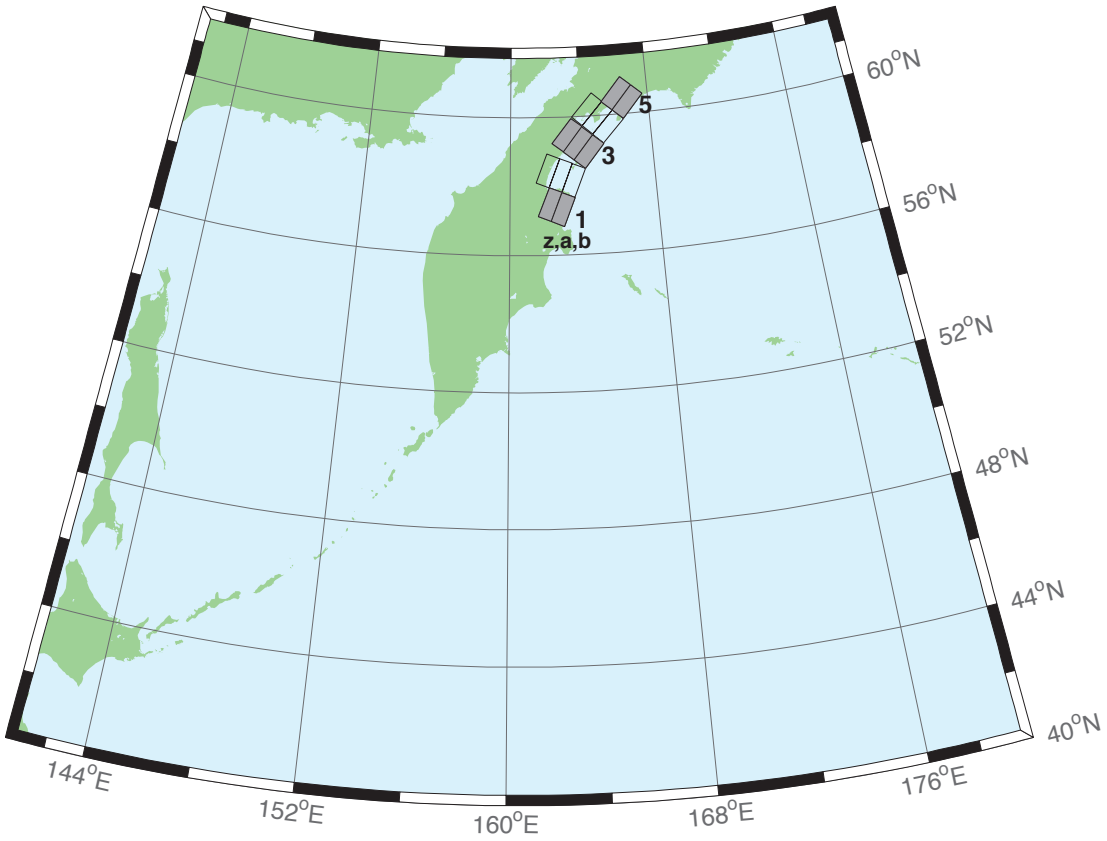

Figure B.4: Kamchatka–Bering Subduction Zone (KBSZ) unit sources.

Table B.4: Earthquake parameters for Kamchatka–Bering Subduction Zone (KBSZ) unit sources.

Segment	Description	Longitude (°E)	Latitude (°N)	Strike (°)	Dip (°)	Depth (km)
KBSZ–1a	Kamchatka–Bering	161.8374	57.5485	201.5	29	26.13
KBSZ–1b	Kamchatka–Bering	162.5162	57.4030	202.1	25	5
KBSZ–2a	Kamchatka–Bering	162.4410	58.3816	201.7	29	26.13
KBSZ–2b	Kamchatka–Bering	163.1344	58.2343	202.3	25	5
KBSZ–2z	Kamchatka–Bering	161.7418	58.5249	201.1	29	50.37
KBSZ–3a	Kamchatka–Bering	163.5174	59.3493	218.9	29	26.13
KBSZ–3b	Kamchatka–Bering	164.1109	59.1001	219.4	25	5
KBSZ–3z	Kamchatka–Bering	162.9150	59.5958	218.4	29	50.37
KBSZ–4a	Kamchatka–Bering	164.7070	60.0632	222.2	29	26.13
KBSZ–4b	Kamchatka–Bering	165.2833	59.7968	222.7	25	5
KBSZ–4z	Kamchatka–Bering	164.1212	60.3270	221.7	29	50.37
KBSZ–5a	Kamchatka–Bering	165.8652	60.7261	220.5	29	26.13
KBSZ–5b	Kamchatka–Bering	166.4692	60.4683	221	25	5

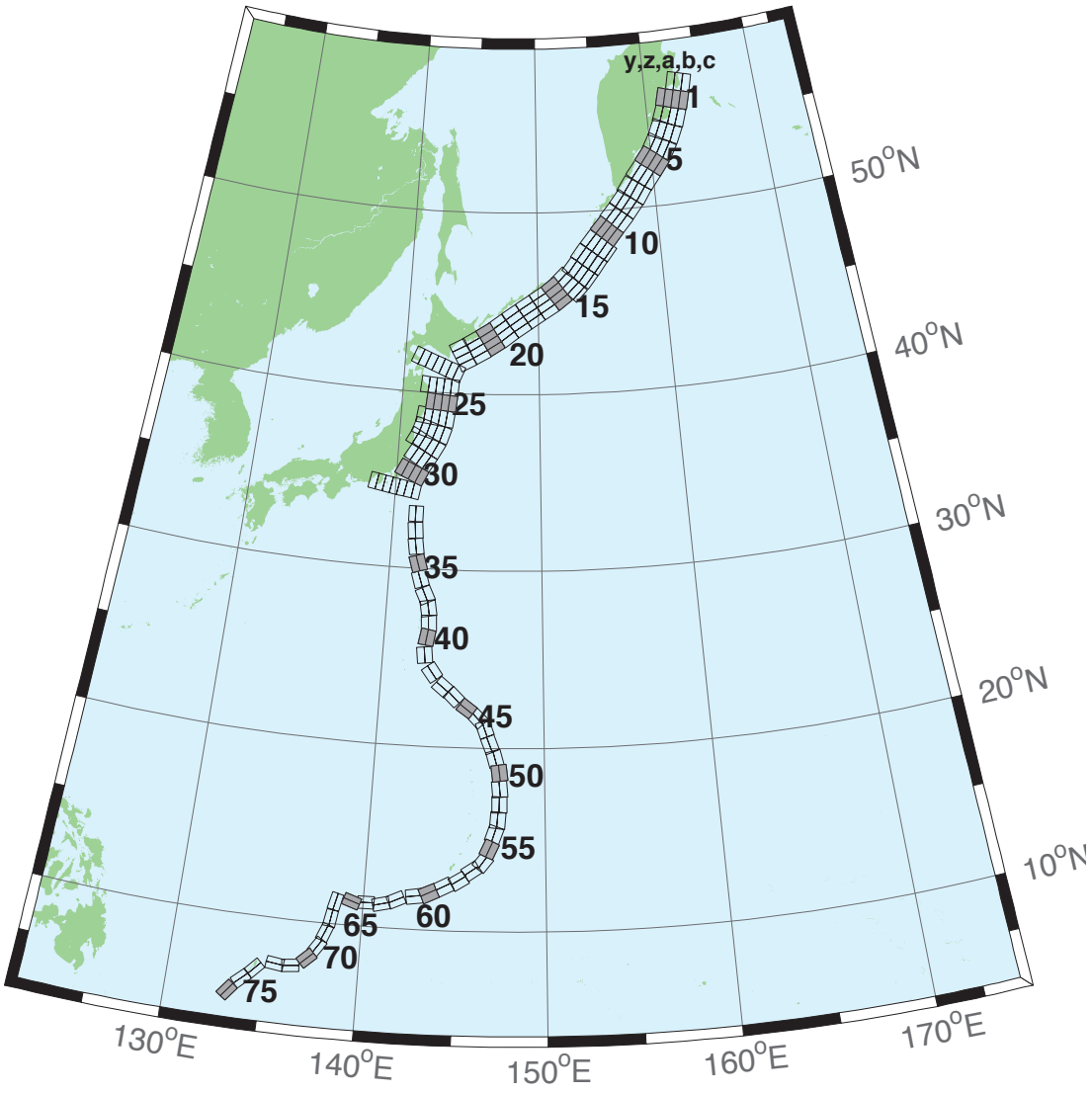

Figure B.5: Kamchatka–Kuril–Japan–Izu–Mariana–Yap Subduction Zone (KISZ) unit sources.

Table B.5: Earthquake parameters for Kamchatka–Kuril–Japan–Izu–Mariana–Yap Subduction Zone (KISZ) unit sources.

Segment	Description	Longitude (°E)	Latitude (°N)	Strike (°)	Dip (°)	Depth (km)
KISZ–0a	Kamchatka–Kuril–Japan–Izu–Mariana–Yap	162.8200	56.3667	194.4	29	26.13
KISZ–0b	Kamchatka–Kuril–Japan–Izu–Mariana–Yap	163.5057	56.2677	195	25	5
KISZ–0z	Kamchatka–Kuril–Japan–Izu–Mariana–Yap	162.1309	56.4618	193.8	29	50.37
KISZ–1a	Kamchatka–Kuril–Japan–Izu–Mariana–Yap	162.4318	55.5017	195	29	26.13
KISZ–1b	Kamchatka–Kuril–Japan–Izu–Mariana–Yap	163.1000	55.4000	195	25	5
KISZ–1y	Kamchatka–Kuril–Japan–Izu–Mariana–Yap	161.0884	55.7050	195	29	74.61
KISZ–1z	Kamchatka–Kuril–Japan–Izu–Mariana–Yap	161.7610	55.6033	195	29	50.37
KISZ–2a	Kamchatka–Kuril–Japan–Izu–Mariana–Yap	161.9883	54.6784	200	29	26.13
KISZ–2b	Kamchatka–Kuril–Japan–Izu–Mariana–Yap	162.6247	54.5440	200	25	5
KISZ–2y	Kamchatka–Kuril–Japan–Izu–Mariana–Yap	160.7072	54.9471	200	29	74.61
KISZ–2z	Kamchatka–Kuril–Japan–Izu–Mariana–Yap	161.3488	54.8127	200	29	50.37
KISZ–3a	Kamchatka–Kuril–Japan–Izu–Mariana–Yap	161.4385	53.8714	204	29	26.13
KISZ–3b	Kamchatka–Kuril–Japan–Izu–Mariana–Yap	162.0449	53.7116	204	25	5
KISZ–3y	Kamchatka–Kuril–Japan–Izu–Mariana–Yap	160.2164	54.1910	204	29	74.61
KISZ–3z	Kamchatka–Kuril–Japan–Izu–Mariana–Yap	160.8286	54.0312	204	29	50.37
KISZ–4a	Kamchatka–Kuril–Japan–Izu–Mariana–Yap	160.7926	53.1087	210	29	26.13
KISZ–4b	Kamchatka–Kuril–Japan–Izu–Mariana–Yap	161.3568	52.9123	210	25	5
KISZ–4y	Kamchatka–Kuril–Japan–Izu–Mariana–Yap	159.6539	53.5015	210	29	74.61
KISZ–4z	Kamchatka–Kuril–Japan–Izu–Mariana–Yap	160.2246	53.3051	210	29	50.37
KISZ–5a	Kamchatka–Kuril–Japan–Izu–Mariana–Yap	160.0211	52.4113	218	29	26.13
KISZ–5b	Kamchatka–Kuril–Japan–Izu–Mariana–Yap	160.5258	52.1694	218	25	5
KISZ–5y	Kamchatka–Kuril–Japan–Izu–Mariana–Yap	159.0005	52.8950	218	29	74.61
KISZ–5z	Kamchatka–Kuril–Japan–Izu–Mariana–Yap	159.5122	52.6531	218	29	50.37
KISZ–6a	Kamchatka–Kuril–Japan–Izu–Mariana–Yap	159.1272	51.7034	218	29	26.13
KISZ–6b	Kamchatka–Kuril–Japan–Izu–Mariana–Yap	159.6241	51.4615	218	25	5
KISZ–6y	Kamchatka–Kuril–Japan–Izu–Mariana–Yap	158.1228	52.1871	218	29	74.61
KISZ–6z	Kamchatka–Kuril–Japan–Izu–Mariana–Yap	158.6263	51.9452	218	29	50.37
KISZ–7a	Kamchatka–Kuril–Japan–Izu–Mariana–Yap	158.2625	50.9549	214	29	26.13
KISZ–7b	Kamchatka–Kuril–Japan–Izu–Mariana–Yap	158.7771	50.7352	214	25	5
KISZ–7y	Kamchatka–Kuril–Japan–Izu–Mariana–Yap	157.2236	51.3942	214	29	74.61
KISZ–7z	Kamchatka–Kuril–Japan–Izu–Mariana–Yap	157.7443	51.1745	214	29	50.37
KISZ–8a	Kamchatka–Kuril–Japan–Izu–Mariana–Yap	157.4712	50.2459	218	31	27.7
KISZ–8b	Kamchatka–Kuril–Japan–Izu–Mariana–Yap	157.9433	50.0089	218	27	5
KISZ–8y	Kamchatka–Kuril–Japan–Izu–Mariana–Yap	156.5176	50.7199	218	31	79.2
KISZ–8z	Kamchatka–Kuril–Japan–Izu–Mariana–Yap	156.9956	50.4829	218	31	53.45
KISZ–9a	Kamchatka–Kuril–Japan–Izu–Mariana–Yap	156.6114	49.5583	220	31	27.7
KISZ–9b	Kamchatka–Kuril–Japan–Izu–Mariana–Yap	157.0638	49.3109	220	27	5
KISZ–9y	Kamchatka–Kuril–Japan–Izu–Mariana–Yap	155.6974	50.0533	220	31	79.2
KISZ–9z	Kamchatka–Kuril–Japan–Izu–Mariana–Yap	156.1556	49.8058	220	31	53.45
KISZ–10a	Kamchatka–Kuril–Japan–Izu–Mariana–Yap	155.7294	48.8804	221	31	27.7
KISZ–10b	Kamchatka–Kuril–Japan–Izu–Mariana–Yap	156.1690	48.6278	221	27	5
KISZ–10y	Kamchatka–Kuril–Japan–Izu–Mariana–Yap	154.8413	49.3856	221	31	79.2
KISZ–10z	Kamchatka–Kuril–Japan–Izu–Mariana–Yap	155.2865	49.1330	221	31	53.45
KISZ–11a	Kamchatka–Kuril–Japan–Izu–Mariana–Yap	154.8489	48.1821	219	31	27.7
KISZ–11b	Kamchatka–Kuril–Japan–Izu–Mariana–Yap	155.2955	47.9398	219	27	5
KISZ–11y	Kamchatka–Kuril–Japan–Izu–Mariana–Yap	153.9472	48.6667	219	31	79.2
KISZ–11z	Kamchatka–Kuril–Japan–Izu–Mariana–Yap	154.3991	48.4244	219	31	53.45
KISZ–11c	Kamchatka–Kuril–Japan–Izu–Mariana–Yap	156.0358	47.5374	39	57.89	4.602
KISZ–12a	Kamchatka–Kuril–Japan–Izu–Mariana–Yap	153.9994	47.4729	217	31	27.7
KISZ–12b	Kamchatka–Kuril–Japan–Izu–Mariana–Yap	154.4701	47.2320	217	27	5
KISZ–12y	Kamchatka–Kuril–Japan–Izu–Mariana–Yap	153.0856	47.9363	217	31	79.2
KISZ–12z	Kamchatka–Kuril–Japan–Izu–Mariana–Yap	153.5435	47.7046	217	31	53.45
KISZ–12c	Kamchatka–Kuril–Japan–Izu–Mariana–Yap	155.2208	46.8473	37	57.89	4.602
KISZ–13a	Kamchatka–Kuril–Japan–Izu–Mariana–Yap	153.2239	46.7564	218	31	27.7
KISZ–13b	Kamchatka–Kuril–Japan–Izu–Mariana–Yap	153.6648	46.5194	218	27	5
KISZ–13y	Kamchatka–Kuril–Japan–Izu–Mariana–Yap	152.3343	47.2304	218	31	79.2
KISZ–13z	Kamchatka–Kuril–Japan–Izu–Mariana–Yap	152.7801	46.9934	218	31	53.45
KISZ–13c	Kamchatka–Kuril–Japan–Izu–Mariana–Yap	154.3957	46.1257	38	57.89	4.602
KISZ–14a	Kamchatka–Kuril–Japan–Izu–Mariana–Yap	152.3657	46.1514	225	23	24.54
KISZ–14b	Kamchatka–Kuril–Japan–Izu–Mariana–Yap	152.7855	45.8591	225	23	5

Continued on next page

Table B.5 – continued

Segment	Description	Longitude (°E)	Latitude (°N)	Strike (°)	Dip (°)	Depth (km)
KISZ–14y	Kamchatka–Kuril–Japan–Izu–Mariana–Yap	151.5172	46.7362	225	23	63.62
KISZ–14z	Kamchatka–Kuril–Japan–Izu–Mariana–Yap	151.9426	46.4438	225	23	44.08
KISZ–14c	Kamchatka–Kuril–Japan–Izu–Mariana–Yap	153.4468	45.3976	45	57.89	4.602
KISZ–15a	Kamchatka–Kuril–Japan–Izu–Mariana–Yap	151.4663	45.5963	233	25	23.73
KISZ–15b	Kamchatka–Kuril–Japan–Izu–Mariana–Yap	151.8144	45.2712	233	22	5
KISZ–15y	Kamchatka–Kuril–Japan–Izu–Mariana–Yap	150.7619	46.2465	233	25	65.99
KISZ–15z	Kamchatka–Kuril–Japan–Izu–Mariana–Yap	151.1151	45.9214	233	25	44.86
KISZ–16a	Kamchatka–Kuril–Japan–Izu–Mariana–Yap	150.4572	45.0977	237	25	23.73
KISZ–16b	Kamchatka–Kuril–Japan–Izu–Mariana–Yap	150.7694	44.7563	237	22	5
KISZ–16y	Kamchatka–Kuril–Japan–Izu–Mariana–Yap	149.8253	45.7804	237	25	65.99
KISZ–16z	Kamchatka–Kuril–Japan–Izu–Mariana–Yap	150.1422	45.4390	237	25	44.86
KISZ–17a	Kamchatka–Kuril–Japan–Izu–Mariana–Yap	149.3989	44.6084	237	25	23.73
KISZ–17b	Kamchatka–Kuril–Japan–Izu–Mariana–Yap	149.7085	44.2670	237	22	5
KISZ–17y	Kamchatka–Kuril–Japan–Izu–Mariana–Yap	148.7723	45.2912	237	25	65.99
KISZ–17z	Kamchatka–Kuril–Japan–Izu–Mariana–Yap	149.0865	44.9498	237	25	44.86
KISZ–18a	Kamchatka–Kuril–Japan–Izu–Mariana–Yap	148.3454	44.0982	235	25	23.73
KISZ–18b	Kamchatka–Kuril–Japan–Izu–Mariana–Yap	148.6687	43.7647	235	22	5
KISZ–18y	Kamchatka–Kuril–Japan–Izu–Mariana–Yap	147.6915	44.7651	235	25	65.99
KISZ–18z	Kamchatka–Kuril–Japan–Izu–Mariana–Yap	148.0194	44.4316	235	25	44.86
KISZ–19a	Kamchatka–Kuril–Japan–Izu–Mariana–Yap	147.3262	43.5619	233	25	23.73
KISZ–19b	Kamchatka–Kuril–Japan–Izu–Mariana–Yap	147.6625	43.2368	233	22	5
KISZ–19y	Kamchatka–Kuril–Japan–Izu–Mariana–Yap	146.6463	44.2121	233	25	65.99
KISZ–19z	Kamchatka–Kuril–Japan–Izu–Mariana–Yap	146.9872	43.8870	233	25	44.86
KISZ–20a	Kamchatka–Kuril–Japan–Izu–Mariana–Yap	146.3513	43.0633	237	25	23.73
KISZ–20b	Kamchatka–Kuril–Japan–Izu–Mariana–Yap	146.6531	42.7219	237	22	5
KISZ–20y	Kamchatka–Kuril–Japan–Izu–Mariana–Yap	145.7410	43.7461	237	25	65.99
KISZ–20z	Kamchatka–Kuril–Japan–Izu–Mariana–Yap	146.0470	43.4047	237	25	44.86
KISZ–21a	Kamchatka–Kuril–Japan–Izu–Mariana–Yap	145.3331	42.5948	239	25	23.73
KISZ–21b	Kamchatka–Kuril–Japan–Izu–Mariana–Yap	145.6163	42.2459	239	22	5
KISZ–21y	Kamchatka–Kuril–Japan–Izu–Mariana–Yap	144.7603	43.2927	239	25	65.99
KISZ–21z	Kamchatka–Kuril–Japan–Izu–Mariana–Yap	145.0475	42.9438	239	25	44.86
KISZ–22a	Kamchatka–Kuril–Japan–Izu–Mariana–Yap	144.3041	42.1631	242	25	23.73
KISZ–22b	Kamchatka–Kuril–Japan–Izu–Mariana–Yap	144.5605	41.8037	242	22	5
KISZ–22y	Kamchatka–Kuril–Japan–Izu–Mariana–Yap	143.7854	42.8819	242	25	65.99
KISZ–22z	Kamchatka–Kuril–Japan–Izu–Mariana–Yap	144.0455	42.5225	242	25	44.86
KISZ–23a	Kamchatka–Kuril–Japan–Izu–Mariana–Yap	143.2863	41.3335	202	21	21.28
KISZ–23b	Kamchatka–Kuril–Japan–Izu–Mariana–Yap	143.8028	41.1764	202	19	5
KISZ–23v	Kamchatka–Kuril–Japan–Izu–Mariana–Yap	140.6816	42.1189	202	21	110.9
KISZ–23w	Kamchatka–Kuril–Japan–Izu–Mariana–Yap	141.2050	41.9618	202	21	92.95
KISZ–23x	Kamchatka–Kuril–Japan–Izu–Mariana–Yap	141.7273	41.8047	202	21	75.04
KISZ–23y	Kamchatka–Kuril–Japan–Izu–Mariana–Yap	142.2482	41.6476	202	21	57.12
KISZ–23z	Kamchatka–Kuril–Japan–Izu–Mariana–Yap	142.7679	41.4905	202	21	39.2
KISZ–24a	Kamchatka–Kuril–Japan–Izu–Mariana–Yap	142.9795	40.3490	185	21	21.28
KISZ–24b	Kamchatka–Kuril–Japan–Izu–Mariana–Yap	143.5273	40.3125	185	19	5
KISZ–24x	Kamchatka–Kuril–Japan–Izu–Mariana–Yap	141.3339	40.4587	185	21	75.04
KISZ–24y	Kamchatka–Kuril–Japan–Izu–Mariana–Yap	141.8827	40.4221	185	21	57.12
KISZ–24z	Kamchatka–Kuril–Japan–Izu–Mariana–Yap	142.4312	40.3856	185	21	39.2
KISZ–25a	Kamchatka–Kuril–Japan–Izu–Mariana–Yap	142.8839	39.4541	185	21	21.28
KISZ–25b	Kamchatka–Kuril–Japan–Izu–Mariana–Yap	143.4246	39.4176	185	19	5
KISZ–25y	Kamchatka–Kuril–Japan–Izu–Mariana–Yap	141.8012	39.5272	185	21	57.12
KISZ–25z	Kamchatka–Kuril–Japan–Izu–Mariana–Yap	142.3426	39.4907	185	21	39.2
KISZ–26a	Kamchatka–Kuril–Japan–Izu–Mariana–Yap	142.7622	38.5837	188	21	21.28
KISZ–26b	Kamchatka–Kuril–Japan–Izu–Mariana–Yap	143.2930	38.5254	188	19	5
KISZ–26x	Kamchatka–Kuril–Japan–Izu–Mariana–Yap	141.1667	38.7588	188	21	75.04
KISZ–26y	Kamchatka–Kuril–Japan–Izu–Mariana–Yap	141.6990	38.7004	188	21	57.12
KISZ–26z	Kamchatka–Kuril–Japan–Izu–Mariana–Yap	142.2308	38.6421	188	21	39.2
KISZ–27a	Kamchatka–Kuril–Japan–Izu–Mariana–Yap	142.5320	37.7830	198	21	21.28
KISZ–27b	Kamchatka–Kuril–Japan–Izu–Mariana–Yap	143.0357	37.6534	198	19	5
KISZ–27x	Kamchatka–Kuril–Japan–Izu–Mariana–Yap	141.0142	38.1717	198	21	75.04
KISZ–27y	Kamchatka–Kuril–Japan–Izu–Mariana–Yap	141.5210	38.0421	198	21	57.12
KISZ–27z	Kamchatka–Kuril–Japan–Izu–Mariana–Yap	142.0269	37.9126	198	21	39.2
KISZ–28a	Kamchatka–Kuril–Japan–Izu–Mariana–Yap	142.1315	37.0265	208	21	21.28

Continued on next page

Table B.5 – continued

Segment	Description	Longitude (°E)	Latitude (°N)	Strike (°)	Dip (°)	Depth (km)
KISZ–28b	Kamchatka–Kuril–Japan–Izu–Mariana–Yap	142.5941	36.8297	208	19	5
KISZ–28x	Kamchatka–Kuril–Japan–Izu–Mariana–Yap	140.7348	37.6171	208	21	75.04
KISZ–28y	Kamchatka–Kuril–Japan–Izu–Mariana–Yap	141.2016	37.4202	208	21	57.12
KISZ–28z	Kamchatka–Kuril–Japan–Izu–Mariana–Yap	141.6671	37.2234	208	21	39.2
KISZ–29a	Kamchatka–Kuril–Japan–Izu–Mariana–Yap	141.5970	36.2640	211	21	21.28
KISZ–29b	Kamchatka–Kuril–Japan–Izu–Mariana–Yap	142.0416	36.0481	211	19	5
KISZ–29y	Kamchatka–Kuril–Japan–Izu–Mariana–Yap	140.7029	36.6960	211	21	57.12
KISZ–29z	Kamchatka–Kuril–Japan–Izu–Mariana–Yap	141.1506	36.4800	211	21	39.2
KISZ–30a	Kamchatka–Kuril–Japan–Izu–Mariana–Yap	141.0553	35.4332	205	21	21.28
KISZ–30b	Kamchatka–Kuril–Japan–Izu–Mariana–Yap	141.5207	35.2560	205	19	5
KISZ–30y	Kamchatka–Kuril–Japan–Izu–Mariana–Yap	140.1204	35.7876	205	21	57.12
KISZ–30z	Kamchatka–Kuril–Japan–Izu–Mariana–Yap	140.5883	35.6104	205	21	39.2
KISZ–31a	Kamchatka–Kuril–Japan–Izu–Mariana–Yap	140.6956	34.4789	190	22	22.1
KISZ–31b	Kamchatka–Kuril–Japan–Izu–Mariana–Yap	141.1927	34.4066	190	20	5
KISZ–31v	Kamchatka–Kuril–Japan–Izu–Mariana–Yap	138.2025	34.8405	190	22	115.8
KISZ–31w	Kamchatka–Kuril–Japan–Izu–Mariana–Yap	138.7021	34.7682	190	22	97.02
KISZ–31x	Kamchatka–Kuril–Japan–Izu–Mariana–Yap	139.2012	34.6958	190	22	78.29
KISZ–31y	Kamchatka–Kuril–Japan–Izu–Mariana–Yap	139.6997	34.6235	190	22	59.56
KISZ–31z	Kamchatka–Kuril–Japan–Izu–Mariana–Yap	140.1979	34.5512	190	22	40.83
KISZ–32a	Kamchatka–Kuril–Japan–Izu–Mariana–Yap	141.0551	33.0921	180	32	23.48
KISZ–32b	Kamchatka–Kuril–Japan–Izu–Mariana–Yap	141.5098	33.0921	180	21.69	5
KISZ–33a	Kamchatka–Kuril–Japan–Izu–Mariana–Yap	141.0924	32.1047	173.8	27.65	20.67
KISZ–33b	Kamchatka–Kuril–Japan–Izu–Mariana–Yap	141.5596	32.1473	173.8	18.27	5
KISZ–34a	Kamchatka–Kuril–Japan–Izu–Mariana–Yap	141.1869	31.1851	172.1	25	18.26
KISZ–34b	Kamchatka–Kuril–Japan–Izu–Mariana–Yap	141.6585	31.2408	172.1	15.38	5
KISZ–35a	Kamchatka–Kuril–Japan–Izu–Mariana–Yap	141.4154	30.1707	163	25	17.12
KISZ–35b	Kamchatka–Kuril–Japan–Izu–Mariana–Yap	141.8662	30.2899	163	14.03	5
KISZ–36a	Kamchatka–Kuril–Japan–Izu–Mariana–Yap	141.6261	29.2740	161.7	25.73	18.71
KISZ–36b	Kamchatka–Kuril–Japan–Izu–Mariana–Yap	142.0670	29.4012	161.7	15.91	5
KISZ–37a	Kamchatka–Kuril–Japan–Izu–Mariana–Yap	142.0120	28.3322	154.7	20	14.54
KISZ–37b	Kamchatka–Kuril–Japan–Izu–Mariana–Yap	142.4463	28.5124	154.7	11	5
KISZ–38a	Kamchatka–Kuril–Japan–Izu–Mariana–Yap	142.2254	27.6946	170.3	20	14.54
KISZ–38b	Kamchatka–Kuril–Japan–Izu–Mariana–Yap	142.6955	27.7659	170.3	11	5
KISZ–39a	Kamchatka–Kuril–Japan–Izu–Mariana–Yap	142.3085	26.9127	177.2	24.23	17.42
KISZ–39b	Kamchatka–Kuril–Japan–Izu–Mariana–Yap	142.7674	26.9325	177.2	14.38	5
KISZ–40a	Kamchatka–Kuril–Japan–Izu–Mariana–Yap	142.2673	26.1923	189.4	26.49	22.26
KISZ–40b	Kamchatka–Kuril–Japan–Izu–Mariana–Yap	142.7090	26.1264	189.4	20.2	5
KISZ–41a	Kamchatka–Kuril–Japan–Izu–Mariana–Yap	142.1595	25.0729	173.7	22.07	19.08
KISZ–41b	Kamchatka–Kuril–Japan–Izu–Mariana–Yap	142.6165	25.1184	173.7	16.36	5
KISZ–42a	Kamchatka–Kuril–Japan–Izu–Mariana–Yap	142.7641	23.8947	143.5	21.54	18.4
KISZ–42b	Kamchatka–Kuril–Japan–Izu–Mariana–Yap	143.1321	24.1432	143.5	15.54	5
KISZ–43a	Kamchatka–Kuril–Japan–Izu–Mariana–Yap	143.5281	23.0423	129.2	23.02	18.77
KISZ–43b	Kamchatka–Kuril–Japan–Izu–Mariana–Yap	143.8128	23.3626	129.2	15.99	5
KISZ–44a	Kamchatka–Kuril–Japan–Izu–Mariana–Yap	144.2230	22.5240	134.6	28.24	18.56
KISZ–44b	Kamchatka–Kuril–Japan–Izu–Mariana–Yap	144.5246	22.8056	134.6	15.74	5
KISZ–45a	Kamchatka–Kuril–Japan–Izu–Mariana–Yap	145.0895	21.8866	125.8	36.73	22.79
KISZ–45b	Kamchatka–Kuril–Japan–Izu–Mariana–Yap	145.3171	22.1785	125.8	20.84	5
KISZ–46a	Kamchatka–Kuril–Japan–Izu–Mariana–Yap	145.6972	21.3783	135.9	30.75	20.63
KISZ–46b	Kamchatka–Kuril–Japan–Izu–Mariana–Yap	145.9954	21.6469	135.9	18.22	5
KISZ–47a	Kamchatka–Kuril–Japan–Izu–Mariana–Yap	146.0406	20.9341	160.1	29.87	19.62
KISZ–47b	Kamchatka–Kuril–Japan–Izu–Mariana–Yap	146.4330	21.0669	160.1	17	5
KISZ–48a	Kamchatka–Kuril–Japan–Izu–Mariana–Yap	146.3836	20.0690	158	32.75	19.68
KISZ–48b	Kamchatka–Kuril–Japan–Izu–Mariana–Yap	146.7567	20.2108	158	17.07	5
KISZ–49a	Kamchatka–Kuril–Japan–Izu–Mariana–Yap	146.6689	19.3123	164.5	25.07	21.41
KISZ–49b	Kamchatka–Kuril–Japan–Izu–Mariana–Yap	147.0846	19.4212	164.5	19.16	5
KISZ–50a	Kamchatka–Kuril–Japan–Izu–Mariana–Yap	146.9297	18.5663	172.1	22	22.1
KISZ–50b	Kamchatka–Kuril–Japan–Izu–Mariana–Yap	147.3650	18.6238	172.1	20	5
KISZ–51a	Kamchatka–Kuril–Japan–Izu–Mariana–Yap	146.9495	17.7148	175.1	22.06	22.04
KISZ–51b	Kamchatka–Kuril–Japan–Izu–Mariana–Yap	147.3850	17.7503	175.1	19.93	5
KISZ–52a	Kamchatka–Kuril–Japan–Izu–Mariana–Yap	146.9447	16.8869	180	25.51	18.61
KISZ–52b	Kamchatka–Kuril–Japan–Izu–Mariana–Yap	147.3683	16.8869	180	15.79	5
KISZ–53a	Kamchatka–Kuril–Japan–Izu–Mariana–Yap	146.8626	16.0669	185.2	27.39	18.41

Continued on next page

Table B.5 – continued

Segment	Description	Longitude (°E)	Latitude (°N)	Strike (°)	Dip (°)	Depth (km)
KISZ–53b	Kamchatka–Kuril–Japan–Izu–Mariana–Yap	147.2758	16.0309	185.2	15.56	5
KISZ–54a	Kamchatka–Kuril–Japan–Izu–Mariana–Yap	146.7068	15.3883	199.1	28.12	20.91
KISZ–54b	Kamchatka–Kuril–Japan–Izu–Mariana–Yap	147.0949	15.2590	199.1	18.56	5
KISZ–55a	Kamchatka–Kuril–Japan–Izu–Mariana–Yap	146.4717	14.6025	204.3	29.6	26.27
KISZ–55b	Kamchatka–Kuril–Japan–Izu–Mariana–Yap	146.8391	14.4415	204.3	25.18	5
KISZ–56a	Kamchatka–Kuril–Japan–Izu–Mariana–Yap	146.1678	13.9485	217.4	32.04	26.79
KISZ–56b	Kamchatka–Kuril–Japan–Izu–Mariana–Yap	146.4789	13.7170	217.4	25.84	5
KISZ–57a	Kamchatka–Kuril–Japan–Izu–Mariana–Yap	145.6515	13.5576	235.8	37	24.54
KISZ–57b	Kamchatka–Kuril–Japan–Izu–Mariana–Yap	145.8586	13.2609	235.8	23	5
KISZ–58a	Kamchatka–Kuril–Japan–Izu–Mariana–Yap	144.9648	12.9990	237.8	37.72	24.54
KISZ–58b	Kamchatka–Kuril–Japan–Izu–Mariana–Yap	145.1589	12.6984	237.8	23	5
KISZ–59a	Kamchatka–Kuril–Japan–Izu–Mariana–Yap	144.1799	12.6914	242.9	34.33	22.31
KISZ–59b	Kamchatka–Kuril–Japan–Izu–Mariana–Yap	144.3531	12.3613	242.9	20.25	5
KISZ–60a	Kamchatka–Kuril–Japan–Izu–Mariana–Yap	143.3687	12.3280	244.9	30.9	20.62
KISZ–60b	Kamchatka–Kuril–Japan–Izu–Mariana–Yap	143.5355	11.9788	244.9	18.2	5
KISZ–61a	Kamchatka–Kuril–Japan–Izu–Mariana–Yap	142.7051	12.1507	261.8	35.41	25.51
KISZ–61b	Kamchatka–Kuril–Japan–Izu–Mariana–Yap	142.7582	11.7883	261.8	24.22	5
KISZ–62a	Kamchatka–Kuril–Japan–Izu–Mariana–Yap	141.6301	11.8447	245.7	39.86	34.35
KISZ–62b	Kamchatka–Kuril–Japan–Izu–Mariana–Yap	141.7750	11.5305	245.7	35.94	5
KISZ–63a	Kamchatka–Kuril–Japan–Izu–Mariana–Yap	140.8923	11.5740	256.2	42	38.46
KISZ–63b	Kamchatka–Kuril–Japan–Izu–Mariana–Yap	140.9735	11.2498	256.2	42	5
KISZ–64a	Kamchatka–Kuril–Japan–Izu–Mariana–Yap	140.1387	11.6028	269.6	42.48	38.77
KISZ–64b	Kamchatka–Kuril–Japan–Izu–Mariana–Yap	140.1410	11.2716	269.6	42.48	5
KISZ–65a	Kamchatka–Kuril–Japan–Izu–Mariana–Yap	139.4595	11.5883	288.7	44.16	39.83
KISZ–65b	Kamchatka–Kuril–Japan–Izu–Mariana–Yap	139.3541	11.2831	288.7	44.16	5
KISZ–66a	Kamchatka–Kuril–Japan–Izu–Mariana–Yap	138.1823	11.2648	193.1	45	40.36
KISZ–66b	Kamchatka–Kuril–Japan–Izu–Mariana–Yap	138.4977	11.1929	193.1	45	5
KISZ–67a	Kamchatka–Kuril–Japan–Izu–Mariana–Yap	137.9923	10.3398	189.8	45	40.36
KISZ–67b	Kamchatka–Kuril–Japan–Izu–Mariana–Yap	138.3104	10.2856	189.8	45	5
KISZ–68a	Kamchatka–Kuril–Japan–Izu–Mariana–Yap	137.7607	9.6136	201.7	45	40.36
KISZ–68b	Kamchatka–Kuril–Japan–Izu–Mariana–Yap	138.0599	9.4963	201.7	45	5
KISZ–69a	Kamchatka–Kuril–Japan–Izu–Mariana–Yap	137.4537	8.8996	213.5	45	40.36
KISZ–69b	Kamchatka–Kuril–Japan–Izu–Mariana–Yap	137.7215	8.7241	213.5	45	5
KISZ–70a	Kamchatka–Kuril–Japan–Izu–Mariana–Yap	137.0191	8.2872	226.5	45	40.36
KISZ–70b	Kamchatka–Kuril–Japan–Izu–Mariana–Yap	137.2400	8.0569	226.5	45	5
KISZ–71a	Kamchatka–Kuril–Japan–Izu–Mariana–Yap	136.3863	7.9078	263.9	45	40.36
KISZ–71b	Kamchatka–Kuril–Japan–Izu–Mariana–Yap	136.4202	7.5920	263.9	45	5
KISZ–72a	Kamchatka–Kuril–Japan–Izu–Mariana–Yap	135.6310	7.9130	276.9	45	40.36
KISZ–72b	Kamchatka–Kuril–Japan–Izu–Mariana–Yap	135.5926	7.5977	276.9	45	5
KISZ–73a	Kamchatka–Kuril–Japan–Izu–Mariana–Yap	134.3296	7.4541	224	45	40.36
KISZ–73b	Kamchatka–Kuril–Japan–Izu–Mariana–Yap	134.5600	7.2335	224	45	5
KISZ–74a	Kamchatka–Kuril–Japan–Izu–Mariana–Yap	133.7125	6.8621	228.1	45	40.36
KISZ–74b	Kamchatka–Kuril–Japan–Izu–Mariana–Yap	133.9263	6.6258	228.1	45	5
KISZ–75a	Kamchatka–Kuril–Japan–Izu–Mariana–Yap	133.0224	6.1221	217.7	45	40.36
KISZ–75b	Kamchatka–Kuril–Japan–Izu–Mariana–Yap	133.2751	5.9280	217.7	45	5

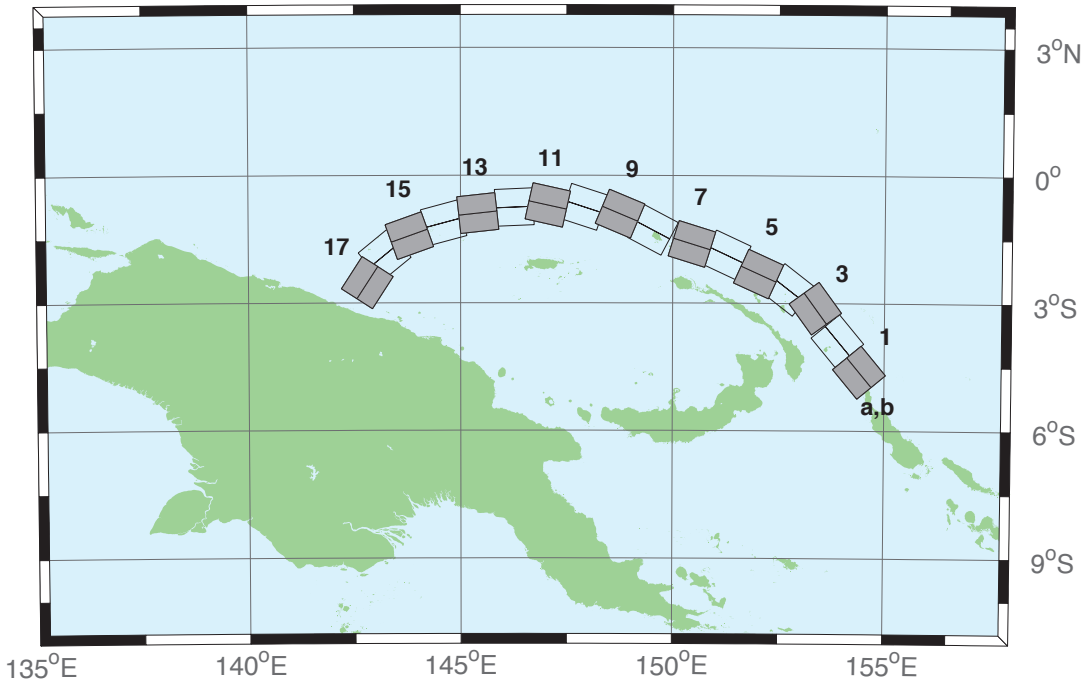

Figure B.6: Manus–Oceanic Convergent Boundary Subduction Zone (MOSZ) unit sources.

Table B.6: Earthquake parameters for Manus–Oceanic Convergent Boundary Subduction Zone (MOSZ) unit sources.

Segment	Description	Longitude (°E)	Latitude (°N)	Strike (°)	Dip (°)	Depth (km)
MOSZ–1a	Manus–Oceanic Convergent Boundary	154.0737	-4.8960	140.2	15	15.88
MOSZ–1b	Manus–Oceanic Convergent Boundary	154.4082	-4.6185	140.2	15	2.94
MOSZ–2a	Manus–Oceanic Convergent Boundary	153.5589	-4.1575	140.2	15	15.91
MOSZ–2b	Manus–Oceanic Convergent Boundary	153.8931	-3.8800	140.2	15	2.97
MOSZ–3a	Manus–Oceanic Convergent Boundary	153.0151	-3.3716	143.9	15	16.64
MOSZ–3b	Manus–Oceanic Convergent Boundary	153.3662	-3.1160	143.9	15	3.7
MOSZ–4a	Manus–Oceanic Convergent Boundary	152.4667	-3.0241	127.7	15	17.32
MOSZ–4b	Manus–Oceanic Convergent Boundary	152.7321	-2.6806	127.7	15	4.38
MOSZ–5a	Manus–Oceanic Convergent Boundary	151.8447	-2.7066	114.3	15	17.57
MOSZ–5b	Manus–Oceanic Convergent Boundary	152.0235	-2.3112	114.3	15	4.63
MOSZ–6a	Manus–Oceanic Convergent Boundary	151.0679	-2.2550	115	15	17.66
MOSZ–6b	Manus–Oceanic Convergent Boundary	151.2513	-1.8618	115	15	4.72
MOSZ–7a	Manus–Oceanic Convergent Boundary	150.3210	-2.0236	107.2	15	17.73
MOSZ–7b	Manus–Oceanic Convergent Boundary	150.4493	-1.6092	107.2	15	4.79
MOSZ–8a	Manus–Oceanic Convergent Boundary	149.3226	-1.6666	117.8	15	17.83
MOSZ–8b	Manus–Oceanic Convergent Boundary	149.5251	-1.2829	117.8	15	4.89
MOSZ–9a	Manus–Oceanic Convergent Boundary	148.5865	-1.3017	112.7	15	17.84
MOSZ–9b	Manus–Oceanic Convergent Boundary	148.7540	-0.9015	112.7	15	4.9
MOSZ–10a	Manus–Oceanic Convergent Boundary	147.7760	-1.1560	108	15	17.78
MOSZ–10b	Manus–Oceanic Convergent Boundary	147.9102	-0.7434	108	15	4.84
MOSZ–11a	Manus–Oceanic Convergent Boundary	146.9596	-1.1226	102.5	15	17.54
MOSZ–11b	Manus–Oceanic Convergent Boundary	147.0531	-0.6990	102.5	15	4.6
MOSZ–12a	Manus–Oceanic Convergent Boundary	146.2858	-1.1820	87.48	15	17.29
MOSZ–12b	Manus–Oceanic Convergent Boundary	146.2667	-0.7486	87.48	15	4.35
MOSZ–13a	Manus–Oceanic Convergent Boundary	145.4540	-1.3214	83.75	15	17.34
MOSZ–13b	Manus–Oceanic Convergent Boundary	145.4068	-0.8901	83.75	15	4.4
MOSZ–14a	Manus–Oceanic Convergent Boundary	144.7151	-1.5346	75.09	15	17.21
MOSZ–14b	Manus–Oceanic Convergent Boundary	144.6035	-1.1154	75.09	15	4.27
MOSZ–15a	Manus–Oceanic Convergent Boundary	143.9394	-1.8278	70.43	15	16.52
MOSZ–15b	Manus–Oceanic Convergent Boundary	143.7940	-1.4190	70.43	15	3.58
MOSZ–16a	Manus–Oceanic Convergent Boundary	143.4850	-2.2118	50.79	15	15.86
MOSZ–16b	Manus–Oceanic Convergent Boundary	143.2106	-1.8756	50.79	15	2.92
MOSZ–17a	Manus–Oceanic Convergent Boundary	143.1655	-2.7580	33	15	16.64
MOSZ–17b	Manus–Oceanic Convergent Boundary	142.8013	-2.5217	33	15	3.7

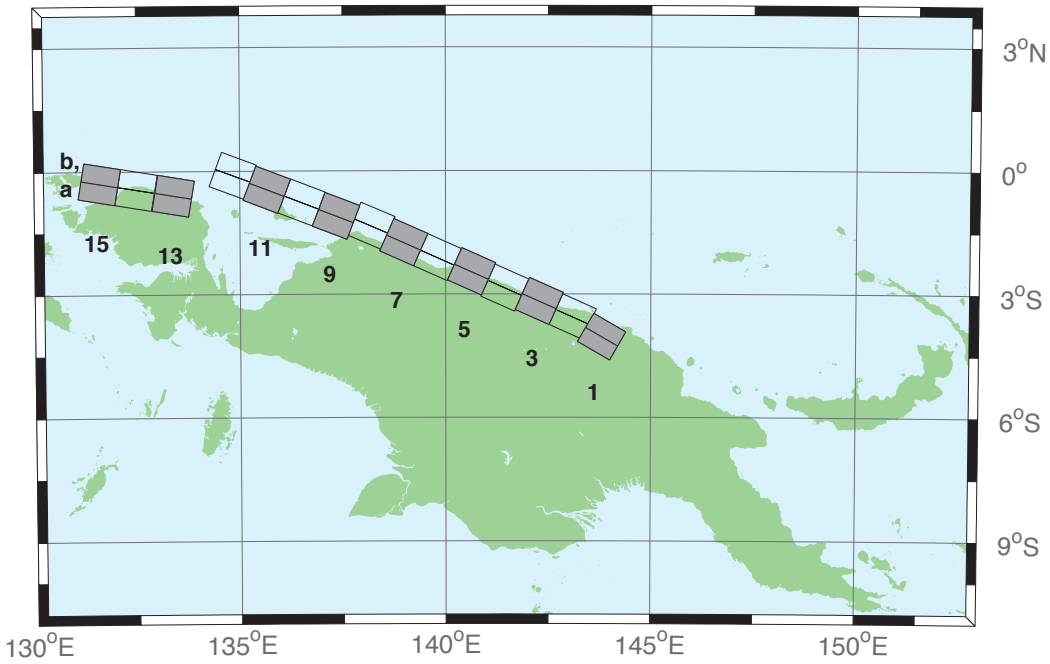

Figure B.7: New Guinea Subduction Zone (NGSZ) unit sources.

Table B.7: Earthquake parameters for New Guinea Subduction Zone (NGSZ) unit sources.

Segment	Description	Longitude (°E)	Latitude (°N)	Strike (°)	Dip (°)	Depth (km)
NGSZ–1a	New Guinea	143.6063	-4.3804	120	29	25.64
NGSZ–1b	New Guinea	143.8032	-4.0402	120	29	1.4
NGSZ–2a	New Guinea	142.9310	-3.9263	114	27.63	20.1
NGSZ–2b	New Guinea	143.0932	-3.5628	114	21.72	1.6
NGSZ–3a	New Guinea	142.1076	-3.5632	114	20.06	18.73
NGSZ–3b	New Guinea	142.2795	-3.1778	114	15.94	5
NGSZ–4a	New Guinea	141.2681	-3.2376	114	21	17.76
NGSZ–4b	New Guinea	141.4389	-2.8545	114	14.79	5
NGSZ–5a	New Guinea	140.4592	-2.8429	114	21.26	16.14
NGSZ–5b	New Guinea	140.6296	-2.4605	114	12.87	5
NGSZ–6a	New Guinea	139.6288	-2.4960	114	22.72	15.4
NGSZ–6b	New Guinea	139.7974	-2.1175	114	12	5
NGSZ–7a	New Guinea	138.8074	-2.1312	114	21.39	15.4
NGSZ–7b	New Guinea	138.9776	-1.7491	114	12	5
NGSZ–8a	New Guinea	138.0185	-1.7353	113.1	18.79	15.14
NGSZ–8b	New Guinea	138.1853	-1.3441	113.1	11.7	5
NGSZ–9a	New Guinea	137.1805	-1.5037	111	15.24	13.23
NGSZ–9b	New Guinea	137.3358	-1.0991	111	9.47	5
NGSZ–10a	New Guinea	136.3418	-1.1774	111	13.51	11.09
NGSZ–10b	New Guinea	136.4983	-0.7697	111	7	5
NGSZ–11a	New Guinea	135.4984	-0.8641	111	11.38	12.49
NGSZ–11b	New Guinea	135.6562	-0.4530	111	8.62	5
NGSZ–12a	New Guinea	134.6759	-0.5216	110.5	10	13.68
NGSZ–12b	New Guinea	134.8307	-0.1072	110.5	10	5
NGSZ–13a	New Guinea	133.3065	-1.0298	99.5	10	13.68
NGSZ–13b	New Guinea	133.3795	-0.5935	99.5	10	5
NGSZ–14a	New Guinea	132.4048	-0.8816	99.5	10	13.68
NGSZ–14b	New Guinea	132.4778	-0.4453	99.5	10	5
NGSZ–15a	New Guinea	131.5141	-0.7353	99.5	10	13.68
NGSZ–15b	New Guinea	131.5871	-0.2990	99.5	10	5

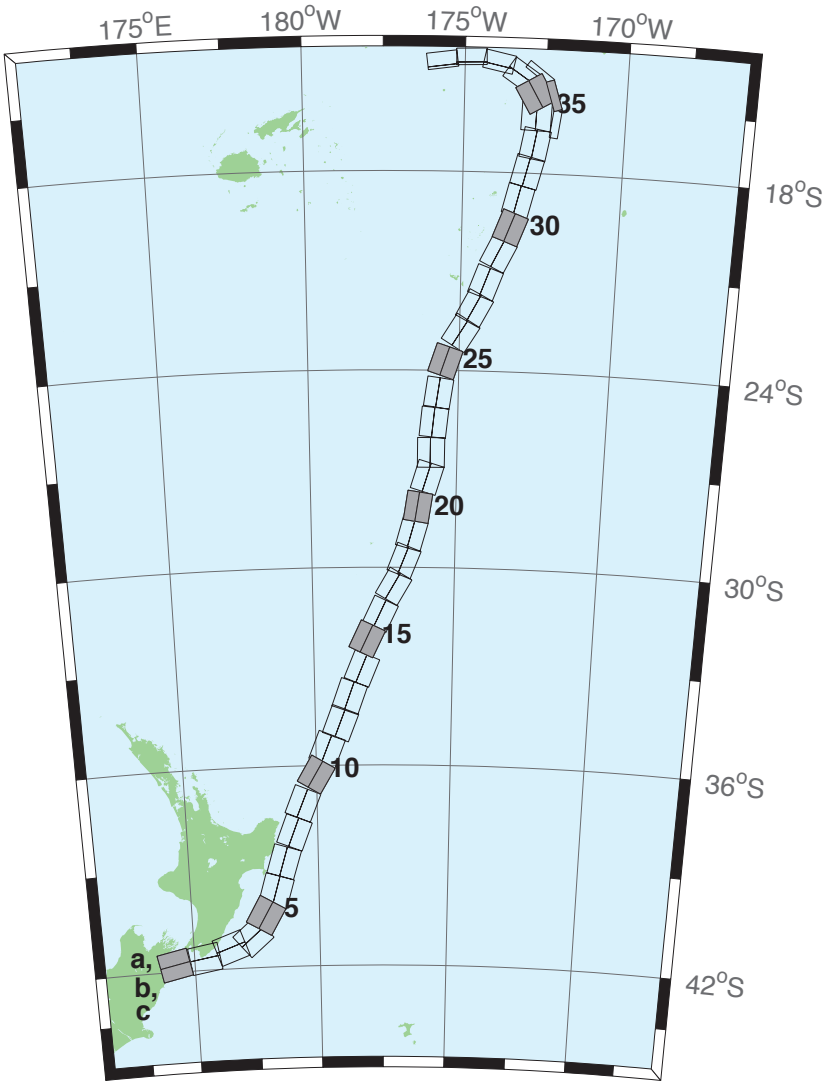

Figure B.8: New Zealand–Kermadec–Tonga Subduction Zone (NTSZ) unit sources.

Table B.8: Earthquake parameters for New Zealand–Kermadec–Tonga Subduction Zone (NTSZ) unit sources.

Segment	Description	Longitude (°E)	Latitude (°N)	Strike (°)	Dip (°)	Depth (km)
NTSZ–1a	New Zealand–Kermadec–Tonga	174.0985	-41.3951	258.6	24	25.34
NTSZ–1b	New Zealand–Kermadec–Tonga	174.2076	-41.7973	258.6	24	5
NTSZ–2a	New Zealand–Kermadec–Tonga	175.3289	-41.2592	260.6	29.38	23.17
NTSZ–2b	New Zealand–Kermadec–Tonga	175.4142	-41.6454	260.6	21.31	5
NTSZ–3a	New Zealand–Kermadec–Tonga	176.2855	-40.9950	250.7	29.54	21.74
NTSZ–3b	New Zealand–Kermadec–Tonga	176.4580	-41.3637	250.7	19.56	5
NTSZ–4a	New Zealand–Kermadec–Tonga	177.0023	-40.7679	229.4	24.43	18.87
NTSZ–4b	New Zealand–Kermadec–Tonga	177.3552	-41.0785	229.4	16.1	5
NTSZ–5a	New Zealand–Kermadec–Tonga	177.4114	-40.2396	210	18.8	19.29
NTSZ–5b	New Zealand–Kermadec–Tonga	177.8951	-40.4525	210	16.61	5
NTSZ–6a	New Zealand–Kermadec–Tonga	177.8036	-39.6085	196.7	18.17	15.8
NTSZ–6b	New Zealand–Kermadec–Tonga	178.3352	-39.7310	196.7	12.48	5
NTSZ–7a	New Zealand–Kermadec–Tonga	178.1676	-38.7480	197	28.1	17.85
NTSZ–7b	New Zealand–Kermadec–Tonga	178.6541	-38.8640	197	14.89	5
NTSZ–8a	New Zealand–Kermadec–Tonga	178.6263	-37.8501	201.4	31.47	18.78
NTSZ–8b	New Zealand–Kermadec–Tonga	179.0788	-37.9899	201.4	16	5
NTSZ–9a	New Zealand–Kermadec–Tonga	178.9833	-36.9770	202.2	29.58	20.02
NTSZ–9b	New Zealand–Kermadec–Tonga	179.4369	-37.1245	202.2	17.48	5
NTSZ–10a	New Zealand–Kermadec–Tonga	179.5534	-36.0655	210.6	32.1	20.72
NTSZ–10b	New Zealand–Kermadec–Tonga	179.9595	-36.2593	210.6	18.32	5
NTSZ–11a	New Zealand–Kermadec–Tonga	179.9267	-35.3538	201.7	25	16.09
NTSZ–11b	New Zealand–Kermadec–Tonga	180.3915	-35.5040	201.7	12.81	5
NTSZ–12a	New Zealand–Kermadec–Tonga	180.4433	-34.5759	201.2	25	15.46
NTSZ–12b	New Zealand–Kermadec–Tonga	180.9051	-34.7230	201.2	12.08	5
NTSZ–13a	New Zealand–Kermadec–Tonga	180.7990	-33.7707	199.8	25.87	19.06
NTSZ–13b	New Zealand–Kermadec–Tonga	181.2573	-33.9073	199.8	16.33	5
NTSZ–14a	New Zealand–Kermadec–Tonga	181.2828	-32.9288	202.4	31.28	22.73
NTSZ–14b	New Zealand–Kermadec–Tonga	181.7063	-33.0751	202.4	20.77	5
NTSZ–15a	New Zealand–Kermadec–Tonga	181.4918	-32.0035	205.4	32.33	22.64
NTSZ–15b	New Zealand–Kermadec–Tonga	181.8967	-32.1665	205.4	20.66	5
NTSZ–16a	New Zealand–Kermadec–Tonga	181.9781	-31.2535	205.5	34.29	23.59
NTSZ–16b	New Zealand–Kermadec–Tonga	182.3706	-31.4131	205.5	21.83	5
NTSZ–17a	New Zealand–Kermadec–Tonga	182.4819	-30.3859	210.3	37.6	25.58
NTSZ–17b	New Zealand–Kermadec–Tonga	182.8387	-30.5655	210.3	24.3	5
NTSZ–18a	New Zealand–Kermadec–Tonga	182.8176	-29.6545	201.6	37.65	26.13
NTSZ–18b	New Zealand–Kermadec–Tonga	183.1985	-29.7856	201.6	25	5
NTSZ–19a	New Zealand–Kermadec–Tonga	183.0622	-28.8739	195.7	34.41	26.13
NTSZ–19b	New Zealand–Kermadec–Tonga	183.4700	-28.9742	195.7	25	5
NTSZ–20a	New Zealand–Kermadec–Tonga	183.2724	-28.0967	188.8	38	26.13
NTSZ–20b	New Zealand–Kermadec–Tonga	183.6691	-28.1508	188.8	25	5
NTSZ–21a	New Zealand–Kermadec–Tonga	183.5747	-27.1402	197.1	32.29	24.83
NTSZ–21b	New Zealand–Kermadec–Tonga	183.9829	-27.2518	197.1	23.37	5
NTSZ–22a	New Zealand–Kermadec–Tonga	183.6608	-26.4975	180	29.56	18.63
NTSZ–22b	New Zealand–Kermadec–Tonga	184.0974	-26.4975	180	15.82	5
NTSZ–23a	New Zealand–Kermadec–Tonga	183.7599	-25.5371	185.8	32.42	20.56
NTSZ–23b	New Zealand–Kermadec–Tonga	184.1781	-25.5752	185.8	18.13	5
NTSZ–24a	New Zealand–Kermadec–Tonga	183.9139	-24.6201	188.2	33.31	23.73
NTSZ–24b	New Zealand–Kermadec–Tonga	184.3228	-24.6734	188.2	22	5
NTSZ–25a	New Zealand–Kermadec–Tonga	184.1266	-23.5922	198.5	29.34	19.64
NTSZ–25b	New Zealand–Kermadec–Tonga	184.5322	-23.7163	198.5	17.03	5
NTSZ–26a	New Zealand–Kermadec–Tonga	184.6613	-22.6460	211.7	30.26	19.43
NTSZ–26b	New Zealand–Kermadec–Tonga	185.0196	-22.8497	211.7	16.78	5
NTSZ–27a	New Zealand–Kermadec–Tonga	185.0879	-21.9139	207.9	31.73	20.67
NTSZ–27b	New Zealand–Kermadec–Tonga	185.4522	-22.0928	207.9	18.27	5
NTSZ–28a	New Zealand–Kermadec–Tonga	185.4037	-21.1758	200.5	32.44	21.76
NTSZ–28b	New Zealand–Kermadec–Tonga	185.7849	-21.3084	200.5	19.58	5
NTSZ–29a	New Zealand–Kermadec–Tonga	185.8087	-20.2629	206.4	32.47	20.4
NTSZ–29b	New Zealand–Kermadec–Tonga	186.1710	-20.4312	206.4	17.94	5
NTSZ–30a	New Zealand–Kermadec–Tonga	186.1499	-19.5087	200.9	32.98	22.46
NTSZ–30b	New Zealand–Kermadec–Tonga	186.5236	-19.6432	200.9	20.44	5

Continued on next page

Table B.8 – continued

Segment	Description	Longitude (°E)	Latitude (°N)	Strike (°)	Dip (°)	Depth (km)
NTSZ–31a	New Zealand–Kermadec–Tonga	186.3538	-18.7332	193.9	34.41	21.19
NTSZ–31b	New Zealand–Kermadec–Tonga	186.7339	-18.8221	193.9	18.89	5
NTSZ–32a	New Zealand–Kermadec–Tonga	186.5949	-17.8587	194.1	30	19.12
NTSZ–32b	New Zealand–Kermadec–Tonga	186.9914	-17.9536	194.1	16.4	5
NTSZ–33a	New Zealand–Kermadec–Tonga	186.8172	-17.0581	190	33.15	23.34
NTSZ–33b	New Zealand–Kermadec–Tonga	187.2047	-17.1237	190	21.52	5
NTSZ–34a	New Zealand–Kermadec–Tonga	186.7814	-16.2598	182.1	15	13.41
NTSZ–34b	New Zealand–Kermadec–Tonga	187.2330	-16.2759	182.1	9.68	5
NTSZ–34c	New Zealand–Kermadec–Tonga	187.9697	-16.4956	7.62	57.06	6.571
NTSZ–35a	New Zealand–Kermadec–Tonga	186.8000	-15.8563	149.8	15	12.17
NTSZ–35b	New Zealand–Kermadec–Tonga	187.1896	-15.6384	149.8	8.24	5
NTSZ–35c	New Zealand–Kermadec–Tonga	187.8776	-15.6325	342.4	57.06	6.571
NTSZ–36a	New Zealand–Kermadec–Tonga	186.5406	-15.3862	123.9	40.44	36.72
NTSZ–36b	New Zealand–Kermadec–Tonga	186.7381	-15.1025	123.9	39.38	5
NTSZ–36c	New Zealand–Kermadec–Tonga	187.3791	-14.9234	307	57.06	6.571
NTSZ–37a	New Zealand–Kermadec–Tonga	185.9883	-14.9861	102	68.94	30.99
NTSZ–37b	New Zealand–Kermadec–Tonga	186.0229	-14.8282	102	31.32	5
NTSZ–38a	New Zealand–Kermadec–Tonga	185.2067	-14.8259	88.4	80	26.13
NTSZ–38b	New Zealand–Kermadec–Tonga	185.2044	-14.7479	88.4	25	5
NTSZ–39a	New Zealand–Kermadec–Tonga	184.3412	-14.9409	82.55	80	26.13
NTSZ–39b	New Zealand–Kermadec–Tonga	184.3307	-14.8636	82.55	25	5

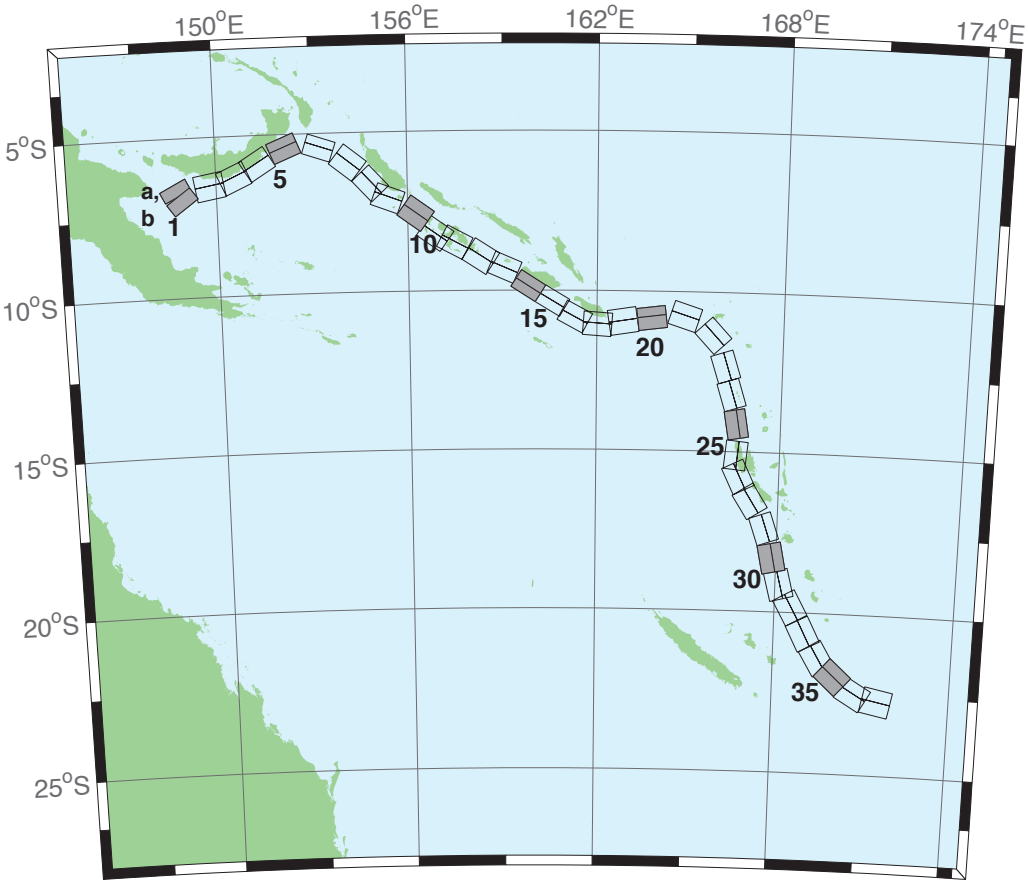

Figure B.9: New Britain–Solomons–Vanuatu Subduction Zone (NVSZ) unit sources.

Table B.9: Earthquake parameters for New Britain–Solomons–Vanuatu Subduction Zone (NVSZ) unit sources.

Segment	Description	Longitude (°E)	Latitude (°N)	Strike (°)	Dip (°)	Depth (km)
NVSZ–1a	New Britain–Solomons–Vanuatu	148.6217	-6.4616	243.2	32.34	15.69
NVSZ–1b	New Britain–Solomons–Vanuatu	148.7943	-6.8002	234.2	12.34	5
NVSZ–2a	New Britain–Solomons–Vanuatu	149.7218	-6.1459	260.1	35.1	16.36
NVSZ–2b	New Britain–Solomons–Vanuatu	149.7856	-6.5079	260.1	13.13	5
NVSZ–3a	New Britain–Solomons–Vanuatu	150.4075	-5.9659	245.7	42.35	18.59
NVSZ–3b	New Britain–Solomons–Vanuatu	150.5450	-6.2684	245.7	15.77	5
NVSZ–4a	New Britain–Solomons–Vanuatu	151.1095	-5.5820	238.2	42.41	23.63
NVSZ–4b	New Britain–Solomons–Vanuatu	151.2851	-5.8639	238.2	21.88	5
NVSZ–5a	New Britain–Solomons–Vanuatu	152.0205	-5.1305	247.7	49.22	32.39
NVSZ–5b	New Britain–Solomons–Vanuatu	152.1322	-5.4020	247.7	33.22	5
NVSZ–6a	New Britain–Solomons–Vanuatu	153.3450	-5.1558	288.6	53.53	33.59
NVSZ–6b	New Britain–Solomons–Vanuatu	153.2595	-5.4089	288.6	34.87	5
NVSZ–7a	New Britain–Solomons–Vanuatu	154.3814	-5.6308	308.3	39.72	19.18
NVSZ–7b	New Britain–Solomons–Vanuatu	154.1658	-5.9017	308.3	16.48	5
NVSZ–8a	New Britain–Solomons–Vanuatu	155.1097	-6.3511	317.2	45.33	22.92
NVSZ–8b	New Britain–Solomons–Vanuatu	154.8764	-6.5656	317.2	21	5
NVSZ–9a	New Britain–Solomons–Vanuatu	155.5027	-6.7430	290.5	48.75	22.92
NVSZ–9b	New Britain–Solomons–Vanuatu	155.3981	-7.0204	290.5	21	5
NVSZ–10a	New Britain–Solomons–Vanuatu	156.4742	-7.2515	305.9	36.88	27.62
NVSZ–10b	New Britain–Solomons–Vanuatu	156.2619	-7.5427	305.9	26.9	5
NVSZ–11a	New Britain–Solomons–Vanuatu	157.0830	-7.8830	305.4	32.97	29.72
NVSZ–11b	New Britain–Solomons–Vanuatu	156.8627	-8.1903	305.4	29.63	5
NVSZ–12a	New Britain–Solomons–Vanuatu	157.6537	-8.1483	297.9	37.53	28.57
NVSZ–12b	New Britain–Solomons–Vanuatu	157.4850	-8.4630	297.9	28.13	5
NVSZ–13a	New Britain–Solomons–Vanuatu	158.5089	-8.5953	302.7	33.62	23.02
NVSZ–13b	New Britain–Solomons–Vanuatu	158.3042	-8.9099	302.7	21.12	5
NVSZ–14a	New Britain–Solomons–Vanuatu	159.1872	-8.9516	293.3	38.44	34.06
NVSZ–14b	New Britain–Solomons–Vanuatu	159.0461	-9.2747	293.3	35.54	5
NVSZ–15a	New Britain–Solomons–Vanuatu	159.9736	-9.5993	302.8	46.69	41.38
NVSZ–15b	New Britain–Solomons–Vanuatu	159.8044	-9.8584	302.8	46.69	5
NVSZ–16a	New Britain–Solomons–Vanuatu	160.7343	-10.0574	301	46.05	41
NVSZ–16b	New Britain–Solomons–Vanuatu	160.5712	-10.3246	301	46.05	5
NVSZ–17a	New Britain–Solomons–Vanuatu	161.4562	-10.5241	298.4	40.12	37.22
NVSZ–17b	New Britain–Solomons–Vanuatu	161.2900	-10.8263	298.4	40.12	5
NVSZ–18a	New Britain–Solomons–Vanuatu	162.0467	-10.6823	274.1	40.33	29.03
NVSZ–18b	New Britain–Solomons–Vanuatu	162.0219	-11.0238	274.1	28.72	5
NVSZ–19a	New Britain–Solomons–Vanuatu	162.7818	-10.5645	261.3	34.25	24.14
NVSZ–19b	New Britain–Solomons–Vanuatu	162.8392	-10.9315	261.3	22.51	5
NVSZ–20a	New Britain–Solomons–Vanuatu	163.7222	-10.5014	262.9	50.35	26.3
NVSZ–20b	New Britain–Solomons–Vanuatu	163.7581	-10.7858	262.9	25.22	5
NVSZ–21a	New Britain–Solomons–Vanuatu	164.9445	-10.4183	287.9	40.31	23.3
NVSZ–21b	New Britain–Solomons–Vanuatu	164.8374	-10.7442	287.9	21.47	5
NVSZ–22a	New Britain–Solomons–Vanuatu	166.0261	-11.1069	317.1	42.39	20.78
NVSZ–22b	New Britain–Solomons–Vanuatu	165.7783	-11.3328	317.1	18.4	5
NVSZ–23a	New Britain–Solomons–Vanuatu	166.5179	-12.2260	342.4	47.95	22.43
NVSZ–23b	New Britain–Solomons–Vanuatu	166.2244	-12.3171	342.4	20.4	5
NVSZ–24a	New Britain–Solomons–Vanuatu	166.7236	-13.1065	342.6	47.13	28.52
NVSZ–24b	New Britain–Solomons–Vanuatu	166.4241	-13.1979	342.6	28.06	5
NVSZ–25a	New Britain–Solomons–Vanuatu	166.8914	-14.0785	350.3	54.1	31.16
NVSZ–25b	New Britain–Solomons–Vanuatu	166.6237	-14.1230	350.3	31.55	5
NVSZ–26a	New Britain–Solomons–Vanuatu	166.9200	-15.1450	365.6	50.46	29.05
NVSZ–26b	New Britain–Solomons–Vanuatu	166.6252	-15.1170	365.6	28.75	5
NVSZ–27a	New Britain–Solomons–Vanuatu	167.0053	-15.6308	334.2	44.74	25.46
NVSZ–27b	New Britain–Solomons–Vanuatu	166.7068	-15.7695	334.2	24.15	5
NVSZ–28a	New Britain–Solomons–Vanuatu	167.4074	-16.3455	327.5	41.53	22.44
NVSZ–28b	New Britain–Solomons–Vanuatu	167.1117	-16.5264	327.5	20.42	5
NVSZ–29a	New Britain–Solomons–Vanuatu	167.9145	-17.2807	341.2	49.1	24.12
NVSZ–29b	New Britain–Solomons–Vanuatu	167.6229	-17.3757	341.2	22.48	5
NVSZ–30a	New Britain–Solomons–Vanuatu	168.2220	-18.2353	348.6	44.19	23.99
NVSZ–30b	New Britain–Solomons–Vanuatu	167.8895	-18.2991	348.6	22.32	5

Continued on next page

Table B.9 – continued

Segment	Description	Longitude (°E)	Latitude (°N)	Strike (°)	Dip (°)	Depth (km)
NVSZ–31a	New Britain–Solomons–Vanuatu	168.5022	-19.0510	345.6	42.2	22.26
NVSZ–31b	New Britain–Solomons–Vanuatu	168.1611	-19.1338	345.6	20.2	5
NVSZ–32a	New Britain–Solomons–Vanuatu	168.8775	-19.6724	331.1	42.03	21.68
NVSZ–32b	New Britain–Solomons–Vanuatu	168.5671	-19.8338	331.1	19.49	5
NVSZ–33a	New Britain–Solomons–Vanuatu	169.3422	-20.4892	332.9	40.25	22.4
NVSZ–33b	New Britain–Solomons–Vanuatu	169.0161	-20.6453	332.9	20.37	5
NVSZ–34a	New Britain–Solomons–Vanuatu	169.8304	-21.2121	329.1	39	22.73
NVSZ–34b	New Britain–Solomons–Vanuatu	169.5086	-21.3911	329.1	20.77	5
NVSZ–35a	New Britain–Solomons–Vanuatu	170.3119	-21.6945	311.9	39	22.13
NVSZ–35b	New Britain–Solomons–Vanuatu	170.0606	-21.9543	311.9	20.03	5
NVSZ–36a	New Britain–Solomons–Vanuatu	170.9487	-22.1585	300.4	39.42	23.5
NVSZ–36b	New Britain–Solomons–Vanuatu	170.7585	-22.4577	300.4	21.71	5
NVSZ–37a	New Britain–Solomons–Vanuatu	171.6335	-22.3087	281.3	30	22.1
NVSZ–37b	New Britain–Solomons–Vanuatu	171.5512	-22.6902	281.3	20	5

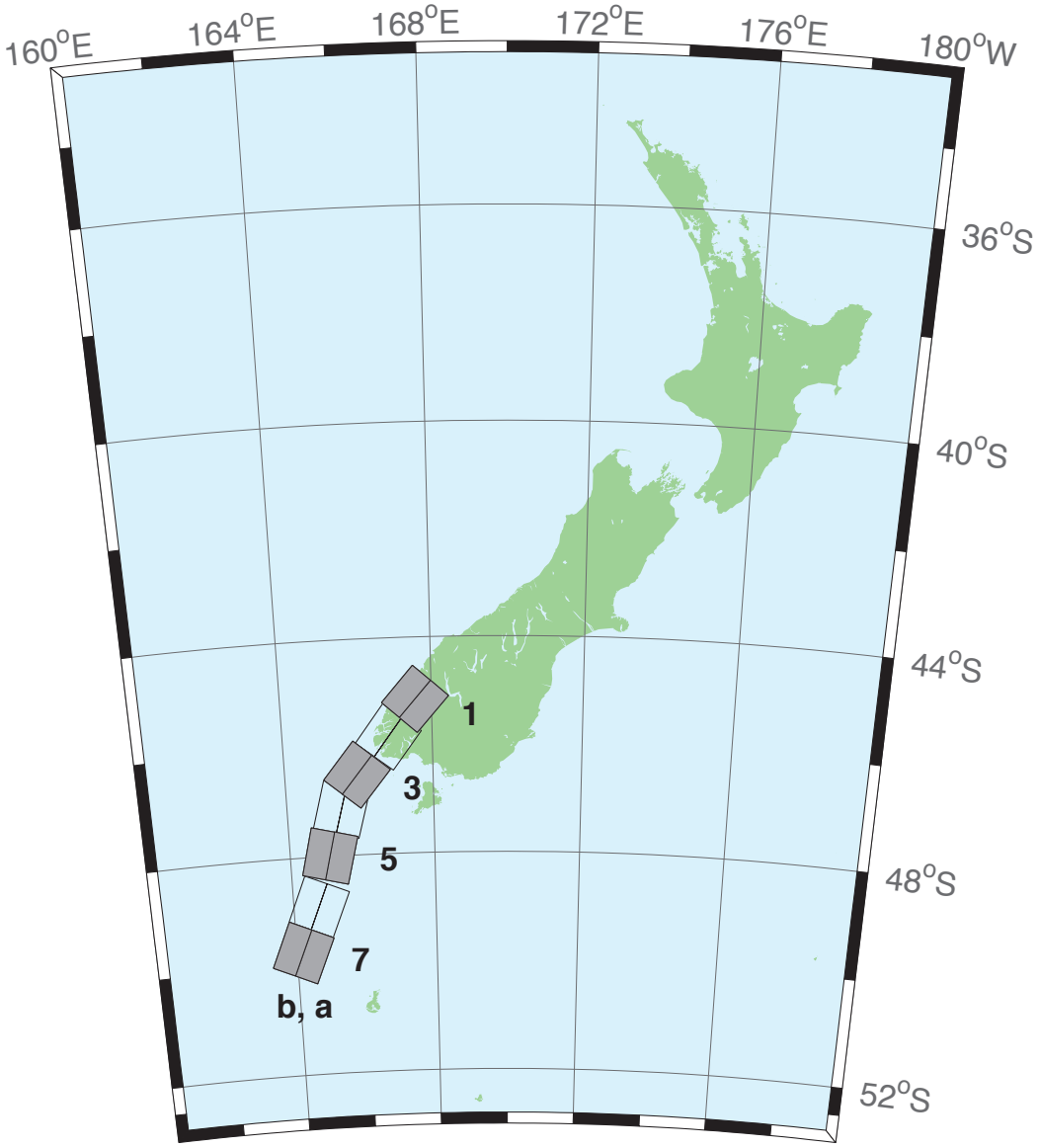

Figure B.10: New Zealand–Puysegur Subduction Zone (NPSZ) unit sources.

Table B.10: Earthquake parameters for New Zealand–Puysegur Subduction Zone (NPSZ) unit sources.

Segment	Description	Longitude (°E)	Latitude (°N)	Strike (°)	Dip (°)	Depth (km)
NZSZ–1a	New Zealand–Puysegur	168.0294	-45.4368	41.5	15	17.94
NZSZ–1b	New Zealand–Puysegur	167.5675	-45.1493	41.5	15	5
NZSZ–2a	New Zealand–Puysegur	167.3256	-46.0984	37.14	15	17.94
NZSZ–2b	New Zealand–Puysegur	166.8280	-45.8365	37.14	15	5
NZSZ–3a	New Zealand–Puysegur	166.4351	-46.7897	39.53	15	17.94
NZSZ–3b	New Zealand–Puysegur	165.9476	-46.5136	39.53	15	5
NZSZ–4a	New Zealand–Puysegur	166.0968	-47.2583	15.38	15	17.94
NZSZ–4b	New Zealand–Puysegur	165.4810	-47.1432	15.38	15	5
NZSZ–5a	New Zealand–Puysegur	165.7270	-48.0951	13.94	15	17.94
NZSZ–5b	New Zealand–Puysegur	165.0971	-47.9906	13.94	15	5
NZSZ–6a	New Zealand–Puysegur	165.3168	-49.0829	22.71	15	17.94
NZSZ–6b	New Zealand–Puysegur	164.7067	-48.9154	22.71	15	5
NZSZ–7a	New Zealand–Puysegur	164.8017	-49.9193	23.25	15	17.94
NZSZ–7b	New Zealand–Puysegur	164.1836	-49.7480	23.25	15	5

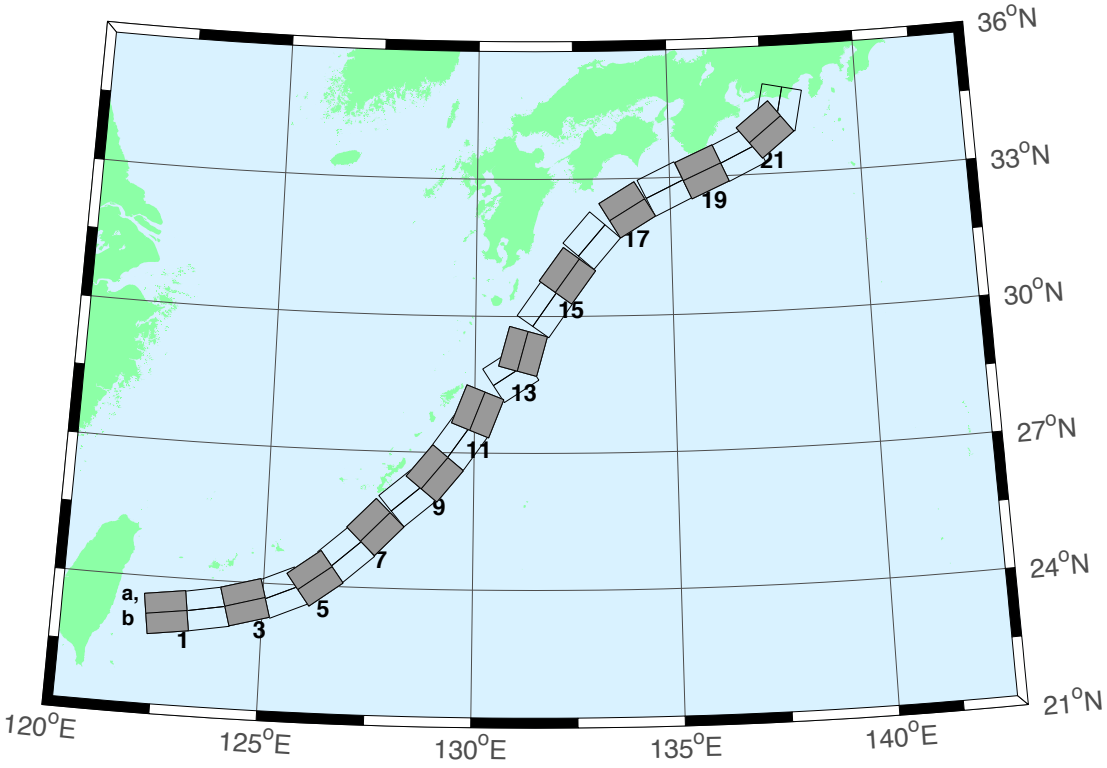

Figure B.11: Ryukyu–Kyushu–Nankai Subduction Zone (RNSZ) unit sources.

Table B.11: Earthquake parameters for Ryukyu–Kyushu–Nankai Subduction Zone (RNSZ) unit sources.

Segment	Description	Longitude (°E)	Latitude (°N)	Strike (°)	Dip (°)	Depth (km)
RNSZ–1a	Ryukyu–Kyushu–Nankai	122.6672	23.6696	262	14	11.88
RNSZ–1b	Ryukyu–Kyushu–Nankai	122.7332	23.2380	262	10	3.2
RNSZ–2a	Ryukyu–Kyushu–Nankai	123.5939	23.7929	259.9	18.11	12.28
RNSZ–2b	Ryukyu–Kyushu–Nankai	123.6751	23.3725	259.9	10	3.6
RNSZ–3a	Ryukyu–Kyushu–Nankai	124.4604	23.9777	254.6	19.27	14.65
RNSZ–3b	Ryukyu–Kyushu–Nankai	124.5830	23.5689	254.6	12.18	4.1
RNSZ–4a	Ryukyu–Kyushu–Nankai	125.2720	24.2102	246.8	18	20.38
RNSZ–4b	Ryukyu–Kyushu–Nankai	125.4563	23.8177	246.8	16	6.6
RNSZ–5a	Ryukyu–Kyushu–Nankai	125.9465	24.5085	233.6	18	20.21
RNSZ–5b	Ryukyu–Kyushu–Nankai	126.2241	24.1645	233.6	16	6.43
RNSZ–6a	Ryukyu–Kyushu–Nankai	126.6349	25.0402	228.7	17.16	19.55
RNSZ–6b	Ryukyu–Kyushu–Nankai	126.9465	24.7176	228.7	15.16	6.47
RNSZ–7a	Ryukyu–Kyushu–Nankai	127.2867	25.6343	224	15.85	17.98
RNSZ–7b	Ryukyu–Kyushu–Nankai	127.6303	25.3339	224	13.56	6.26
RNSZ–8a	Ryukyu–Kyushu–Nankai	128.0725	26.3146	229.7	14.55	14.31
RNSZ–8b	Ryukyu–Kyushu–Nankai	128.3854	25.9831	229.7	9.64	5.94
RNSZ–9a	Ryukyu–Kyushu–Nankai	128.6642	26.8177	219.2	15.4	12.62
RNSZ–9b	Ryukyu–Kyushu–Nankai	129.0391	26.5438	219.2	8	5.66
RNSZ–10a	Ryukyu–Kyushu–Nankai	129.2286	27.4879	215.2	17	12.55
RNSZ–10b	Ryukyu–Kyushu–Nankai	129.6233	27.2402	215.2	8.16	5.45
RNSZ–11a	Ryukyu–Kyushu–Nankai	129.6169	28.0741	201.3	17	12.91
RNSZ–11b	Ryukyu–Kyushu–Nankai	130.0698	27.9181	201.3	8.8	5.26
RNSZ–12a	Ryukyu–Kyushu–Nankai	130.6175	29.0900	236.7	16.42	13.05
RNSZ–12b	Ryukyu–Kyushu–Nankai	130.8873	28.7299	236.7	9.57	4.74
RNSZ–13a	Ryukyu–Kyushu–Nankai	130.7223	29.3465	195.2	20.25	15.89
RNSZ–13b	Ryukyu–Kyushu–Nankai	131.1884	29.2362	195.2	12.98	4.66
RNSZ–14a	Ryukyu–Kyushu–Nankai	131.3467	30.3899	215.1	22.16	19.73
RNSZ–14b	Ryukyu–Kyushu–Nankai	131.7402	30.1507	215.1	17.48	4.71
RNSZ–15a	Ryukyu–Kyushu–Nankai	131.9149	31.1450	216	15.11	16.12
RNSZ–15b	Ryukyu–Kyushu–Nankai	132.3235	30.8899	216	13.46	4.48
RNSZ–16a	Ryukyu–Kyushu–Nankai	132.5628	31.9468	220.9	10.81	10.88
RNSZ–16b	Ryukyu–Kyushu–Nankai	132.9546	31.6579	220.9	7.19	4.62
RNSZ–17a	Ryukyu–Kyushu–Nankai	133.6125	32.6956	239	10.14	12.01
RNSZ–17b	Ryukyu–Kyushu–Nankai	133.8823	32.3168	239	8.41	4.7
RNSZ–18a	Ryukyu–Kyushu–Nankai	134.6416	33.1488	244.7	10.99	14.21
RNSZ–18b	Ryukyu–Kyushu–Nankai	134.8656	32.7502	244.5	10.97	4.7
RNSZ–19a	Ryukyu–Kyushu–Nankai	135.6450	33.5008	246.5	14.49	14.72
RNSZ–19b	Ryukyu–Kyushu–Nankai	135.8523	33.1021	246.5	11.87	4.44
RNSZ–20a	Ryukyu–Kyushu–Nankai	136.5962	33.8506	244.8	15	14.38
RNSZ–20b	Ryukyu–Kyushu–Nankai	136.8179	33.4581	244.8	12	3.98
RNSZ–21a	Ryukyu–Kyushu–Nankai	137.2252	34.3094	231.9	15	15.4
RNSZ–21b	Ryukyu–Kyushu–Nankai	137.5480	33.9680	231.9	12	5
RNSZ–22a	Ryukyu–Kyushu–Nankai	137.4161	34.5249	192.3	15	15.4
RNSZ–22b	Ryukyu–Kyushu–Nankai	137.9301	34.4327	192.3	12	5

Appendix C

SIFT Testing

Authors: Lindsey Wright, Utku Kânoğlu

C.1 Purpose

Forecast models are tested with synthetic tsunami events covering a range of tsunami source locations. Testing is also done with selected historical tsunami events when available.

The purpose of forecast model testing is three-fold. The first objective is to assure that the results obtained with NOAA's tsunami forecast system, which has been released to the Tsunami Warning Centers (TWCs) for operational use, are consistent with those obtained by the researcher during the development of the forecast model. The second objective is to test the forecast model for consistency, accuracy, time efficiency, and quality of results over a range of possible tsunami locations and magnitudes. The third objective is to identify bugs and issues in need of resolution by the researcher who developed the forecast model or by the forecast software development team before the next version release to NOAA's two TWCs.

Local hardware and software applications, and tools familiar to the researcher(s), are used to run the Method of Splitting Tsunamis (MOST) model during the forecast model development. The test results presented in this report lend confidence that the model performs as developed and produces the same results when initiated within the forecast application in an operational setting as those produced by the researcher during the forecast model development. The test results assure those who rely on the Homer tsunami forecast model that consistent results are produced irrespective of system.

C.2 Testing Procedure

The general procedure for forecast model testing is to run a set of synthetic tsunami scenarios and a selected set of historical tsunami events through the forecast system application and compare the results with those obtained by the researcher during the forecast model development and presented in this report. Specific steps taken to test the model include:

1. Identification of testing scenarios, including the standard set of synthetic events, appropriate historical events, and customized synthetic scenarios that may have been used by the researcher(s) in developing the forecast model.

2. Creation of new events to represent customized synthetic scenarios used by the researcher(s) in developing the forecast model, if any.

3. Submission of test model runs with the forecast system, and export of the results from A-, B-, and C-grids, along with time series.

4. Recording applicable metadata, including the specific version of the forecast system used for testing.

5. Examination of forecast model results from the forecast system for instabilities in both time series and plot results.

6. Comparison of forecast model results obtained through the forecast system with those obtained during the forecast model development.

7. Summarization of results with specific mention of quality, consistency, and time efficiency.

8. Reporting of issues identified to modeler and forecast software development team.

9. Retesting the forecast models in the forecast system when reported issues have been addressed or explained.

Synthetic model runs were tested on a DELL PowerEdge R510 computer equipped with two Xeon E5670 processors at 2.93 Ghz, each with 12 MBytes of cache and 32GB memory. The processors are hex core and support hyperthreading, resulting in the computer performing as a 24 processor core machine. Additionally, the testing computer supports 10 Gigabit Ethernet for fast network connections. This computer configuration is similar or the same as the configurations of the computers installed at the TWCs so the compute times should only vary slightly.

C.3 Results

The Homer forecast model was tested with NOAA's tsunami forecast system version 3.2 using four synthetic scenarios and one historical tsunami event. Test results from the forecast system and comparisons with the results obtained during the forecast model development are shown numerically in Table C.1 and graphically in Figures C.1 to C.4. The results show that the forecast model is stable and robust, with consistent and high quality results across geographically distributed tsunami sources and mega-event tsunami magnitudes. The model run time (wall clock time) was 25.45 minutes for 10 hours of simulation time, and 10.16 minutes for 4 hours (Table C.2). This run time is acceptable for 10 minute run time for 4 hours of simulation time and satisfies time efficiency requirements.

Four synthetic events were run on the Homer forecast model. A standard 25 m slip was used for all synthetic cases for comparison purposes. The modeled scenarios were stable for all cases tested, with no instabilities or ringing. Results show that the largest modeled height was 38 cm and originated in the Aleutian–Alaska–Cascadia Subduction Zone (ACSZ) 56–65 source. Amplitudes less than 20 cm were recorded for 3 of the 4 test sources and the smallest signal of 9.6 cm was recorded at the Kamchatka–Yap–Mariana–Izu–Bonin Subduction Zone (KISZ) 22–31 source. All scenarios were similar in shape and amplitude when compared with the results

obtained during development. The 11 March 2011 Japan event was also stable and the wave pattern output from the forecast system appears similar in shape and amplitude when compared to development results (Figures C.5).

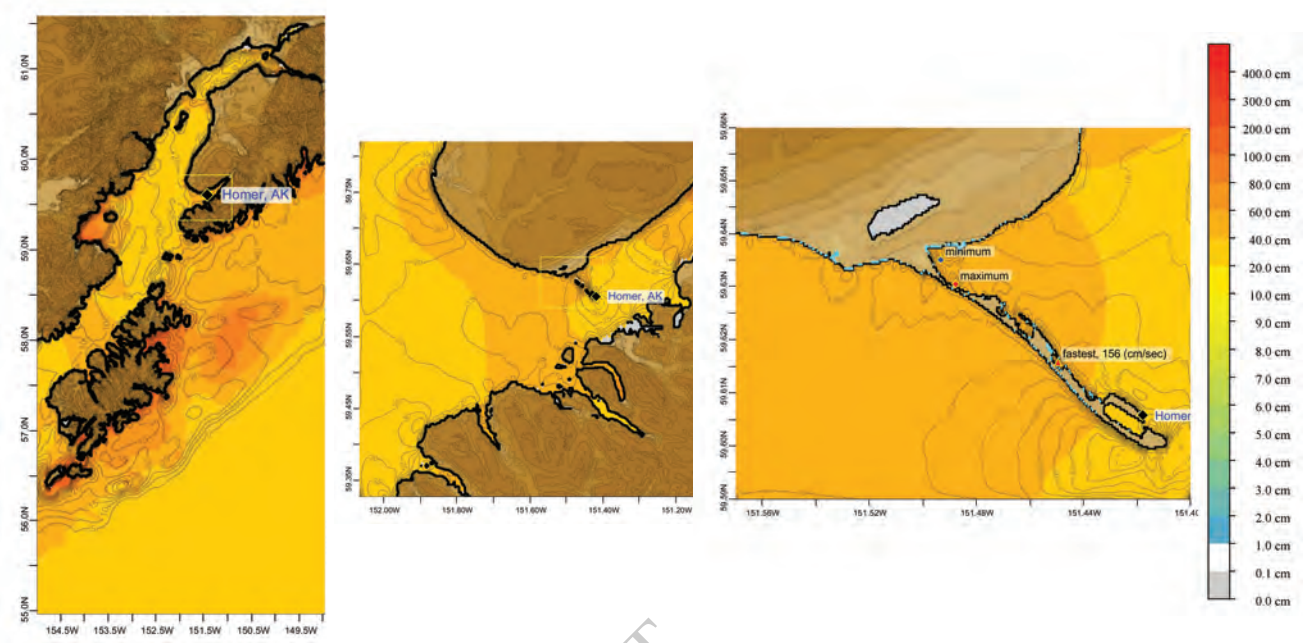

(a) (b) (c)

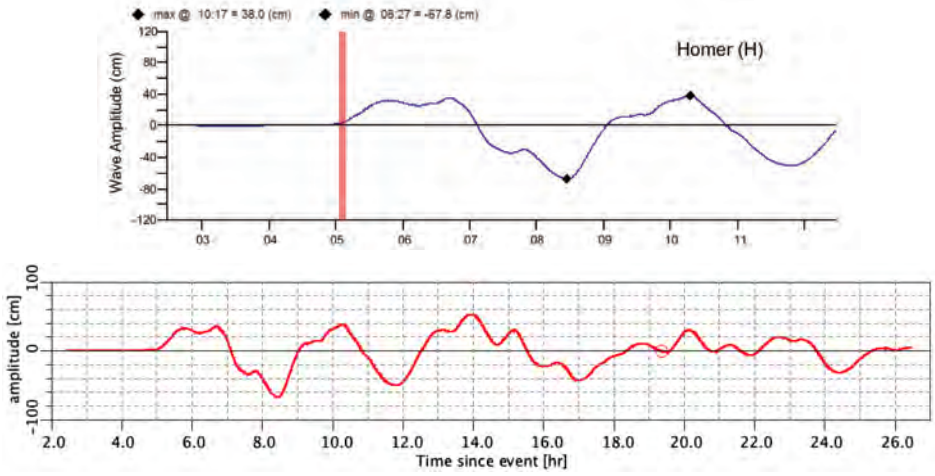

(d)

Figure C.1: Response of the Homer forecast model to synthetic scenario ACSZ 56–65 ($\alpha = 25$). Maximum sea surface elevation for (a) A-grid, b) B-grid, c) C-grid and d) sea surface elevation time series at the C-grid warning point. Sea surface elevation time series obtained during SIFT testing (upper inset) is compared the one obtained during model development (lower inset).

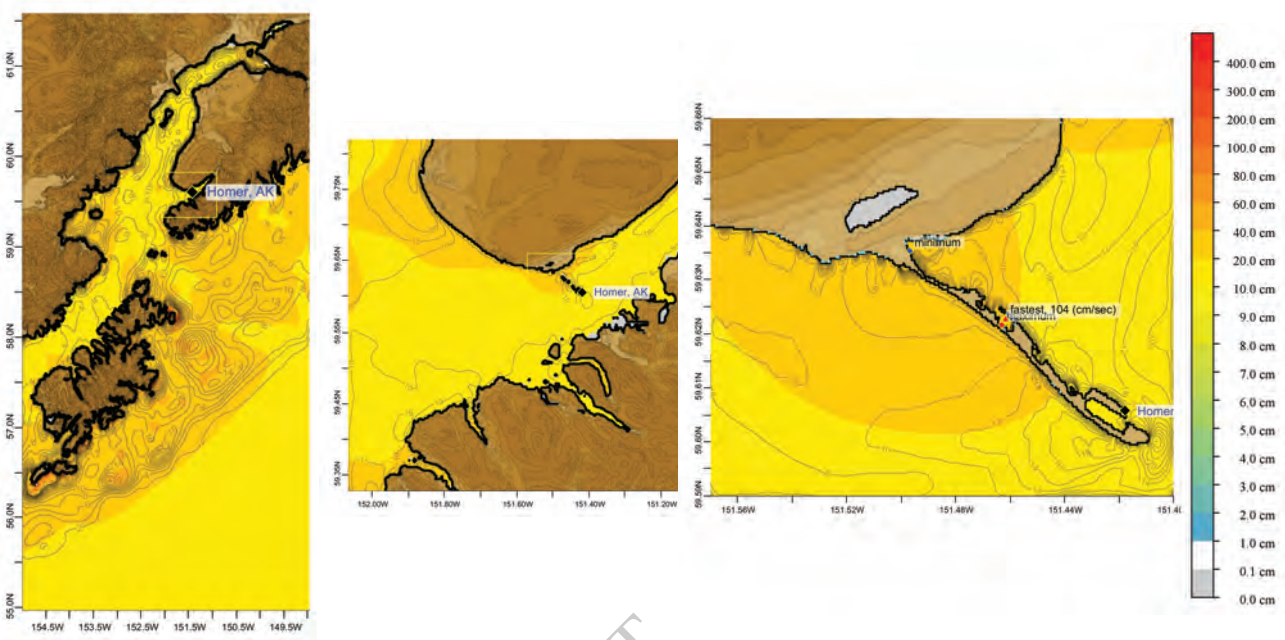

(a) (b) (c)

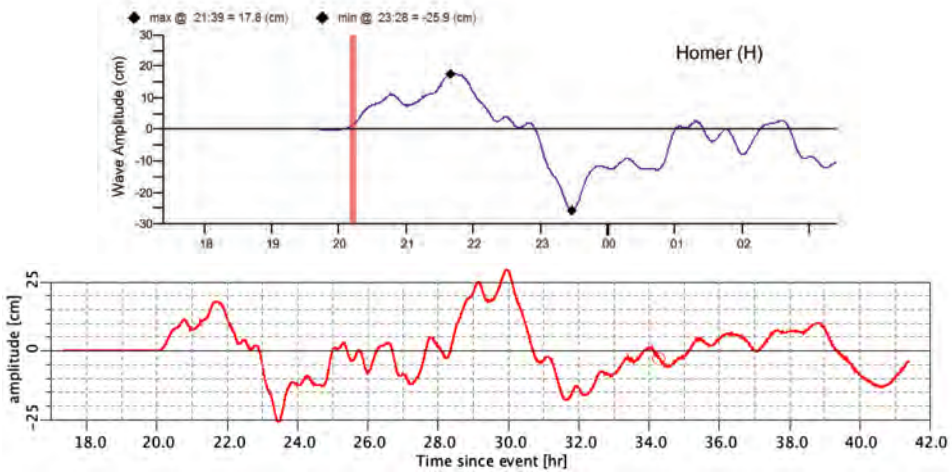

(d)

Figure C.2: Response of the Homer forecast model to synthetic scenario CSSZ 89–98 ($\alpha = 25$). Maximum sea surface elevation for (a) A-grid, b) B-grid, c) C-grid and d) sea surface elevation time series at the C-grid warning point. Sea surface elevation time series obtained during SIFT testing (upper inset) is compared the one obtained during model development (lower inset).

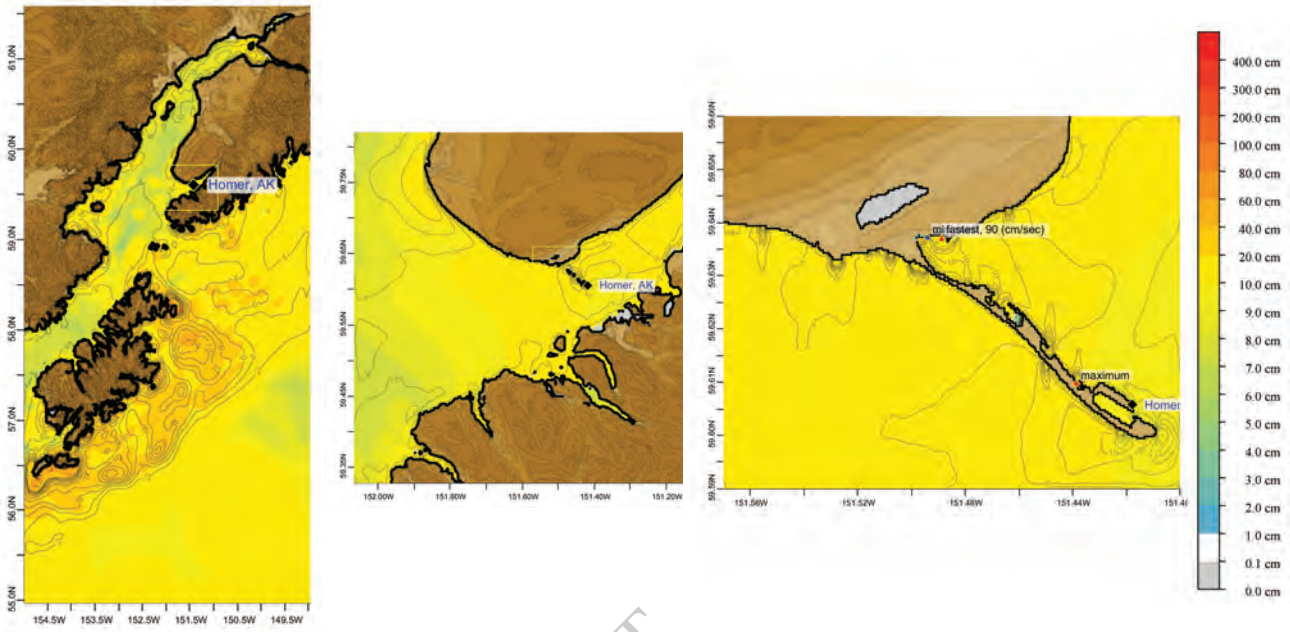

(a) (b) (c)

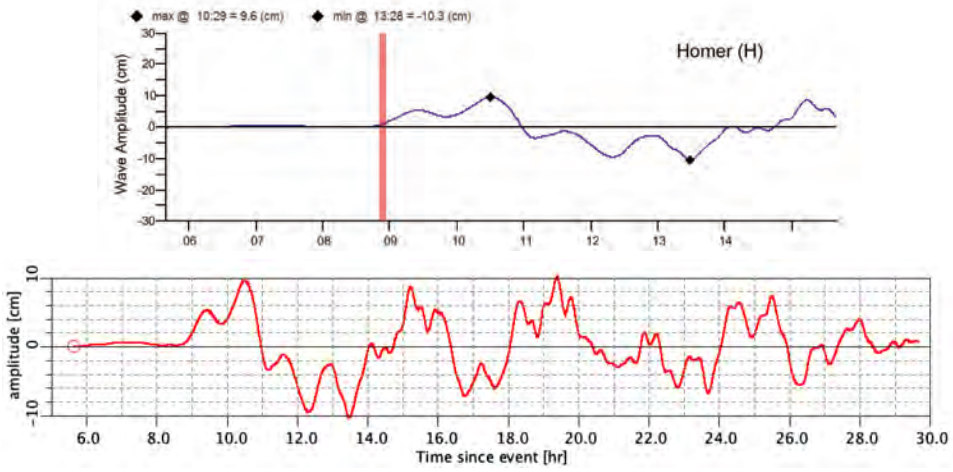

(d)

Figure C.3: Response of the Homer forecast model to synthetic scenario KISZ 22–31 ($\alpha = 25$). Maximum sea surface elevation for (a) A-grid, b) B-grid, c) C-grid and d) sea surface elevation time series at the C-grid warning point. Sea surface elevation time series obtained during SIFT testing (upper inset) is compared the one obtained during model development (lower inset).

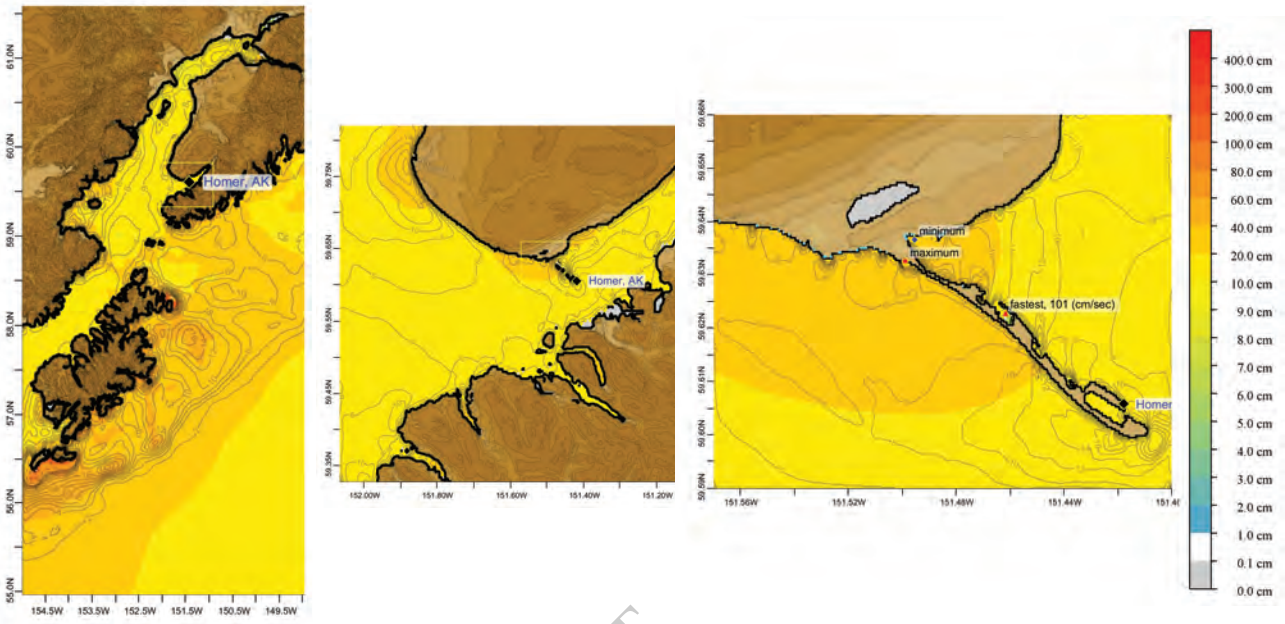

(a) (b) (c)

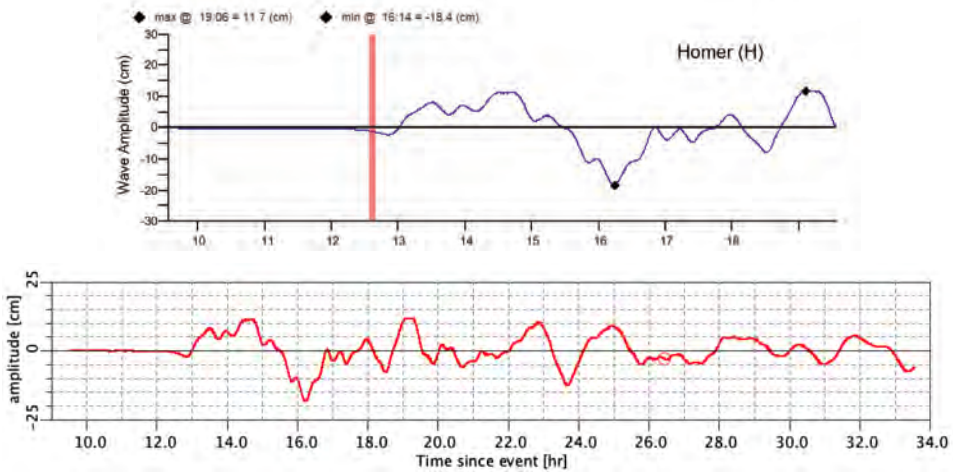

(d)

Figure C.4: Response of the Homer forecast model to synthetic scenario NTSZ 30–39 ($\alpha = 25$). Maximum sea surface elevation for (a) A-grid, b) B-grid, c) C-grid and d) sea surface elevation time series at the C-grid warning point. Sea surface elevation time series obtained during SIFT testing (upper inset) is compared the one obtained during model development (lower inset).

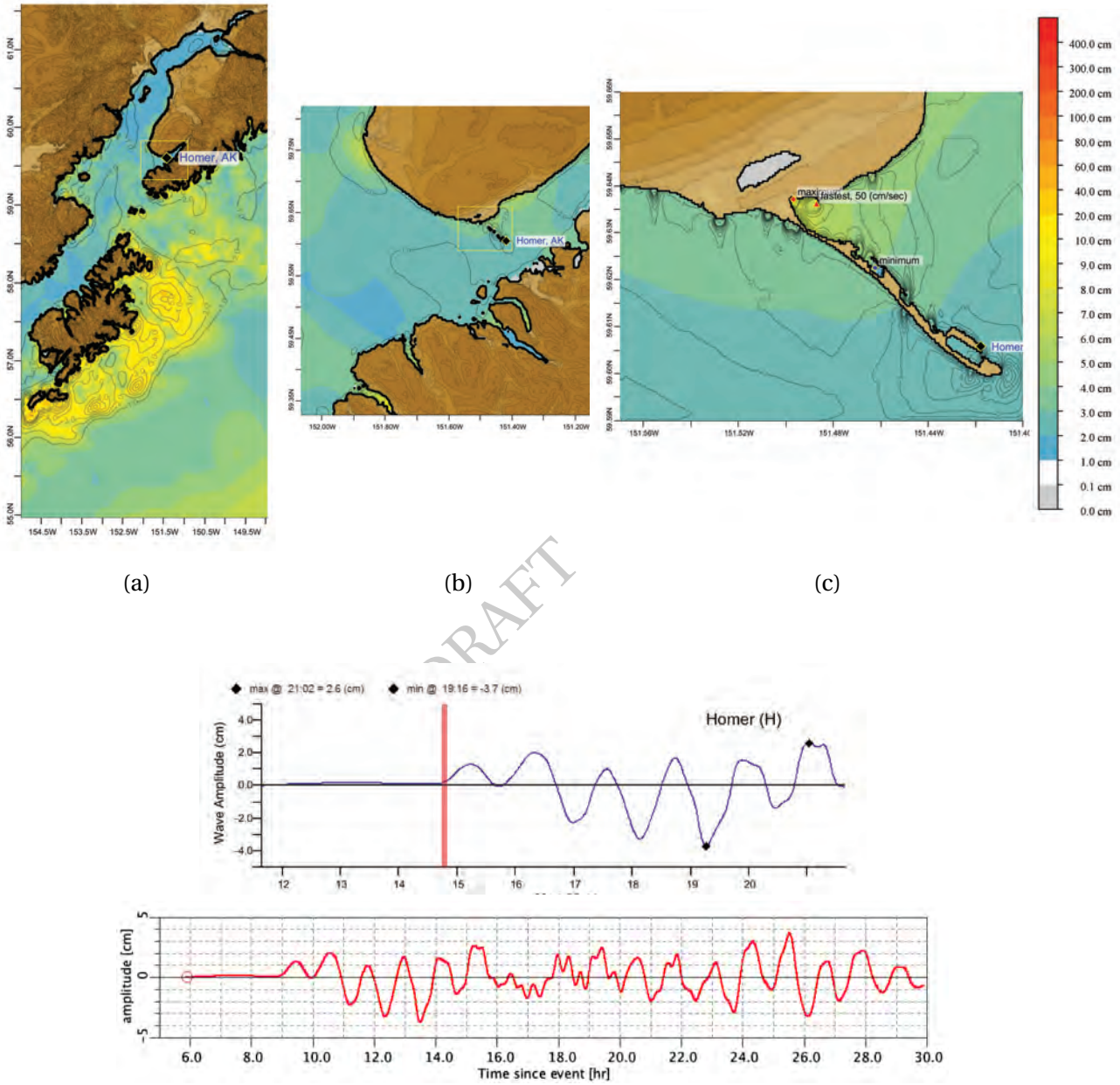

Figure C.5: Response of the Homer forecast model to the 11 March 2011 Japan tsunami. Maximum sea surface elevation for (a) A-grid, b) B-grid, c) C-grid and d) sea surface elevation time series at the C-grid warning point. Sea surface elevation time series obtained during SIFT testing (upper inset) is compared the one obtained during model development (lower inset). Note that while time axes for the SIFT testing is given as UTC, initiation time is used as the reference time during the development.

Table C.1: Run time of the Homer, Alaska forecast model.

Model	Modeled Time (hrs)	Wall Time (min)	4-hour Time (min)	Space (Gb)	12-hour Space (Gb)
LW-acsz56-65.06a.IF_HMR	9.99	24.88	09.96	0.00	0.00
LW-cssz89-98.06b.IF_HMR	9.99	25.25	10.08	0.00	0.00
LW-kisz22-31.06b.IF_HMR	9.99	26.30	10.52	0.00	0.00
LW-ntsz30-39.05c.IF_HMR	9.99	25.45	10.16	0.00	0.00
LW-Tohoku11-01.07a.IF_HMR	9.99	25.37	10.212	0.00	0.00

Table C.2: Table of maximum and minimum amplitudes (cm) at the Homer, Alaska warning point for synthetic and historical events tested using SIFT 3.2 and obtained during development.

Scenario Name	Source Zone	Tsunami Source	α (m)	SIFT Maximum (cm)	Development Maximum (cm)	SIFT Minimum (cm)	Development Minimum (cm)
Mega-tsunami Scenarios							
ACSZ 56–65	Aleutian–Alaska–Cascadia	56a–65a, 56b–65b	25	38.0	38.0	−67.8	−67.8
CSSZ 89–98	Central and South America	89a–98a, 89b–98b	25	17.8	17.8	−25.9	−25.9
KISZ 22–31	Kamchatka–Yap–Mariana–Izu–Bonin	22a–31a, 22b–31b	25	9.6	9.6	−10.3	−10.3
NTSZ 30–39	New Zealand–Kermadec–Tonga	30a–39a, 30b–39b	25	11.7	11.7	−18.4	−18.4
Historical Events							
Tohoku 2011	Kamchatka–Yap–Marina–Izu–Bonin	24b, 25b, 26a–27b	varies	66.217	2.6	−3.7	−3.7

Glossary

Arrival time The time when the first tsunami wave is observed at a particular location, typically given in local and/or universal time, but also commonly noted in minutes or hours relative to the time of the earthquake.

Bathymetry The measurement of water depth of an undisturbed body of water.

Cascadia Subduction Zone Fault that extends from Cape Mendocino in Northern California northward to mid-Vancouver Island Canada. The fault marks the convergence boundary where the Juan de Fuca tectonic plate is being subducted under the margin of the North America plate.

Current speed The scalar rate of water motion measured as distance/time.

Current velocity Movement of water expressed as a vector quantity. Velocity is the distance of movement per time coupled with direction of motion.

Digital Elevation Model (DEM) A digital representation of bathymetry or topography based on regional survey data or satellite imagery. Data are arrays of regularly spaced elevations referenced to a map projection of the geographic coordinate system.

Epicenter The point on the surface of the earth that is directly above the focus of an earthquake.

Focus The point beneath the surface of the earth where a rupture or energy release occurs due to a buildup of stress or the movement of earth's tectonic plates relative to one another.

Inundation The horizontal inland extent of land that a tsunami penetrates, generally measured perpendicularly to a shoreline.

Marigram Tide gauge recording of wave level as a function of time at a particular location. The instrument used for recording is termed a marigraph.

Moment magnitude (M_W) The magnitude of an earthquake on a logarithmic scale in terms of the energy released. Moment magnitude is based on the size and characteristics of a fault rupture as determined from long-period seismic waves.

Method of Splitting Tsunamis (MOST) A suite of numerical simulation codes used to provide estimates of the three processes of tsunami evolution: tsunami generation, propagation, and inundation.

Near–field A particular location at which the earth's deformation due to energy release affects the modeling solution.

Propagation database A basin-wide database of pre-computed water elevations and flow velocities at uniformly spaced grid points throughout the world oceans. Values are computed from tsunamis generated by earthquakes with a fault rupture at any one of discrete 100 × 50 km unit sources along worldwide subduction zones.

Runup Vertical difference between the elevation of tsunami inundation and the sea level at the time of a tsunami. Runup is the elevation of the highest point of land inundated by a tsunami as measured relative to a stated datum, such as mean sea level.

Short-term Inundation Forecasting for Tsunamis (SIFT) A tsunami forecast system that integrates tsunami observations in the deep-ocean with numerical models to provide an estimate of tsunami wave arrival and amplitude at specific coastal locations while a tsunami propagates across an ocean basin.

Subduction zone A submarine region of the earth's crust at which two or more tectonic plates converge to cause one plate to sink under another, overriding plate. Subduction zones are regions of high seismic activity.

Synthetic event Hypothetical events based on computer simulations or theory of possible or even likely future scenarios.

Tidal wave Term frequently used incorrectly as a synonym for tsunami. A tsunami is unrelated to the predictable periodic rise and fall of sea level due to the gravitational attractions of the moon and sun: the tide.

Tide The predictable rise and fall of a body of water (ocean, sea, bay, etc.) due to the gravitational attractions of the moon and sun.

Tide gauge An instrument for measuring the rise and fall of a column of water over time at a particular location.

Tele–tsunami or distant tsunami or far–field tsunami Most commonly, a tsunami originating from a source greater than 1000 km away from a particular location. In some contexts, a tele-tsunami is one that propagates through deep-ocean before reaching a particular location without regard to distance separation.

Travel time The time it takes for a tsunami to travel from the generating source to a particular location.

Tsunami A Japanese term that literally translates to "harbor wave." Tsunamis are a series of long–period shallow water waves that are generated by the sudden displacement of water due to subsea disturbances such as earthquakes, submarine landslides, or volcanic eruptions. Less commonly, meteoric impact to the ocean or meteorological forcing can generate a tsunami.

Tsunami hazard assessment A systematic investigation of seismically active regions of the world oceans to determine their potential tsunami impact at a particular location. Numerical

models are typically used to characterize tsunami generation, propagation, and inundation, and to quantify the risk posed to a particular community from tsunamis generated in each source region investigated.

Tsunami propagation The directional movement of a tsunami wave outward from the source of generation. The speed at which a tsunami propagates depends on the depth of the water column in which the wave is traveling. Tsunamis travel at a speed of 700 km/hr (450 mi/hr) over the average depth of 4000 m in the open deep Pacific Ocean.

Tsunami source Location of tsunami origin, most typically an underwater earthquake epicenter. Tsunamis are also generated by submarine landslides, underwater volcanic eruptions, or, less commonly, by meteoric impact of the ocean.

Wave amplitude The maximum vertical rise or drop of a column of water as measured from wave crest (peak) or trough to a defined mean water level state.

Wave crest or peak The highest part of a wave or maximum rise above a defined mean water level state, such as mean lower low water.

Wave height The vertical difference between the highest part of a specific wave (crest) and it's corresponding lowest point (trough).

Wavelength The horizontal distance between two successive wave crests or troughs.

Wave period The length of time between the passage of two successive wave crests or troughs as measured at a fixed location.

Wave trough The lowest part of a wave or the maximum drop below a defined mean water level state, such as mean lower low water.